ceramics

MDPI

Review

Binary Oxide Ceramics (TiO_2, ZnO, Al_2O_3, SiO_2, CeO_2, Fe_2O_3, and WO_3) for Solar Cell Applications: A Comparative and Bibliometric Analysis

Yana Suchikova [1,*], Serhii Nazarovets [2], Marina Konuhova [3] and Anatoli I. Popov [3,*]

[1] Scientific Department, Berdyansk State Pedagogical University, 69061 Zaporizhzhia, Ukraine
[2] Library, Borys Grinchenko Kyiv Metropolitan University, 04053 Kyiv, Ukraine; serhii.nazarovets@gmail.com
[3] Institute of Solid State Physics, University of Latvia, 8 Kengaraga, 1063 Riga, Latvia; marina.konuhova@cfi.lu.lv
* Correspondence: yanasuchikova@gmail.com (Y.S.); popov@latnet.lv (A.I.P.)

Abstract

Binary oxide ceramics have emerged as key materials in solar energy research due to their versatility, chemical stability, and tunable electronic properties. This study presents a comparative analysis of seven prominent oxides (TiO_2, ZnO, Al_2O_3, SiO_2, CeO_2, Fe_2O_3, and WO_3), focusing on their functional roles in silicon, perovskite, dye-sensitized, and thin-film solar cells. A bibliometric analysis covering over 50,000 publications highlights TiO_2 and ZnO as the most widely studied materials, serving as electron transport layers, antireflective coatings, and buffer layers. Al_2O_3 and SiO_2 demonstrate highly specialized applications in surface passivation and interface engineering, while CeO_2 offers UV-blocking capability and Fe_2O_3 shows potential as an absorber material in photoelectrochemical systems. WO_3 is noted for its multifunctionality and suitability for scalable, high-rate processing. Together, these findings suggest that binary oxide ceramics are poised to transition from supporting roles to essential components of stable, efficient, and environmentally safer next-generation solar cells.

Keywords: oxide ceramics; solar cells; photoconversion; TiO_2; ZnO; SiO_2; Al_2O_3; CeO_2; Fe_2O_3; WO_3; bibliometric analysis

Received: 1 August 2025
Revised: 7 September 2025
Accepted: 22 September 2025
Published: 23 September 2025

Citation: Suchikova, Y.; Nazarovets, S.; Konuhova, M.; Popov, A.I. Binary Oxide Ceramics (TiO_2, ZnO, Al_2O_3, SiO_2, CeO_2, Fe_2O_3, and WO_3) for Solar Cell Applications: A Comparative and Bibliometric Analysis. *Ceramics* **2025**, *8*, 119. https://doi.org/10.3390/ceramics8040119

1. Introduction

Traditionally, solar energy has been closely associated with materials such as silicon [1–3], cadmium telluride [4–6], and copper indium gallium selenide (CIGS) [7–9]. Silicon, in particular, has dominated the photovoltaic device market due to its abundance, relatively low cost, and well-established manufacturing processes [10–13]. Silicon-based solar cells have been the cornerstone of solar energy production, offering high efficiency and long-term stability [14–16]. These materials are widely recognized for their ability to effectively convert sunlight into electricity, making them the standard choice for most commercial and residential solar energy systems [17–20].

Cadmium telluride (CdTe) is another key material in the field of solar energy, particularly in thin-film solar cells [21–23]. CdTe has gained popularity due to its high absorption coefficient and relatively low production cost, making it a competitive alternative to silicon for specific applications [24–26]. However, concerns about cadmium toxicity and the limited availability of tellurium have prompted the search for safer and more sustainable alternatives [27,28].

Copper indium gallium selenide (CIGS) represents another category of thin-film solar cells that has attracted attention due to its high efficiency and flexibility [29–31]. CIGS cells offer higher efficiencies than other thin-film technologies and can be applied to a variety of substrates, including flexible materials, opening up new opportunities for solar energy applications [32–34]. Despite these advantages, the complexity of the material composition and associated manufacturing challenges have limited their widespread adoption compared to silicon-based technologies [35,36].

As the solar energy sector continues to grow and evolve, there has been a significant push to diversify the range of materials used in solar cells [37–42]. Researchers are exploring novel materials that may offer higher efficiency, lower production costs, or better performance under specific environmental conditions. This expansion has led to the investigation of organic photovoltaic materials [43,44], perovskites [45,46], and quantum dots [47,48], among others.

In particular, perovskite solar cells are attracting significant interest due to their high efficiency and ease of fabrication [47,48]. These materials have rapidly progressed from laboratory experiments to near-commercialization, offering efficiencies that rival traditional silicon solar cells. However, challenges related to long-term stability and the presence of lead in many perovskite compositions remain serious issues that must be resolved before widespread adoption is possible [49,50].

Quantum dot solar cells represent another frontier in solar energy research, offering the potential for high efficiency through multiple exciton generation [51,52]. These nanoscale semiconductor particles can be engineered to possess specific optical properties, making them easily tunable for various applications [53,54]. However, quantum dot technologies face challenges such as stability and scalability that must be overcome.

Organic photovoltaics (OPV) [55,56] have emerged as a promising field due to their potential for low-cost production and mechanical flexibility, although they currently lag behind traditional materials in terms of efficiency and stability.

This expansion of material options reflects ongoing efforts in solar energy to enhance the efficiency, affordability, and versatility of solar cells. By moving beyond traditional materials, the industry seeks to develop next-generation solar technologies capable of meeting the rising global demand for renewable energy and addressing the limitations of current systems [57].

In recent years, the solar energy field has begun to explore the potential of oxide ceramics as alternative materials for photovoltaic and related applications [58]. Known for their durability, thermal stability, and diverse electrical properties, oxide ceramics offer a promising avenue for improving the performance and longevity of solar cells [59–62]. Unlike traditional semiconductors, oxide ceramics provide a unique combination of features, including high chemical resistance and the ability to operate under extreme environmental conditions, making them ideal candidates for use in advanced solar technologies [63–66].

The growing interest in oxide ceramics for solar applications stems from their ability to play multiple roles within solar cells, such as serving as transparent conducting oxides, photoanodes, or passivation layers [67–70]. These materials can enhance light absorption, increase charge carrier mobility, and reduce recombination losses, thereby potentially improving the overall efficiency of solar cells [71–74]. Furthermore, the versatility of oxide ceramics allows them to be integrated into various types of solar cells, including dye-sensitized solar cells [75,76], perovskite solar cells [77,78], and even novel technologies such as photoelectrochemical cells for hydrogen production [79,80].

Key binary oxide ceramics (Table 1), such as titanium dioxide (TiO_2) [81–84] and zinc oxide (ZnO) [85,86], have already proven to be critical components in several solar technologies [87–89]. TiO_2, for instance, is widely used as a photoanode in dye-sensitized

solar cells due to its excellent photocatalytic properties and high stability [90,91]. ZnO, with its favorable electron transport characteristics, is frequently used as a transparent electrode or photoanode in various solar cell designs [92]. These materials, along with others such as aluminum oxide (Al_2O_3) [93–95], silicon dioxide (SiO_2) [96,97], and cerium dioxide (CeO_2) [98–100], are being extensively investigated for their potential to create more efficient and durable solar cells.

Fe_2O_3 (hematite) is considered a promising material due to its abundance, environmental friendliness, and ability to absorb visible light [101–103]. The bandgap of Fe_2O_3 makes it particularly attractive for photoelectrochemical solar cells, where it is often used as a photoanode [104,105]. Its high chemical stability and durability enable its use in harsh environments, such as acidic or alkaline media. WO_3 (tungsten trioxide) is another promising material for solar technologies due to its electrochromic and photocatalytic properties [106–108]. The bandgap of WO_3 allows it to absorb light in the near-UV spectrum, making it useful in hybrid solar cells [109,110]. WO_3 is often employed as a photoanode in photoelectrochemical cells for hydrogen production [111], as well as an active material in multilayer anti-reflective coatings for solar panels [112].

Table 1. Physico-electrical parameters of oxide ceramic materials used in photovoltaic structures *.

Oxide Material	Band Gap (Eg, eV)	Conductivity Type	Electron Mobility ($cm^2 \cdot V^{-1} \cdot s^{-1}$)	Dielectric Constant (εr)	Electron Affinity (χ, eV)	Ref
TiO_2 (anatase/rutile)	2.9–3.4 (direct/indirect)	n-type (O-vacancy, donor-doped)	~0.1–1 (up to 15 in crystals)	25–1000 †	3.9–4.3	[113–116]
ZnO (wurtzite)	3.1–3.4	n-type (intrinsic/doped)	10–300	7–12 (up to ~25 for Co/Mn-doped)	4.2–4.5	[117–119]
Al_2O_3 (sapphire)	8.5–9.5	Insulator	~ ($\leq 10^{-9}$ S cm^{-1})	6–12	1.0–2.6	[120–122]
SiO_2 (quartz, glass)	8.0–9.2	Insulator	—	3.7–4.3	0.8–1.1	[123–125]
CeO_2 (ceria)	2.8–3.5	n-type (Ce^{3+}, O-vacancies)	10^{-4}–1 (small-polaron hopping)	16–35	3.3–3.7	[126–129]
Fe_2O_3 (hematite)	1.9–2.3	n-type (poor σ)	10^{-4}–0.1	5–120	4.3–5.0	[130–133]
WO_3 (monoclinic)	2.4–3.2	n-type (O-deficient)	0.1–30	10–10^5 ‡	3.2–3.6	[134–136]

† For heavily reduced or H-implanted rutile TiO_2, εr > 1000 has been reported; the listed range of 25–1000 covers both typical and "giant" values (the typical range is 25–120). ‡ WO_3 near the phase transition (~16 °C) shows peak εr ≈ 10^5; the operational range includes the most commonly used values of 10–10^5. * Note: All parameters are reported as generalized ranges because their values depend on synthesis route, crystallinity, defect concentration, doping level, measurement frequency, and other experimental conditions.

The integration of oxide ceramics into solar energy systems represents a significant shift toward the development of materials that not only improve efficiency but also offer enhanced durability [106,107]. As the demand for more reliable and cost-effective solar energy solutions continues to grow, the role of oxide ceramics is expected to increase, driving further innovation in the field.

While numerous studies have been conducted on specific oxide materials or their applications in solar technologies, no comprehensive bibliometric and comparative investigation has been conducted that evaluates various oxide ceramics across a wide range of

solar applications. This gap in the literature highlights the need for a holistic analysis that not only identifies current trends but also provides insight into potential future directions for research and development.

The primary objective of this study is to conduct an in-depth bibliometric and comparative analysis of oxide ceramics used in solar energy, with a focus on understanding research trends, key materials, and their impact on the field. This study aims to identify which oxide ceramics are most prominent in solar energy research, how interest in these materials has evolved, and which materials hold the most significant potential for future development in this field.

The results of this study will be valuable for researchers, industry professionals, and policymakers, as they offer a clearer understanding of the current state of the field and its future direction. By mapping the research landscape, this study will help identify the most influential work, emerging areas of interest, and potential opportunities for innovation. Furthermore, it will serve as a resource for scholars seeking to build on existing knowledge, supporting more targeted and impactful research on the use of oxide ceramics in solar energy.

2. Methodology

This study employed a combined methodology that integrates bibliometric analysis, descriptive statistics, and thematic interpretation of results. This approach enables the identification of general research trends as well as an in-depth examination of each material's specific role in solar energy applications. All data that was used for this research may be found at Zenodo: https://doi.org/10.5281/zenodo.15829792.

The focus of this review was restricted to seven binary oxides—TiO_2, ZnO, Al_2O_3, SiO_2, CeO_2, Fe_2O_3, and WO_3—based on a set of clearly defined criteria. First, each of these oxides intersects with major photovoltaic architectures (c-Si, PSC, OPV, DSSC, PEC), thereby ensuring broad technological relevance. Second, they exhibit functional complementarity across key device roles, including electron and hole transport (TiO_2, ZnO, WO_3), passivation and interfacial control (Al_2O_3, SiO_2), optical filtering and stability enhancement (CeO_2), and light absorption (Fe_2O_3, WO_3). Third, they are characterized by a sufficient bibliometric corpus, providing a robust publication base for comparative statistical analysis. Other oxides such as SnO_2 (a well-established TCO/ETL in PSCs) and Fe_3O_4 (with known roles in PV) were acknowledged as relevant but were excluded to maintain methodological consistency and comparability across the selected set. Their omission avoids introducing stoichiometric and functional heterogeneity that could complicate bibliometric interpretation. Nevertheless, we note that SnO_2 and Fe_3O_4 represent potential candidates for future "sensitivity appendices" or extended studies, where their trajectories may be compared against the seven selected benchmarks.

2.1. Bibliometric Analysis

Bibliometric analysis is a quantitative method used to assess the structure, dynamics, and trends of scientific research through the systematic examination of publications, citations, and metadata [137–139]. Traditionally employed in scientometrics and library sciences, this approach is gaining relevance in materials science, where it allows researchers to uncover patterns of technological development, identify leading contributors and emerging topics, and assess the maturity and interdisciplinarity of specific material systems [140–143].

In the context of solar energy research, bibliometric tools provide valuable insights into how specific materials, such as binary metal oxides, are integrated into device architectures, studied across disciplines, and adopted by different scientific communities [144–147]. By quantitatively assessing publication trends, citation impact, and keyword co-occurrence,

bibliometric analysis complements experimental and theoretical approaches, offering a macroscopic view of knowledge production and research activity [148–151].

This study applies bibliometric analysis to map the research landscape surrounding seven key oxide ceramics (TiO_2, ZnO, SiO_2, Al_2O_3, CeO_2, Fe_2O_3, and WO_3) in solar energy applications. The goal is to identify thematic concentrations, leading authors and institutions, geographical distribution, and collaboration networks, as well as to compare material-specific trends in attention and utilization.

2.1.1. Database Selection and Search Strategy

The analysis was conducted using data retrieved from the Web of Science Core Collection, which was selected due to its broad coverage of peer-reviewed literature in science and technology [152–154]. To ensure a systematic and comprehensive approach, a detailed search strategy was developed to identify publications related to the studied oxide materials (Figure 1).

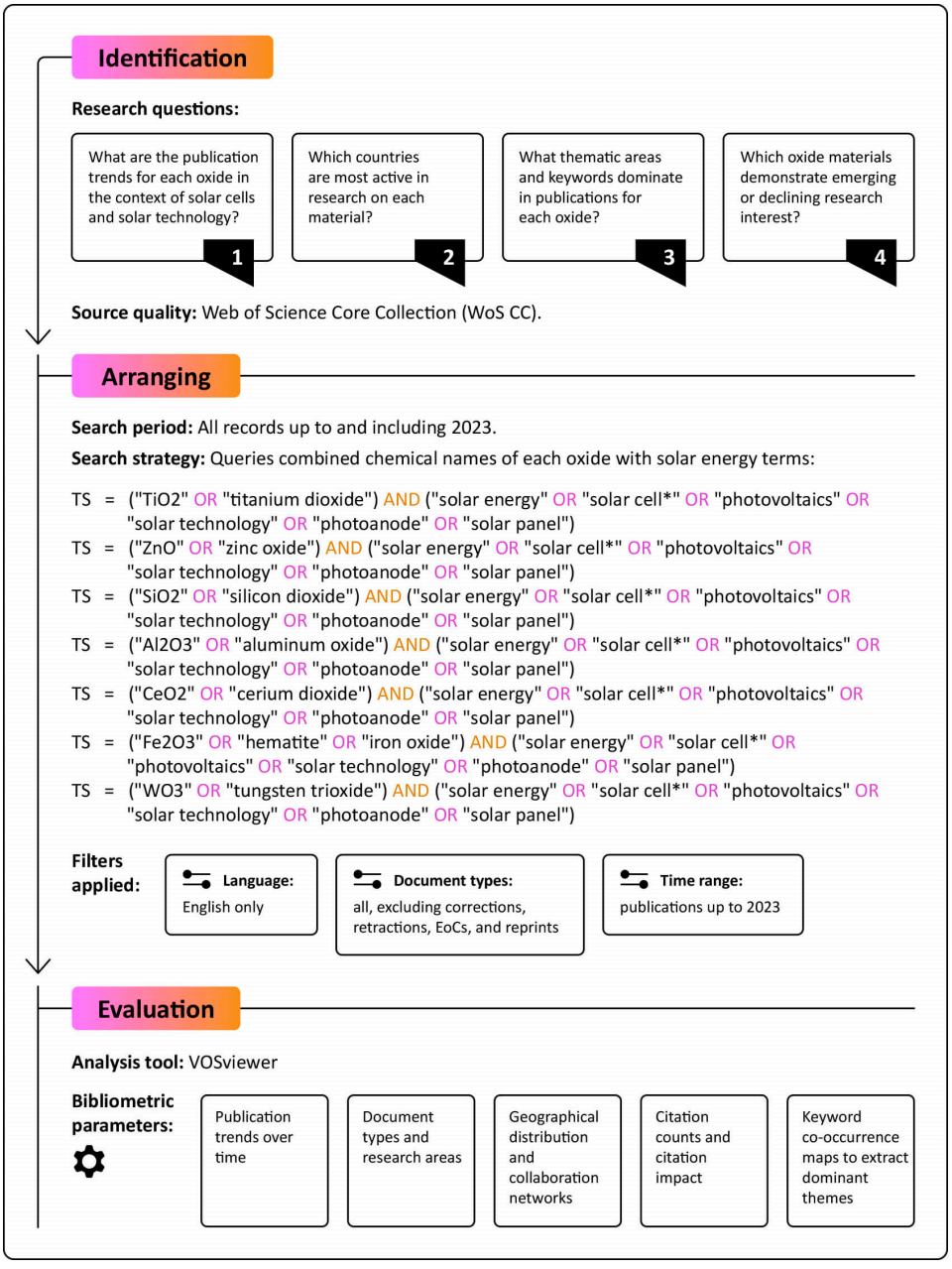

Figure 1. Design of the Bibliometric Analysis.

Search queries targeted each oxide individually by combining its chemical names with keywords associated with solar energy applications. For titanium dioxide (TiO_2), the query used was TS = ("TiO_2" OR "titanium dioxide") AND TS = ("solar energy" OR "solar cell*" OR "photovoltaic devices" OR "solar technology" OR "photoanode" OR "solar panel"). Similar queries were constructed for zinc oxide (ZnO), silicon dioxide (SiO_2), aluminum oxide (Al_2O_3), cerium dioxide (CeO_2), hematite or iron oxide (Fe_2O_3), and tungsten trioxide (WO_3). These queries combined the oxide names with terms such as "solar energy," "solar cells," "photovoltaic devices," "solar technologies," "photoanode," and "solar panel" to capture the full scope of solar-related research for each material.

Filters were applied to refine the search results and ensure consistency across datasets. The temporal scope of the study was limited to publications available up to and including the year 2023 and included only articles written in English. All document types were considered, except corrections, editorials, retractions, and reprints, in order to maintain data integrity and relevance.

To quantitatively assess the impact of research related to oxide materials, citation counts were analyzed for each material. This analysis enabled the evaluation of not only the intensity of publication activity but also the scientific weight of research within each segment.

2.1.2. Data Analysis

The retrieved datasets were processed and analyzed using VOSviewer (1.6.20 version), a bibliometric analysis software tool designed for visualizing and exploring patterns in scientific literature [155–157]. For each oxide material, a range of bibliometric parameters was examined to provide a detailed overview of research activity. These included temporal publication trend analysis to identify chronological patterns, distribution of document types to evaluate the nature of contributions, and distribution across research areas to understand each material's interdisciplinary orientation.

Further analysis identified leading journals, authors, and institutions to highlight the key contributors in the field. Geographic contributions were also assessed to explore global research activity, and collaboration networks were visualized to understand international and institutional partnerships. Finally, keyword co-occurrence analysis was conducted to identify thematic trends and research priorities for each oxide material.

2.2. Statistical Analysis

To analyze publication trends related to binary oxide ceramics, descriptive statistical methods were applied to summarize and compare research activity for each material. The computed statistical indicators include the median, mean, standard deviation, coefficient of variation (CV), maximum value, first quartile (Q1), third quartile (Q3), and interquartile range (IQR) (Table 2). These indicators were selected to reflect both the central tendency and variability of the data, enabling a comprehensive assessment of publication dynamics for each material.

All statistical calculations were based on the number of publications per material for the period 1974–2023. Data for each material were sorted in ascending order, and quartiles were calculated using interpolation for noninteger positions. The resulting metrics provide detailed insights into research trends, highlighting both the intensity of scientific activity and its temporal stability.

Table 2. Description of Statistical Indicators.

Statistical Indicator	Description
Median	The central value of an ordered dataset, less affected by outliers.
Mean	The arithmetic average, indicating the overall level of research activity.
Standard Deviation	A measure of data variability relative to the mean.
Coefficient of Variation (CV)	The standard deviation, expressed as a percentage of the mean, reflecting relative variability.
Maximum Value	The highest recorded number of publications.
First Quartile (Q1)	The value below which 25% of the data fall, representing the lower range of activity.
Third Quartile (Q3)	The value below which 75% of the data fall, representing the upper range of activity.
Interquartile Range (IQR)	The range containing the central 50% of the data, enabling assessment of variability without outliers.

2.3. Functional Literature Analysis

In addition to bibliometric and statistical approaches, a structured literature review was conducted to compare the functional roles of selected binary oxide ceramics across different solar cell architectures. This stage of the study aimed to link material properties to their technological relevance in device engineering.

The analysis was based on a systematic review and synthesis of peer-reviewed publications addressing

- The physical, chemical, and optoelectronic properties of TiO_2, ZnO, SiO_2, Al_2O_3, CeO_2, Fe_2O_3, and WO_3;
- Their specific functions in crystalline silicon (c-Si), perovskite (PSC), dye-sensitized (DSSC), thin-film chalcogenide (CIGS, CdTe, CZTS), organic (OSC), and quantum dot (QD) solar cells;
- Comparative advantages, limitations, and integration challenges of each oxide in these technologies.

The analysis was based on a systematic review and synthesis of peer-reviewed To structure the results, the following analytical tools were used:

- A functional role matrix mapping the oxide materials to device architectures and layer functionalities (ETL, HTL, TCO, passivation, buffer, optical interlayer);
- A synthesis of key advantages and limitations drawn from experimental studies and review articles;
- Cross-verification of usage trends with bibliometric co-occurrence data (e.g., TiO_2 + passivation; ZnO + buffer layer).

This triangulated approach enabled a comprehensive assessment of each oxide's contribution to modern photovoltaic engineering, highlighting both mainstream uses and cutting-edge developments.

3. Results

3.1. Evolution of Scientific Interest in Oxide Ceramics for Solar Energy: Results of the Bibliometric Analysis

The bibliometric analysis of publications on oxide ceramics for solar energy applications provides a comprehensive overview of the research landscape. Table 3 summarizes

the volume of literature identified for each of the selected binary oxide materials in the Web of Science Core Collection.

Table 3. Number of publications identified for each oxide material in the context of solar energy applications (Web of Science Core Collection).

Materials	Results from WoS CC
TiO_2 (titanium dioxide)	22,898
ZnO (zinc oxide)	19,092
SiO_2 (silicon dioxide)	4140
Al_2O_3 (aluminum oxide)	3268
Fe_2O_3 (iron oxide)	2633
WO_3 (tungsten trioxide)	2062
CeO_2 (cerium dioxide)	491

Overall, the dominance of TiO_2 (22,898 publications) and ZnO (19,092) in the solar research arena is clearly evident. These are followed in popularity by SiO_2 (4140), Al_2O_3 (3268), Fe_2O_3 (2633), and WO_3 (2062). CeO_2 received the least attention, with 491 publications.

Research on oxide ceramics in the context of solar energy has undergone significant evolution over recent decades, with notable fluctuations in interest across different materials (Figure 2). The earliest publications related to oxide ceramics appeared in the 1970s, focusing on materials such as TiO_2 (1974) and WO_3 (1976). However, until the late 1980s, the overall publication volume remained minimal, with only a few isolated studies. This indicates that the field had a very slow start.

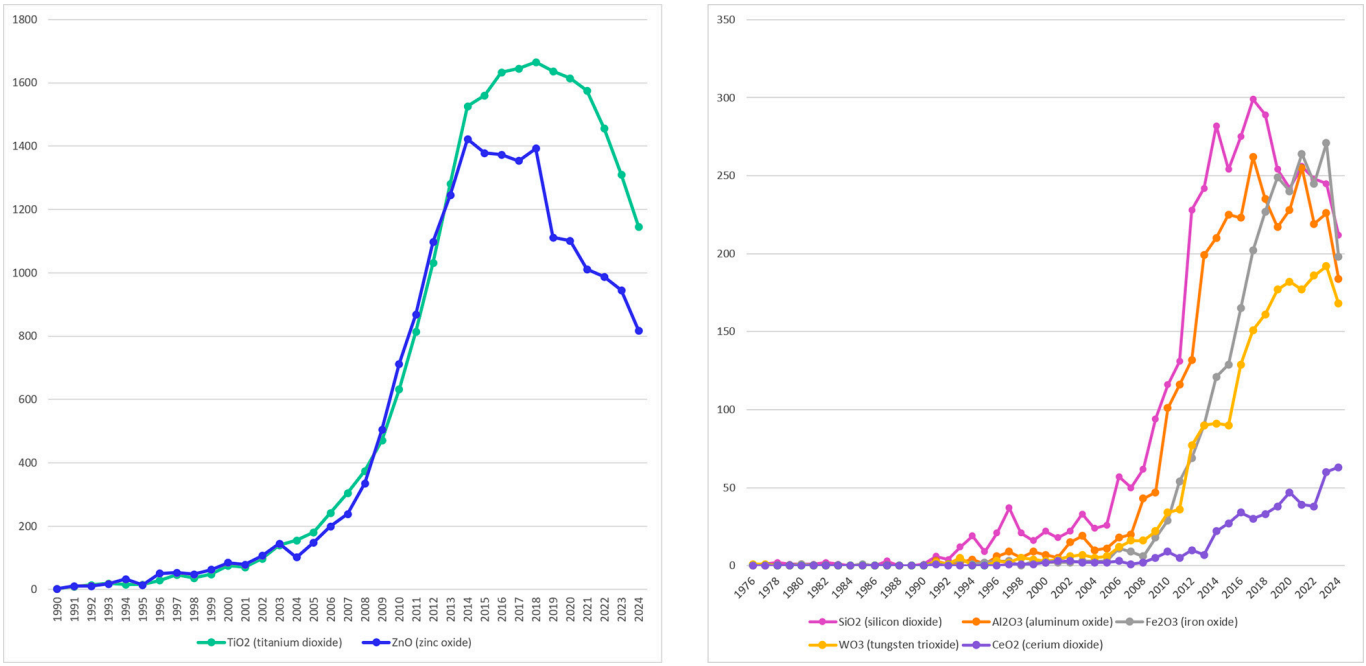

Figure 2. Dynamics of publication numbers for selected binary oxides in the context of solar energy applications (Web of Science Core Collection data, 1970–2024).

The situation began to change in the early 1990s, as interest in oxide materials gradually intensified. This period saw a growth in the number of publications for TiO_2, ZnO, and Fe_2O_3. For instance, TiO_2 showed steady growth, reaching 49 publications by the end of the decade, signaling increasing recognition of this material. ZnO also garnered more attention,

though at a slightly slower pace, while interest in other materials such as Al_2O_3 and WO_3 remained low.

A true breakthrough for oxide ceramics occurred in the 2000s, when publication counts for TiO_2 and ZnO rose sharply, reaching hundreds per year. TiO_2 became the leading subject of research, exceeding 600 publications per year by 2010. ZnO ranked second, following a similar upward trend, though with slightly lower absolute numbers. Al_2O_3, Fe_2O_3, and WO_3 also began to gain traction, albeit at more moderate rates, reaching dozens of publications annually. This reflects a broadening interest in various materials within this category.

The peak of oxide ceramics research occurred in the 2010s. TiO_2 and ZnO reached their highest publication volumes, peaking in the middle of the decade (over 1600 for TiO_2 and 1400 for ZnO). Other materials also hit their peaks during this period: SiO_2 reached 299 publications in 2017, Al_2O_3 peaked at 262 in the same year, Fe_2O_3 at 249 in 2019, and WO_3 at 182 in 2020. CeO_2, despite its overall lower activity, also showed gradual growth, reaching its peak in 2024 with 63 publications. This surge of interest in different materials reflects a broad range of scientific challenges and experimental approaches associated with oxide ceramic research.

In the 2020s, the overall publication rate for most materials began to stabilize or slightly decline, likely due to saturation in certain research areas and a shift in focus toward new materials or concepts. An exception is CeO_2, which continues to show growing interest, possibly due to its niche applications.

Key observations indicate that TiO_2 and ZnO remain the primary subjects of research, while other materials such as Al_2O_3, Fe_2O_3, WO_3, and CeO_2 occupy more specialized niches.

3.2. Publication Trends and Statistical Analysis of Binary Oxide Ceramics

The statistical analysis of publications related to binary oxide ceramics revealed significant differences in research activity among the various materials, as well as substantial fluctuations in publication trends (Table 4). The results provide insight into the relative importance and developmental dynamics of each material in the research field.

Table 4. Statistical analysis of publications on binary oxide ceramics *.

Material	Median	Standard Deviation	Coefficient of Variation (%)	Mean	Maximum	1st Quartile (Q1)	3rd Quartile (Q3)	Interquartile Range (IQR)
TiO_2	119.0	652.44	125.37	520.41	1665	13.75	1180.0	1166.25
ZnO	126.5	529.57	116.50	454.57	1422	15.75	977.25	961.5
SiO_2	25.0	110.43	117.33	94.11	299	5.5	231.5	226.0
Al_2O_3	20.0	100.99	108.16	93.37	262	6.5	213.5	207.0
Fe_2O_3	9.0	98.82	131.36	75.23	271	2.5	147.0	144.5
WO_3	16.0	71.78	118.36	60.65	192	4.25	119.5	115.25
CeO_2	5.0	19.42	114.72	16.93	63	2.0	33.0	31.0

* The mean values are calculated over active years only, i.e., years in which at least one publication on the given oxide was recorded. Years with zero publications were excluded from the denominator in order to provide a meaningful average for periods of active research.

TiO_2 exhibits the highest research intensity, with an average of 520.41 publications and a maximum of 1665 articles in a single year.

SiO_2 is characterized by lower average research indicators: a mean of 94.11 and a maximum of 299 publications. Its median (25.0) and interquartile range (IQR = 226.0) suggest that most years were marked by moderate research activity, without the surges observed for TiO_2 and ZnO. The standard deviation (110.43) and coefficient of variation

(117.33%) indicate relatively stable interest in the material, though without major peaks in research output.

Al_2O_3 showed similar trends to SiO_2, with a mean of 93.37 and a maximum of 262 publications. The median (20.0) and IQR (207.0) suggest that most years had low research activity, interspersed with periodic spikes. The standard deviation (100.99) and coefficient of variation (108.16%) point to significant year-to-year variability, likely driven by developments in specific solar applications.

Fe_2O_3 has the lowest publication median (9.0) among the studied materials but demonstrates moderate overall activity. Its mean is 75.23, and the maximum number of publications is 271, indicating periods of increased attention. The IQR (144.5) and high coefficient of variation (131.36%) reflect uneven but occasionally intense research activity, possibly linked to specific technological innovations.

WO_3 demonstrates moderate research intensity, with an average of 60.65 publications and a maximum of 192 articles. The median (16.0) and IQR (115.25) suggest a concentration of activity in the lower range, with only a few years yielding higher output. The coefficient of variation (118.36%) confirms considerable variability, highlighting that research on WO_3 tends to be more focused but less consistent over time.

CeO_2 has the lowest overall research activity among the materials: an average of 16.93 publications and a maximum of 63. The median (5.0) and IQR (31.0) indicate limited but gradually growing research interest in recent years. The standard deviation (19.42) and coefficient of variation (114.72%) point to a slow yet steady interest in CeO_2, likely due to its niche applications.

The analysis shows that TiO_2 and ZnO dominate the research landscape of binary oxide ceramics, with significantly higher publication metrics and variability compared to other materials. In contrast, SiO_2, Al_2O_3, WO_3, Fe_2O_3, and CeO_2 exhibit more moderate research activity, often tied to specific technological breakthroughs. The high coefficients of variation across all materials emphasize the dynamic nature of research priorities in this field.

3.3. Interdisciplinary Distribution of Research on Oxide Ceramics

The Sankey diagram (Figure 3) illustrates the distribution of scientific interest in the studied materials (TiO_2, ZnO, SiO_2, Al_2O_3, CeO_2, Fe_2O_3, and WO_3) across four key research domains: Energy, Materials Science, Environmental Science, and Physics. The width of each connection corresponds to the number of publications associating a given material with the respective field. This visualization provides insight into the degree of interdisciplinarity of each material and outlines the profiles of their research involvement [158–160].

TiO_2 and ZnO exhibit the broadest scientific activity, with strong representation in all four disciplines. Their leading role in energy and materials science stems from their wide range of functionalities—from charge transport to photocatalysis and structural stabilization in optoelectronics. In parallel, their presence in environmental and physics-related studies demonstrates their functional flexibility and adaptability to diverse technological challenges [161–164].

Fe_2O_3, on the other hand, displays a strong focus on energy research. Its research profile is primarily centered on photoelectrochemical water splitting and hydrogen generation [165–168], reflecting its specialization as a material for renewable energy production under harsh environmental conditions [169,170]. Its limited overlap with physics or environmental science highlights a narrow yet strategically important niche.

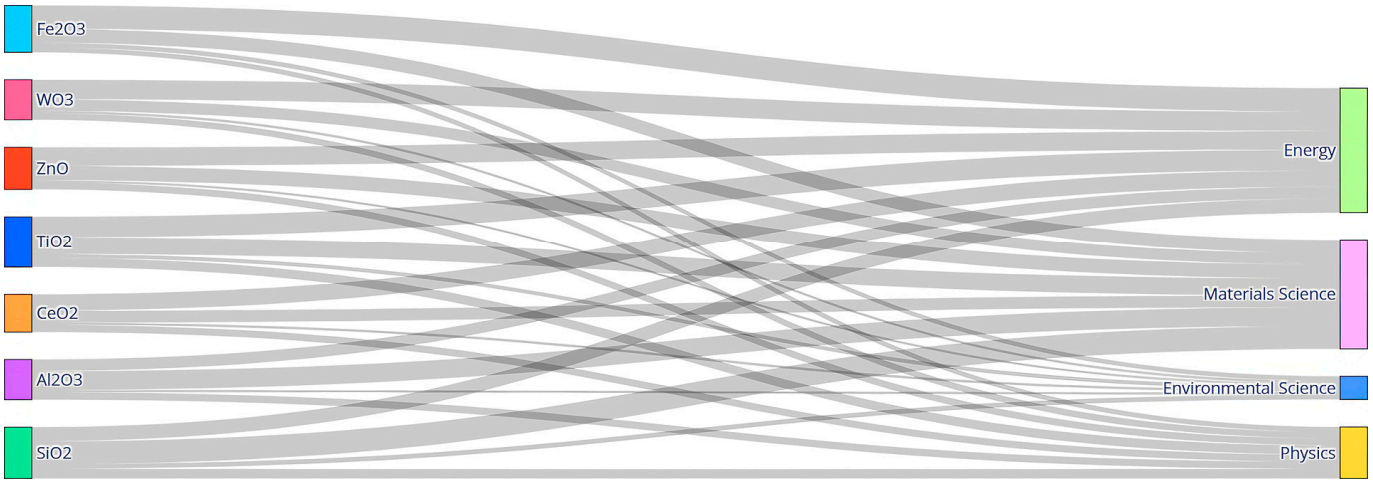

Figure 3. Sankey diagram illustrating the distribution of research focus among binary oxide ceramics across four disciplines: Energy, Materials Science, Environmental Science, and Physics.

WO_3 shows a more balanced distribution across energy, materials science, and environmental science. This structure reflects its multifunctionality: WO_3 is investigated not only in the context of PEC devices [171,172], but also for applications such as electrochromic elements, sensors, and optical control coatings [173,174].

Al_2O_3 and SiO_2 are primarily concentrated in materials science and physics. Their roles are mainly associated with passivation, dielectric separation, interface protection, and the formation of stable layers in complex solar cell architectures [174–180]. These applications align with their physicochemical characteristics—wide bandgap, high stability, and insulating nature [181–183].

CeO_2, while having a smaller overall research volume, shows a relatively even contribution across all four domains. This indicates a growing interest in CeO_2 as a promising material for niche photovoltaic, catalytic, and protective applications [184–186], particularly due to its UV absorption capabilities, redox activity, and high stability [187–190].

Thus, the diagram enables not only an assessment of the research scale for each oxide but also a contextual understanding of how scientific interest is shaped. The varying degrees of cross-sector coverage reflect differences in maturity, specialization, and transdisciplinary potential among the oxides. This has practical implications for developing research strategies and identifying priority directions for future innovations.

3.4. Comparative Analysis of the Most Cited Publications on Binary Oxide Ceramics

An analysis of citation metrics for the most influential publications on binary oxide ceramics highlights significant differences in the impact and research focus of different materials (Table 5).

TiO_2 shows overwhelming dominance in citation counts, followed by ZnO and Fe_2O_3, while materials such as SiO_2, Al_2O_3, WO_3, and CeO_2 contribute in a more specialized but still significant way. These patterns reflect both the scientific maturity of each material's applications and their role within the broader solar energy research landscape.

TiO_2 stands out as the most researched and cited material. The seminal work by O'Regan and Grätzel from 1991 [191], which introduced dye-sensitized solar cells, has garnered over 25,000 citations—far surpassing any other publication in this field. This paper laid the foundation for much of the subsequent TiO_2 research and solidified its reputation as a cornerstone material in solar energy technologies. Other highly cited works on TiO_2 examine its role in photoelectrochemical cells and perovskite solar cells, with citation counts

ranging from 5000 to 18,000. These publications span several decades, indicating TiO_2's sustained influence across multiple generations of solar technology development.

Table 5. Top 5 Most Cited Publications on Binary Oxide Ceramics *.

TiO_2 (Titanium Dioxide)	**Citations**
O'Regan, B., & Grätzel, M. (1991). A low-cost, high-efficiency solar cell based on dye-sensitized colloidal TiO2 films. *Nature*, *353*(6346), 737–740. https://doi.org/10.1038/353737a0 [191]	25,829
Kojima, A., Teshima, K., Shirai, Y., & Miyasaka, T. (2009). Organometal Halide Perovskites as Visible-Light Sensitizers for Photovoltaic Cells. *Journal of the American Chemical Society*, *131*(17), 6050–6051. https://doi.org/10.1021/ja809598r [192]	18,169
Grätzel, M. (2001). Photoelectrochemical cells. Nature, 414(6861), 338–344. https://doi.org/10.1038/35104607 [193]	11,772
Kim, H.-S., Lee, C.-R., Im, J.-H., Lee, K.-B., Moehl, T., Marchioro, A., et al. (2012). Lead Iodide Perovskite Sensitized All-Solid-State Submicron Thin Film Mesoscopic Solar Cell with Efficiency Exceeding 9%. Scientific Reports, 2(1), 591. https://doi.org/10.1038/srep00591 [194]	7149
Nazeeruddin, M. K., Kay, A., Rodicio, I., Humphry-Baker, R., Mueller, E., Liska, P., et al. (1993). Conversion of light to electricity by cis-X2bis(2,2′-bipyridyl-4,4′-dicarboxylate)ruthenium(II) charge-transfer sensitizers (X = Cl-, Br-, I-, CN-, and SCN-) on nanocrystalline titanium dioxide electrodes. Journal of the American Chemical Society, 115(14), 6382–6390. https://doi.org/10.1021/ja00067a063 [195]	5854
ZnO (zinc oxide)	Citations
Grätzel, M. (2001). Photoelectrochemical cells. Nature, 414(6861), 338–344. https://doi.org/10.1038/35104607 [193]	11,772
Law, M., Greene, L. E., Johnson, J. C., Saykally, R., & Yang, P. (2005). Nanowire dye-sensitized solar cells. Nature Materials, 4(6), 455–459. https://doi.org/10.1038/nmat1387 [196]	5135
Grätzel, M. (2003). Dye-sensitized solar cells. Journal of Photochemistry and Photobiology C: Photochemistry Reviews, 4(2), 145–153. https://doi.org/10.1016/S1389-5567(03)00026-1 [197]	4640
Liu, D., & Kelly, T. L. (2014). Perovskite solar cells with a planar heterojunction structure prepared using room-temperature solution processing techniques. Nature Photonics, 8(2), 133–138. https://doi.org/10.1038/nphoton.2013.342 [198]	2383
Liu, B., & Aydil, E. S. (2009). Growth of Oriented Single-Crystalline Rutile TiO 2 Nanorods on Transparent Conducting Substrates for Dye-Sensitized Solar Cells. Journal of the American Chemical Society, 131(11), 3985–3990. https://doi.org/10.1021/ja8078972 [199]	2215
SiO_2 (silicon dioxide)	Citations
Kay, A., Cesar, I., & Grätzel, M. (2006). New Benchmark for Water Photooxidation by Nanostructured α-Fe 2 O 3 Films. Journal of the American Chemical Society, 128(49), 15714–15721. https://doi.org/10.1021/ja064380l [200]	1437
Cushing, S. K., Li, J., Meng, F., Senty, T. R., Suri, S., Zhi, M., et al. (2012). Photocatalytic Activity Enhanced by Plasmonic Resonant Energy Transfer from Metal to Semiconductor. Journal of the American Chemical Society, 134(36), 15033–15041. https://doi.org/10.1021/ja305603t [201]	1032
Palomares, E., Clifford, J. N., Haque, S. A., Lutz, T., & Durrant, J. R. (2003). Control of Charge Recombination Dynamics in Dye Sensitized Solar Cells by the Use of Conformally Deposited Metal Oxide Blocking Layers. Journal of the American Chemical Society, 125(2), 475–482. https://doi.org/10.1021/ja027945w [202]	1029
Zou, S., Liu, Y., Li, J., Liu, C., Feng, R., Jiang, F., et al. (2017). Stabilizing Cesium Lead Halide Perovskite Lattice through Mn(II) Substitution for Air-Stable Light-Emitting Diodes. Journal of the American Chemical Society, 139(33), 11443–11450. https://doi.org/10.1021/jacs.7b04000 [203]	728
Aberle, A. G. (2000). Surface passivation of crystalline silicon solar cells: a review. Progress in Photovoltaics: Research and Applications, 8(5), 473–487. https://doi.org/10.1002/1099-159X(200009/10)8:5%3C473::AID-PIP337%3E3.0.CO;2-D [204]	625

Table 5. *Cont.*

Al_2O_3 (aluminum oxide)	Citations
Palomares, E., Clifford, J. N., Haque, S. A., Lutz, T., & Durrant, J. R. (2003). Control of Charge Recombination Dynamics in Dye Sensitized Solar Cells by the Use of Conformally Deposited Metal Oxide Blocking Layers. Journal of the American Chemical Society, 125(2), 475–482. https://doi.org/10.1021/ja027945w [202]	1886
Mor, G. K., Varghese, O. K., Paulose, M., Shankar, K., & Grimes, C. A. (2006). A review on highly ordered, vertically oriented TiO2 nanotube arrays: Fabrication, material properties, and solar energy applications. Solar Energy Materials and Solar Cells, 90(14), 2011–2075. https://doi.org/10.1016/j.solmat.2006.04.007 [205]	1605
Huang, Z., Geyer, N., Werner, P., de Boor, J., & Gösele, U. (2011). Metal-Assisted Chemical Etching of Silicon: A Review. Advanced Materials, 23(2), 285–308. https://doi.org/10.1002/adma.201001784 [206]	1285
Malinkiewicz, O., Yella, A., Lee, Y. H., Espallargas, G. M., Graetzel, M., Nazeeruddin, M. K., & Bolink, H. J. (2014). Perovskite solar cells employing organic charge-transport layers. Nature Photonics, 8(2), 128–132. https://doi.org/10.1038/nphoton.2013.341 [207]	1029
Niu, G., Li, W., Meng, F., Wang, L., Dong, H., & Qiu, Y. (2014). Study on the stability of CH 3 NH 3 PbI 3 films and the effect of post-modification by aluminum oxide in all-solid-state hybrid solar cells. J. Mater. Chem. A, 2(3), 705–710. https://doi.org/10.1039/C3TA13606J [208]	955
Fe_2O_3 (iron oxide)	Citations
Sivula, K., Le Formal, F., & Grätzel, M. (2011). Solar Water Splitting: Progress Using Hematite (α-Fe_2O_3) Photoelectrodes. ChemSusChem, 4(4), 432–449. https://doi.org/10.1002/cssc.201000416 [209]	2332
Osterloh, F. E. (2013). Inorganic nanostructures for photoelectrochemical and photocatalytic water splitting. Chem. Soc. Rev., 42(6), 2294–2320. https://doi.org/10.1039/C2CS35266D [210]	1776
Kango, S., Kalia, S., Celli, A., Njuguna, J., Habibi, Y., & Kumar, R. (2013). Surface modification of inorganic nanoparticles for development of organic–inorganic nanocomposites—A review. Progress in Polymer Science, 38(8), 1232–1261. https://doi.org/10.1016/j.progpolymsci.2013.02.003 [211]	1685
Park, J. H., Kim, S., & Bard, A. J. (2006). Novel Carbon-Doped TiO 2 Nanotube Arrays with High Aspect Ratios for Efficient Solar Water Splitting. Nano Letters, 6(1), 24–28. https://doi.org/10.1021/nl051807y [212]	1647
Wang, C.-C., Li, J.-R., Lv, X.-L., Zhang, Y.-Q., & Guo, G. (2014). Photocatalytic organic pollutants degradation in metal–organic frameworks. Energy Environ. Sci., 7(9), 2831–2867. https://doi.org/10.1039/C4EE01299B [213]	1444
WO_3 (tungsten trioxide)	Citations
Park, J. H., Kim, S., & Bard, A. J. (2006). Novel Carbon-Doped TiO 2 Nanotube Arrays with High Aspect Ratios for Efficient Solar Water Splitting. Nano Letters, 6(1), 24–28. https://doi.org/10.1021/nl051807y [212]	1647
Bak, T., Nowotny, J., Rekas, M., & Sorrell, C. (2002). Photo-electrochemical hydrogen generation from water using solar energy. Materials-related aspects. International Journal of Hydrogen Energy, 27(10), 991–1022. https://doi.org/10.1016/S0360-3199(02)00022-8 [214]	1346
Granqvist, C. (2000). Electrochromic tungsten oxide films: Review of progress 1993–1998. Solar Energy Materials and Solar Cells, 60(3), 201–262. https://doi.org/10.1016/S0927-0248(99)00088-4 [215]	1324
Meyer, J., Hamwi, S., Kröger, M., Kowalsky, W., Riedl, T., & Kahn, A. (2012). Transition Metal Oxides for Organic Electronics: Energetics, Device Physics and Applications. Advanced Materials, 24(40), 5408–5427. https://doi.org/10.1002/adma.201201630 [216]	1049
Baetens, R., Jelle, B. P., & Gustavsen, A. (2010). Properties, requirements and possibilities of smart windows for dynamic daylight and solar energy control in buildings: A state-of-the-art review. Solar Energy Materials and Solar Cells, 94(2), 87–105. https://doi.org/10.1016/j.solmat.2009.08.021 [217]	1047

Table 5. *Cont.*

CeO_2 (cerium dioxide)	Citations
Liu, X., Iocozzia, J., Wang, Y., Cui, X., Chen, Y., Zhao, S., et al. (2017). Noble metal–metal oxide nanohybrids with tailored nanostructures for efficient solar energy conversion, photocatalysis and environmental remediation. Energy & Environmental Science, 10(2), 402–434. https://doi.org/10.1039/C6EE02265K [218]	832
Corma, A., Atienzar, P., García, H., & Chane-Ching, J.-Y. (2004). Hierarchically mesostructured doped CeO2 with potential for solar-cell use. Nature Materials, 3(6), 394–397. https://doi.org/10.1038/nmat1129 [219]	728
Ou, G., Xu, Y., Wen, B., Lin, R., Ge, B., Tang, Y., et al. (2018). Tuning defects in oxides at room temperature by lithium reduction. Nature Communications, 9(1), 1302. https://doi.org/10.1038/s41467-018-03765-0 [220]	502
Abanades, S., & Flamant, G. (2006). Thermochemical hydrogen production from a two-step solar-driven water-splitting cycle based on cerium oxides. Solar Energy, 80(12), 1611–1623. https://doi.org/10.1016/j.solener.2005.12.005 [221]	491
Boyjoo, Y., Sun, H., Liu, J., Pareek, V. K., & Wang, S. (2017). A review on photocatalysis for air treatment: From catalyst development to reactor design. Chemical Engineering Journal, 310(2, SI), 537–559. https://doi.org/10.1016/j.cej.2016.06.090 [222]	435

* Some publications appear in multiple oxide lists because they reference or use several materials simultaneously. The selection was based on keywords and abstracts, so even if the main focus of the publication is not exclusively on the respective oxide, its role in the research context is confirmed.

ZnO also holds a strong position, with its most cited works receiving between 2000 and 11,000 citations. Key publications focus on its use in dye-sensitized solar cells and nanostructured applications, emphasizing its value as a versatile and cost-effective material. The overlap between ZnO and TiO_2 in several studies underscores their complementary roles in similar technological areas. However, ZnO's citation counts remain significantly lower than those of TiO_2, reflecting its secondary, but still critical, role in the evolution of solar energy applications.

SiO_2 shows more modest citation figures, with its most influential publications ranging from 728 to 1437 citations. These studies primarily explore SiO_2's supporting roles in solar cells, such as surface passivation and photocatalytic enhancement. While its contribution is less transformative than that of TiO_2 or ZnO, SiO_2 remains a fundamental component in optimizing the performance and stability of solar energy systems.

Al_2O_3 shows a similar trend, with top citation counts between 955 and 1886. Its impact centers on areas like charge recombination dynamics and hybrid cell stability. Though its niche applications limit its broader influence, Al_2O_3 has attracted significant attention in these specialized contexts.

Fe_2O_3 has a higher citation range (between 1400 and 2300), reflecting its role in photoelectrochemical water splitting and hydrogen generation. Publications on Fe_2O_3 emphasize its potential for renewable energy storage and production. WO_3 shows a comparable citation profile, with its most cited works receiving between 1000 and 1600 citations. Research on WO_3 highlights its stability and optical properties, particularly for applications like electrochromic films and PEC devices. Although more specialized, WO_3 continues to be a valuable material in niche solar energy technologies.

CeO_2 displays the lowest citation counts among the analyzed materials, with top publications ranging from 400 to 800 citations. Research on CeO_2 is relatively recent and focuses on advanced topics such as defect engineering, photocatalysis, and thermochemical hydrogen production. Its growing relevance indicates emerging potential in specialized solar systems, even though its overall impact remains limited compared to other materials.

Table 6 offers insight not only into the general scientific impact of the materials but also into the evolution of research priorities over time. In the 1990s, TiO_2's dominance was undisputed: it was the material that triggered a breakthrough in solar technologies, as demonstrated by the pivotal publications of 1991 and 1993. In the 2000s, ZnO, SiO_2, and Al_2O_3 joined the landscape, primarily as supporting or alternative components. Beginning in 2006, scientific interest expanded significantly, with key publications emerging on WO_3 and Fe_2O_3, reflecting a growing focus on PEC technologies and photoelectrochemistry.

Table 6. Distribution of Top 5 Publications by Year for Each Oxide.

Year	TiO_2	ZnO	SiO_2	Al_2O_3	Fe_2O_3	WO_3	CeO_2
1991	O'Regan, B., & Grätzel, M. [191] (25,829)	–	–	–	–	–	–
1993	Nazeeruddin et al. [195] (5854)	–	–	–	–	–	–
2000	-	-	Aberle [204] (2000)	-	-	Granqvist [215] (1324)	-
2001	Grätzel [193] (11,772)	Grätzel [193] (11,772)	–	–	–	–	–
2002	-	-	-	-	-	Bak et al. [214] (1346)	-
2003		Grätzel [197] (4640)	Palomares et al. [202] (1029)	Palomares et al. [202] (1886)	–	–	–
2004	-	-	-	-	-	-	Corma et al. [219] (728)
2005	–	Law et al. [196] (5135)	–	–	–	–	–
2006	–	–	Kay et al. [200] (1437)	Mor et al. [205] (1605)	Park et al. [212] (1647)	Park et al. [212] (1647)	Abanades et al. [221] (491)
2009	Kojima et al. [192] (18,169)	Liu, & Aydil, [199] (2215)	–	–	–	–	–
2010	-	-	-	-	-	Baetens et al. [217] (1047)	
2011	–	–	–	Huang et al. [206] (1285)	Sivula et al. [209] (2332)		–

Table 6. *Cont.*

Year	TiO_2	ZnO	SiO_2	Al_2O_3	Fe_2O_3	WO_3	CeO_2
2012	Kim et al. [194] (7149)	–	Cushing et al. [201] (1032)	–	–	Meyer et al. [216] (1049)	–
2013	–	–	–	–	Osterloh [210] (1776), Kango [211] (1685)	–	–
2014	–	Liu & Kelly [198] (2383)	–	Malinkiewicz [207] (1029), Niu et al. [208] (955)	Wang et al. [213] (1444)	–	–
2017	–	–	Zou et al. [203] (728)	–	–	–	Liu et al. [218] (832), Boyjoo et al. [222] (435)
2018	–	–	–	–	–	–	Ou et al. [220] (502)

Simultaneously, the table illustrates the increasing research activity on CeO_2 in the 2010s, marking its transition from a peripheral topic to one of active interest. Although its citation counts do not yet rival those of TiO_2 or ZnO, the thematic focus of recent publications suggests strong potential in areas like hydrogen production and defect engineering. Publications from 2017 to 2018 are particularly significant indicators of which materials may form the next wave in oxide ceramic research for solar energy.

3.5. Global Trends and International Collaboration in Research on Binary Oxides for Solar Energy Applications

3.5.1. Titanium Dioxide

Bibliometric analysis (Figure 4) shows that research on TiO_2 has steadily increased over the past two decades, driven by its applications in photovoltaic systems, photocatalysis, and environmental remediation. China leads the research landscape with the highest number of publications, followed by India, South Korea, and Japan. The United States is also among the leading contributors, although its node overlaps with China in the visualization, making it less visible in the map. Collaboration networks reveal strong global connections, with Germany, Italy, Spain, and France forming influential hubs in Europe. This reflects the worldwide interest in TiO_2 as a key material in energy and environmental technologies.

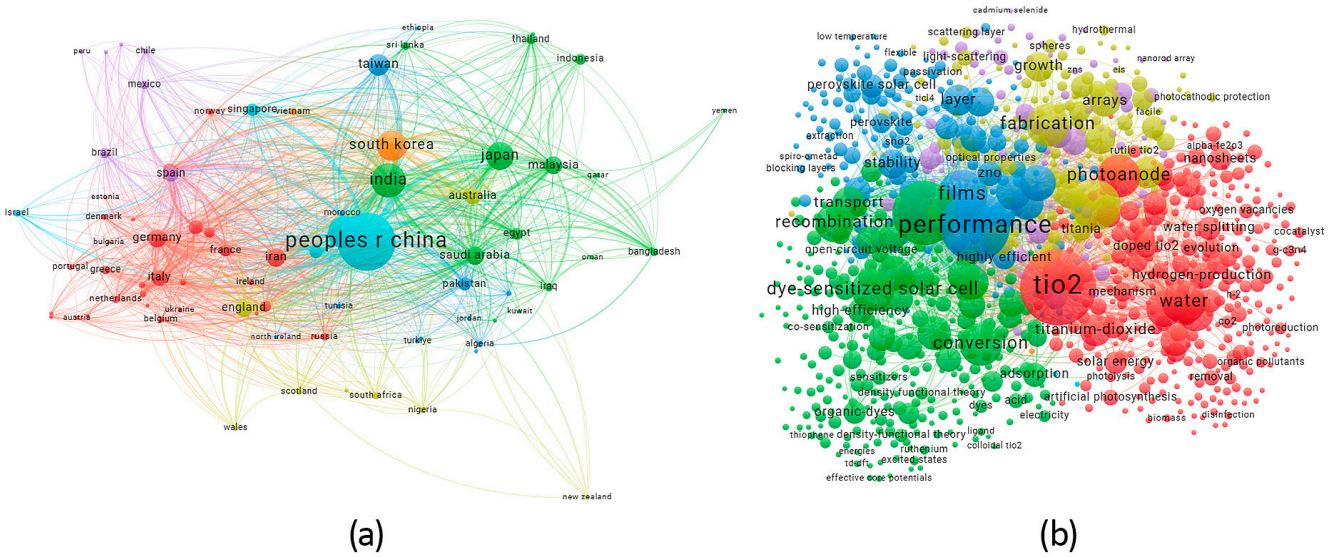

Figure 4. Bibliometric analysis in VOSviewer for TiO_2: (**a**) visualization of international collaboration; (**b**) visualization of keyword clustering. The interactive visualization is available at https://tinyurl.com/245z4qkv, https://tinyurl.com/29ecu8nc (accessed on 7 September 2025).

Keyword analysis reveals major research themes such as "nanostructures," "photoanodes," "efficiency," and "thin films." The role of TiO_2 in dye-sensitized solar cells (DSSC) is well established, with studies highlighting improvements in light harvesting efficiency, stability, and charge separation. Research frequently focuses on nanostructuring approaches, including nanotubes, nanorods, and mesoporous films, to increase surface area and optimize electron transport.

Additionally, TiO_2 doping with elements such as nitrogen or metals has been extensively studied to extend its light absorption into the visible spectrum, making it suitable for broader solar energy applications.

Hydrogen production and water splitting represent another major research direction for TiO_2, where the use of co-catalysts and heterojunction architectures enhances its integration into photoelectrochemical systems. Environmental applications, including pollutant degradation and air purification, further emphasize the versatility of TiO_2, making it a sustained subject of interest across multiple disciplines.

3.5.2. Zinc Oxide

Bibliometric analysis (Figure 5) indicates a steady increase in research output on ZnO, with China, the United States, and India leading global efforts. Germany, France, and South Korea also play important roles, and the collaboration networks show strong partnerships between Asian and European countries. The growing importance of ZnO reflects its versatility in energy conversion, environmental remediation, and advanced electronics.

The keyword network is dominated by terms such as "thin films," "nanostructures," "dye-sensitized solar cells," and "recombination," highlighting ZnO's utility in photovoltaic and catalytic systems. Studies emphasize its high electron mobility, tunable bandgap, and cost-effective synthesis. In DSSCs and hybrid perovskite solar cells, ZnO serves as a transparent conducting oxide (TCO) or electron transport layer, and advances in nanostructuring methods, such as electrospinning and hydrothermal synthesis, have improved its performance. ZnO nanowires, nanoparticles, and quantum dots are actively investigated for their enhanced surface area and light-harvesting capabilities.

ZnO's role in photocatalysis has also drawn considerable attention. Applications include pollutant degradation, hydrogen production, and water purification. Recent

studies combine ZnO with TiO_2 and other materials to form heterojunctions that improve charge separation and catalytic efficiency. These innovations underscore ZnO's critical role in sustainable technologies.

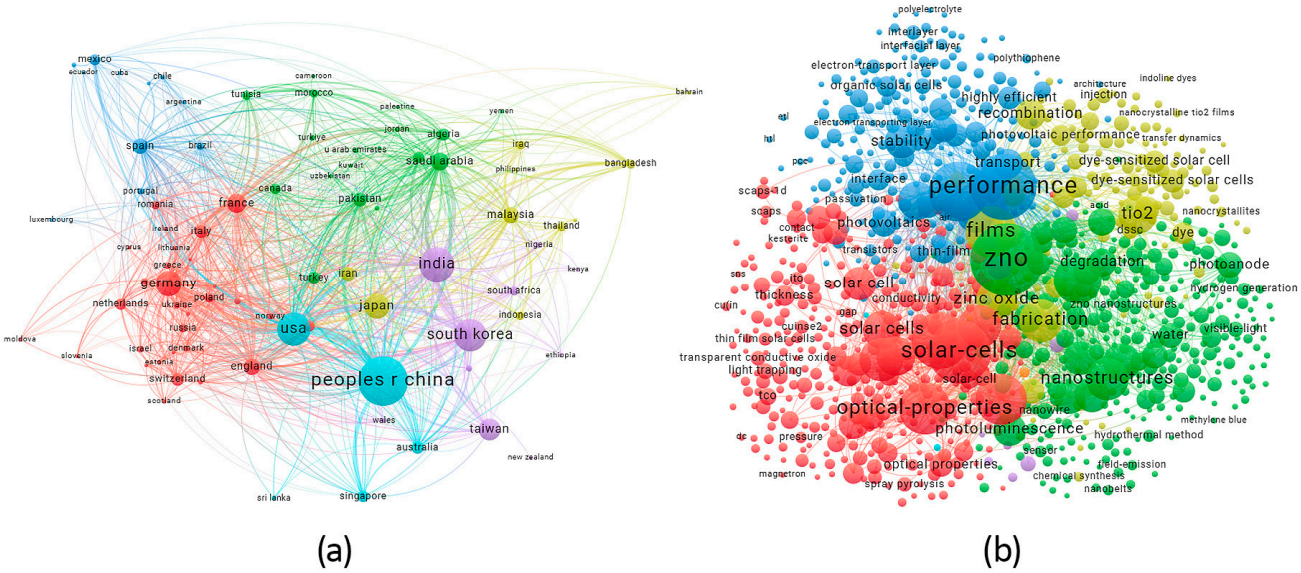

Figure 5. Bibliometric analysis in VOSviewer for ZnO: (**a**) visualization of international collaboration; (**b**) visualization of keyword clustering. The interactive visualization is available at https://tinyurl.com/2cjolpkj, https://tinyurl.com/29k59moj (accessed on 7 September 2025).

3.5.3. Silicon Dioxide

Silicon dioxide (SiO_2), widely recognized for its dielectric and insulating properties, plays a crucial role in enhancing the performance and stability of solar cells. Bibliometric data (Figure 6) identify China and the United States as dominant contributors to SiO_2 research, with strong collaboration networks in Germany, the Netherlands, and South Korea. Patterns of cooperation highlight the cohesion of European research efforts, anchored in partnerships between Germany and neighboring countries such as France and the Netherlands.

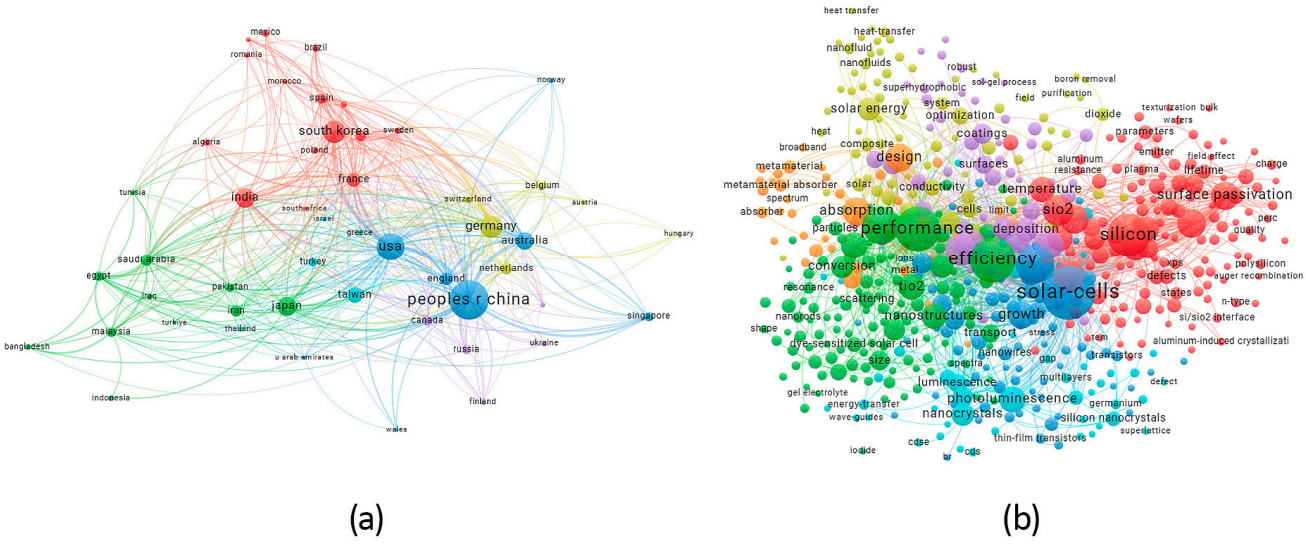

Figure 6. Bibliometric analysis in VOSviewer for SiO_2: (**a**) visualization of international collaboration; (**b**) visualization of keyword clustering. The interactive visualization is available at https://tinyurl.com/23ktygy6, https://tinyurl.com/224hqtyt (accessed on 7 September 2025).

Keyword analysis reveals core themes such as "surface passivation," "coating," and "antireflective layers," reflecting the importance of SiO_2 in minimizing recombination losses and protecting solar cell components. Its applications in thermal management and optical coatings further underscore its versatility. Recent advances include nanoporous SiO_2 structures for light trapping and improved heat dissipation. Sol–gel processing and plasma-enhanced chemical vapor deposition (PECVD) have emerged as prominent methods for producing uniform and durable SiO_2 films.

As an integral part of tandem and thin-film solar cells, SiO_2 continues to serve as a foundational material in photovoltaic research.

3.5.4. Aluminum Oxide

Aluminum oxide (Al_2O_3) has attracted significant attention due to its application in surface passivation, particularly in silicon-based solar cells. Bibliometric data (Figure 7) show a steady increase in research output, with China, the United States, and Germany contributing the largest share globally. The collaboration network highlights strong connections among these countries and other regions, including South Korea, India, and Australia.

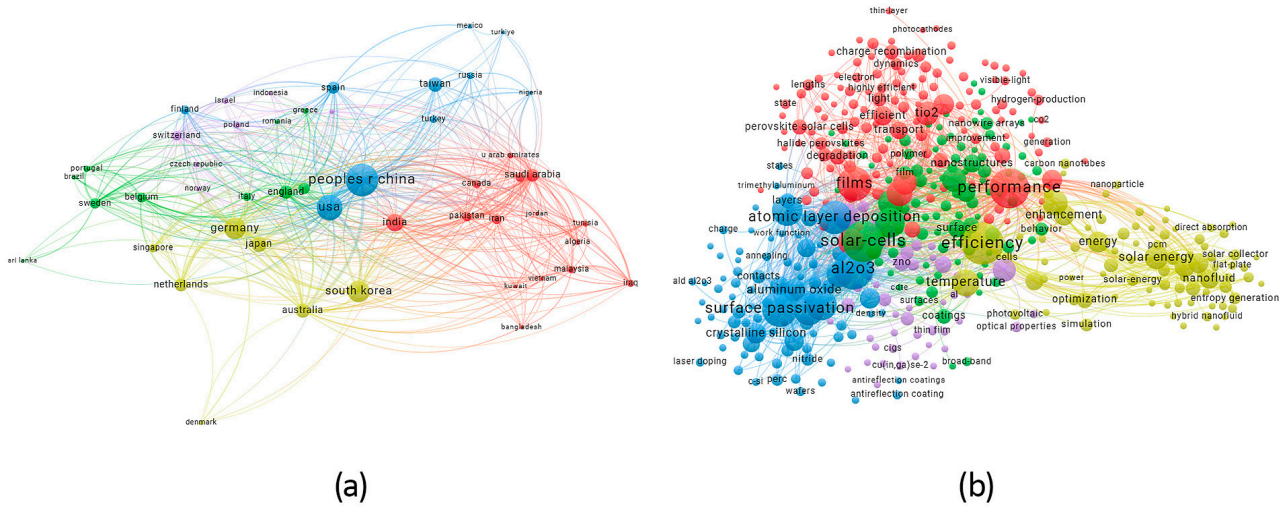

Figure 7. Bibliometric analysis in VOSviewer for Al_2O_3: (**a**) visualization of international collaboration; (**b**) visualization of keyword clustering. The interactive visualization is available at https://tinyurl.com/2dceubry, https://tinyurl.com/22qy7qzs (accessed on 7 September 2025).

Key terms such as "atomic layer deposition," "surface passivation," and "crystalline silicon" dominate the keyword network, illustrating Al_2O_3's role in enhancing the stability and efficiency of photovoltaic systems. ALD methods are frequently used to deposit Al_2O_3 layers with excellent dielectric properties and conformal coverage. Recent developments include the integration of Al_2O_3 into perovskite solar cells and investigations of its potential as a barrier layer under harsh environmental conditions.

3.5.5. Cerium Dioxide

Cerium dioxide (CeO_2) is an emerging material for solar and environmental applications due to its high oxygen storage capacity and redox properties. Bibliometric analysis (Figure 8) reveals that China, India, and the United States are the leading contributors, while collaboration across Europe and the Middle East is expanding. The cooperation network reflects a growing partnership between academic institutions and industrial stakeholders.

The analysis is dominated by keywords such as "nanoparticles," "photocatalysis," and "hydrogen production." CeO_2's catalytic activity makes it ideal for solar-to-hydrogen

conversion and pollutant degradation. Research focuses on the synthesis of CeO_2-based nanocomposites to improve charge transport and catalytic efficiency. Hybrid systems combining CeO_2 with TiO_2 or ZnO have demonstrated enhanced performance in photocatalytic and thermochemical processes. CeO_2's thermal stability and optical properties further expand its potential for solar devices and energy storage systems.

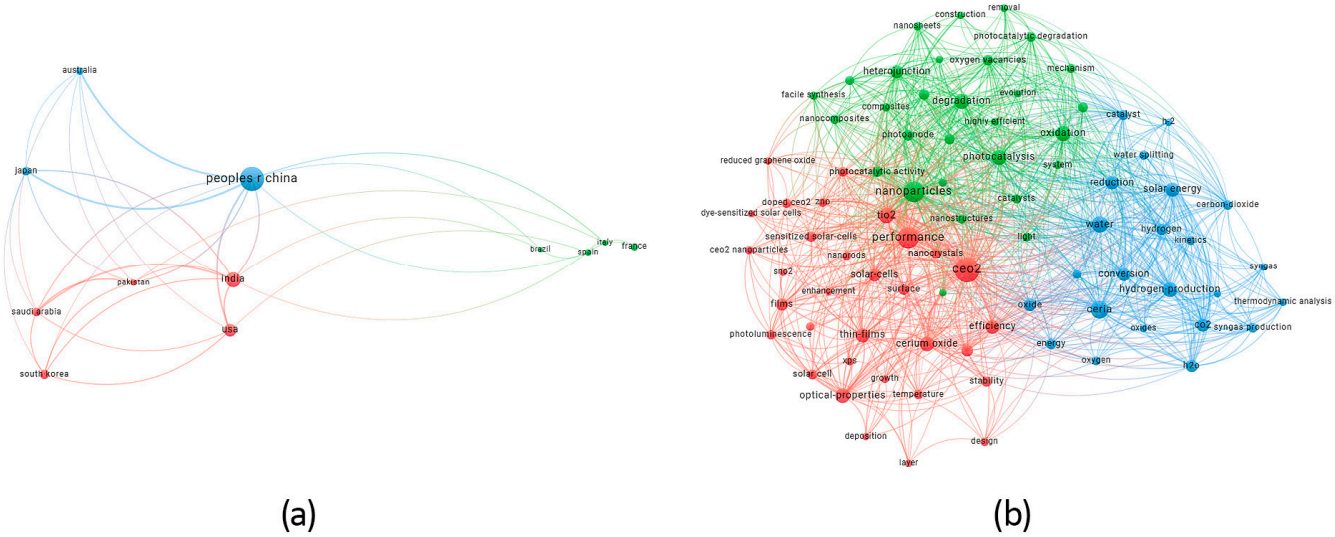

Figure 8. Bibliometric analysis in VOSviewer for CeO_2: (**a**) visualization of international collaboration; (**b**) visualization of keyword clustering. The interactive visualization is available at https://tinyurl.com/25ba3qky, https://tinyurl.com/26wxuydq (accessed on 7 September 2025).

3.5.6. Iron Oxide

Iron oxide (Fe_2O_3), particularly in its hematite form, has been widely studied for applications in photoelectrochemical water splitting and energy storage. Bibliometric data (Figure 9) identify China, the United States, and Germany as leading contributors, with broad international collaboration networks across Europe and Asia. Hematite's abundance and stability make it an attractive material for renewable energy technologies, despite challenges such as its narrow bandgap and low conductivity.

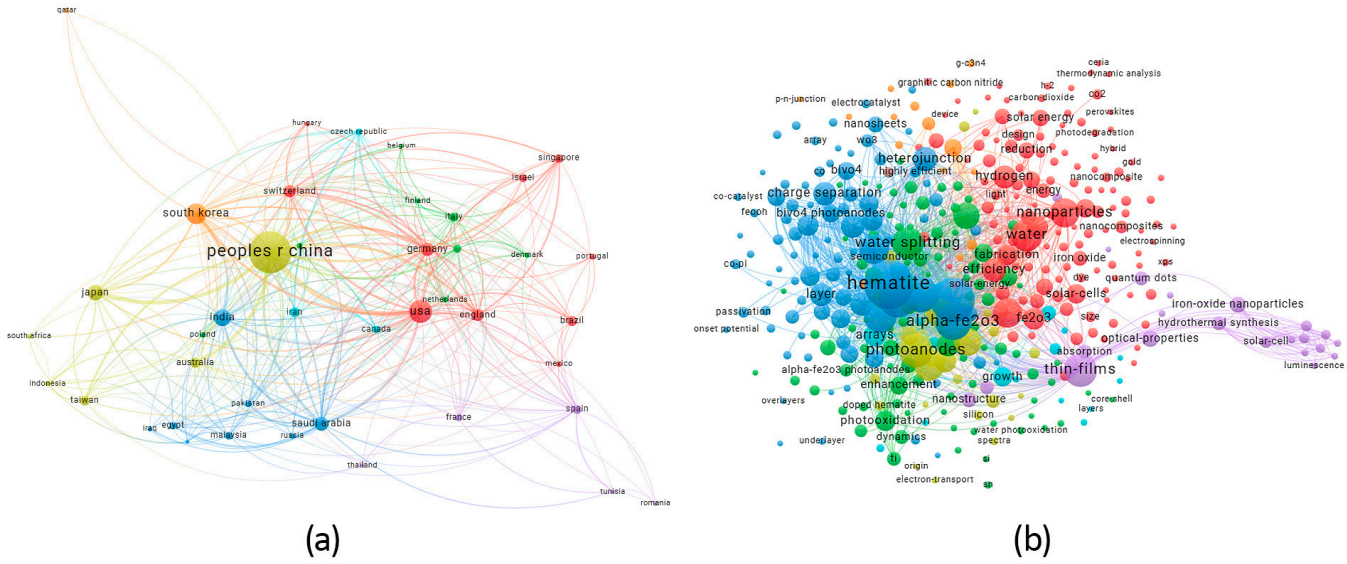

Figure 9. Bibliometric analysis in VOSviewer for Fe_2O_3: (**a**) visualization of international collaboration; (**b**) visualization of keyword clustering. The interactive visualization is available at https://tinyurl.com/26xze96n, https://tinyurl.com/28kszl94 (accessed on 7 September 2025).

Keywords such as "photoanodes," "water splitting," and "hydrogen production" emphasize Fe_2O_3's central role in photoelectrochemical systems. Research focuses on overcoming material limitations through doping, nanostructuring, and the use of co-catalysts. Innovations include heterojunctions and hematite-based tandem systems that improve charge separation and photocurrent efficiency. Additionally, surface passivation strategies and hybrid designs integrating Fe_2O_3 with TiO_2 or WO_3 have demonstrated enhanced performance, solidifying its place at the center of renewable energy research.

3.5.7. Tungsten Trioxide

Research on tungsten trioxide (WO_3) is driven by its applications in photoelectrochemical systems, smart windows, and environmental technologies. Bibliometric analysis (Figure 10) highlights China, the United States, and South Korea as key contributors, with strong collaboration networks in both Europe and Asia. Germany, Japan, and the United Kingdom are also notable players in advancing WO_3-based technologies.

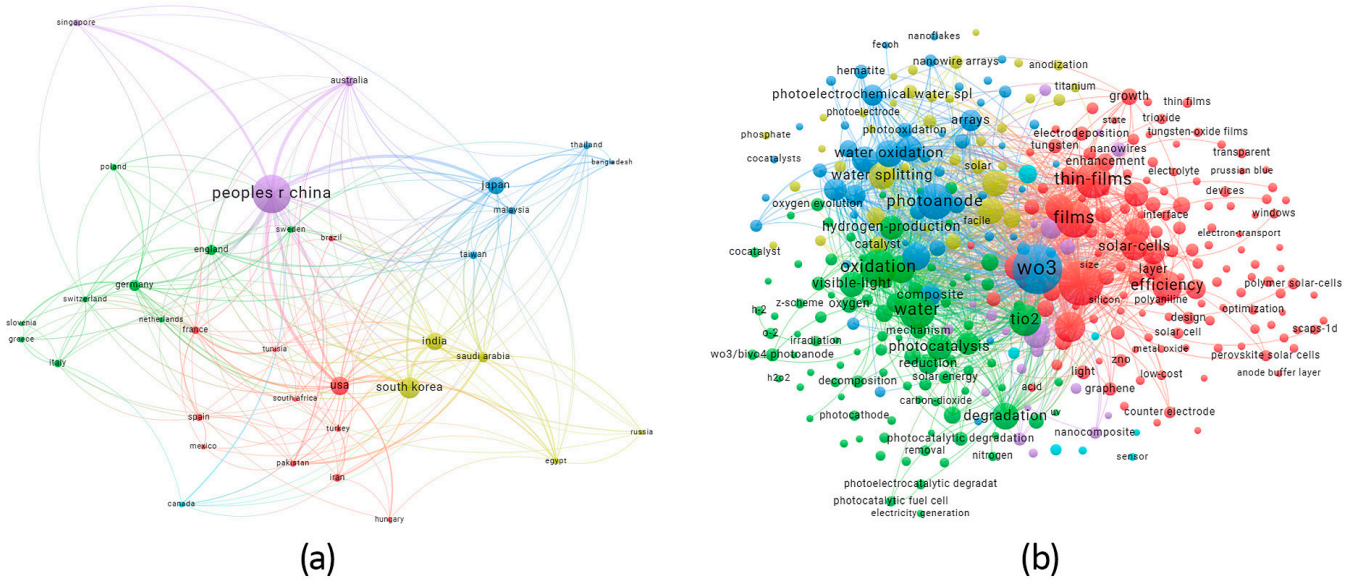

Figure 10. Bibliometric analysis in VOSviewer for WO_3: (**a**) visualization of international collaboration; (**b**) visualization of keyword clustering. The interactive visualization is available at https://tinyurl.com/22smuu6m, https://tinyurl.com/26s56kfs (accessed on 7 September 2025).

The analysis is dominated by keywords such as "photoanodes," "thin films," and "solar cells," reflecting WO_3's versatility in energy and catalytic applications. Studies focus on optimizing WO_3 properties through nanostructuring, doping, and integration with other materials. Recent advances include WO_3-based heterojunctions for improved charge separation and the use of WO_3 thin films in electrochromic devices. Its adaptability and multifunctionality position WO_3 as an important material in addressing global energy and environmental challenges.

4. Comparative Analysis of Oxide Ceramics in Different Types of Solar Cells

The results of the bibliometric analysis demonstrate that binary oxide ceramic materials have diverse applications in solar energy, materials science, and photoelectrochemical technologies. The relevance of each material is defined by its physicochemical properties, its ability to enhance the efficiency of solar devices, and its potential for integration into current and future energy systems.

These oxides serve different roles, such as electron transport layers, hole-blocking layers, surface passivation coatings, or antireflective coatings, across various solar cell technologies, as outlined below. Key properties such as bandgap (electronic structure), optical transparency, chemical stability, and charge transport characteristics make them well suited for specific applications [223–226].

In the following sections, we examine how each oxide is utilized in the main types of solar cells (crystalline silicon solar cells, perovskite solar cells, dye-sensitized solar cells, thin-film chalcogenide cells, quantum dot cells, and emerging organic solar cells) (Figure 11), and explain why their intrinsic properties are advantageous in these systems.

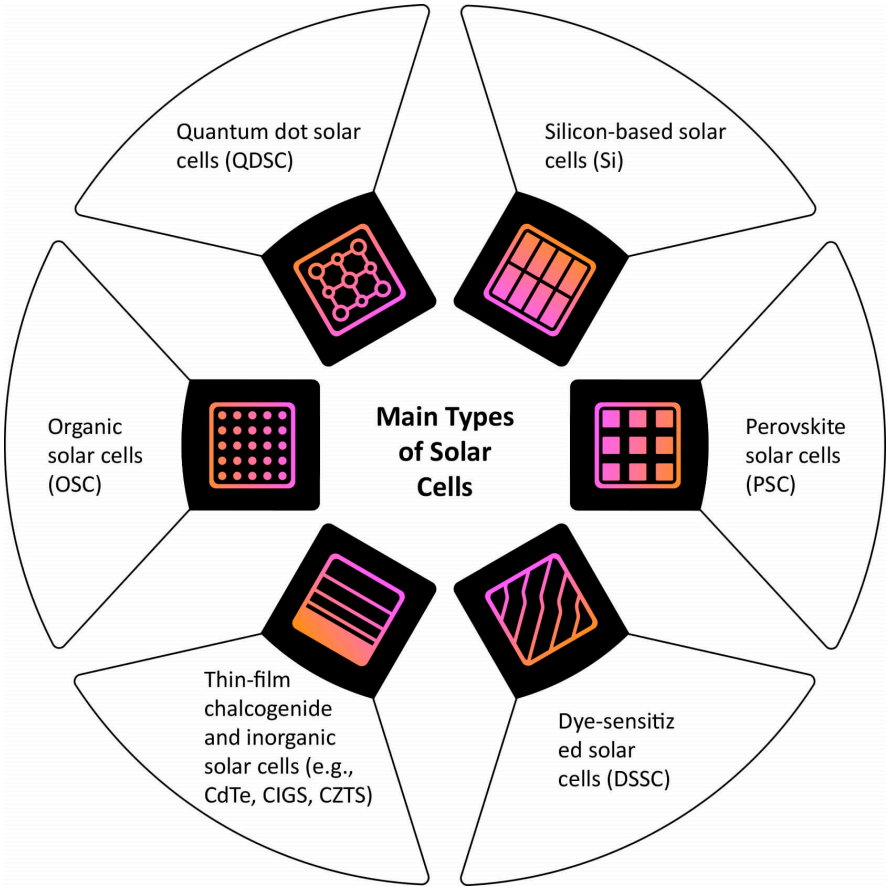

Figure 11. Major types of solar cells.

4.1. Silicon-Based Solar Cells

Silicon-based solar cells, both monocrystalline [226–228] and polycrystalline [229,230], remain the predominant type of solar energy conversion devices due to their high efficiency, long-term stability, and well-established industrial manufacturing processes [231,232]. However, further performance enhancement of silicon photovoltaic devices requires minimizing losses associated with surface recombination of charge carriers and optical losses caused by light reflection [233]. Oxide materials play an important role in addressing these challenges.

One of the most effective and widely used oxide materials for silicon surface passivation is Al_2O_3 [234]. Its application in silicon solar cells is attributed to its excellent passivation properties and high thermal and chemical stability [235]. The deposition of thin Al_2O_3 layers enables the formation of a high-quality interface with silicon [236]. The primary advantage of this material lies in its ability to effectively neutralize surface defects, particularly dangling bonds on silicon atoms [237]. In addition to chemical passivation,

Al_2O_3 exhibits a high density of fixed negative charges [238]. These charges promote field-effect passivation by repelling electrons from the interface, significantly reducing surface recombination on p-type silicon surfaces. As a result, Al_2O_3 layers substantially enhance the open-circuit voltage (V_OC) of silicon solar cells by reducing the defect density at the interface [236,239]. Another important characteristic of Al_2O_3 is its high thermal and chemical stability, which allows it to withstand high-temperature fabrication processes such as contact annealing [240].

Silicon dioxide is one of the most well-established and widely studied materials in silicon photovoltaics [241]. It is mainly used as a surface passivation layer and as a component of antireflective coatings [242]. The main advantage of SiO_2 is its exceptional ability to form a very low density of surface defect states due to the formation of strong and stable bonds with silicon [243]. This is particularly important for ensuring low surface recombination velocities and, consequently, for increasing open-circuit voltage and overall solar cell efficiency. However, unlike Al_2O_3, SiO_2 has a neutral or slightly positive fixed charge, making it less effective for field-effect passivation of p-type silicon surfaces [244–246]. Therefore, SiO_2 is often combined with other oxide or nitride layers in passivated contact structures, such as TOPCon [247,248]. In this architecture, an ultrathin tunneling SiO_2 layer is paired with a highly doped polysilicon layer, enabling efficient charge collection while maintaining excellent surface passivation [249].

In addition to its passivation function, SiO_2 is widely used in optical coatings due to its excellent antireflective properties [250]. Its low refractive index allows it to effectively reduce light losses due to reflection at the surface of silicon cells [251,252]. For example, dual-layer antireflective coatings based on SiO_2 combined with high-index oxides (such as TiO_2) can reduce broadband reflection and significantly enhance solar cell efficiency [253].

Titanium dioxide is well known for its unique properties that make it an attractive material for photovoltaic applications, particularly in silicon solar cells as an antireflective coating or interfacial layer. The choice of TiO_2 for this role is due to its wide bandgap, which ensures high transparency in the visible spectrum [254]. This makes TiO_2 ideal for reducing optical losses at the surface of silicon solar cells [255]. Thanks to its high refractive index, TiO_2 is often used in dual-layer antireflective coatings along with SiO_2 [256]. Such combined layers significantly reduce reflection losses, positively impacting the overall efficiency of silicon photovoltaic devices.

In addition to its optical advantages, TiO_2 can also passivate silicon surfaces, although less effectively than Al_2O_3 or SiO_2 [257]. Thin TiO_2 layers are used to reduce surface recombination of charge carriers, particularly on n-type silicon surfaces or on the rear side of solar cells, contributing to higher open-circuit voltage [258,259]. Due to its chemical stability and low cost, TiO_2 is a favorable material in manufacturing settings [260]. However, its semiconducting nature (n-type) and moderate conductivity must be taken into account, as they may lead to unintended shunting, especially if film thickness or quality is not properly controlled [261]. It is also important to note that achieving optimal performance of TiO_2 layers typically requires thermal treatment, which imposes certain limitations on their use with flexible substrates [262,263].

ZnO is one of the primary candidates for the role of a transparent conducting oxide (TCO) in silicon heterojunctions and thin-film solar cells [264]. Due to its high optical transparency, resulting from its wide bandgap, and its ability to be doped n-type (e.g., with aluminum), ZnO offers excellent properties as a transparent front electrode [265]. Aluminum-doped ZnO (AZO) layers have been successfully used as a lower-cost and more accessible alternative to the more expensive and less abundant indium tin oxide (ITO), demonstrating comparable electrical conductivity and transparency at reduced cost [266].

In addition to its role as a transparent electrode, undoped or lightly doped ZnO can also serve as a buffer layer, minimizing damage during deposition of more conductive oxide layers or facilitating energy level alignment at interfaces [267,268]. However, it is important to note that in conventional silicon solar cells with diffused junctions, the use of ZnO and TiO_2 is less common, as standard technologies typically employ silicon nitride (SiN_x) [269] and screen-printed contact methods [270]. Meanwhile, in advanced heterostructure-based silicon devices, especially thin-film or specialized technologies, these materials demonstrate significant potential for further development.

Despite its many advantages, ZnO has certain limitations. Its surface can react with certain materials or be sensitive to acidic environments, which affects its stability and, consequently, the durability of solar cells [271,272]. Therefore, appropriate processing conditions and additional surface passivation become critically important for the effective use of ZnO in photovoltaic devices.

CeO_2 is a relatively new and experimental material in silicon photovoltaics, but it has already shown potential for improving solar cell performance. Interest in CeO_2 stems from its unique combination of physical and chemical properties, particularly its wide bandgap, which provides high optical transparency across most of the solar spectrum [273]. Owing to these characteristics, CeO_2 can effectively serve as a window layer in silicon heterojunctions [274], similar to materials such as amorphous silicon carbide (a-SiC) [275] or indium tin oxide (ITO) [276] in heterojunction with intrinsic Thin-layer (HIT) cell structures.

Theoretical studies and simulations confirm the promise of CeO_2/n-Si heterojunctions. In such heterostructures, CeO_2 acts not only as a transparent window layer but may also provide additional surface passivation by forming a high-quality interface with silicon [277]. Furthermore, a notable advantage of CeO_2 is its ability to absorb ultraviolet radiation, allowing it to function as a protective layer for silicon structures, mitigating the detrimental effects of UV exposure on the stability of solar cells [278,279]. Despite these promising features, experimental data on the practical use of CeO_2 in commercial devices remain limited. Further research is necessary to optimize deposition methods and improve the film quality of this oxide.

Fe_2O_3 and WO_3 oxides are rarely discussed in the context of silicon solar cell applications, as there is currently no compelling evidence of their effectiveness for passivation or as transparent electrodes in Si-PV.

Thus, each of the oxide materials discussed has unique advantages that make it attractive for specific functions in silicon solar cells (Table 7). Al_2O_3 and SiO_2 are traditionally the most effective materials for silicon passivation, due to their low interface defect densities and chemical inertness when in contact with silicon. Al_2O_3 offers the additional benefit of efficient field-effect passivation due to its negative fixed charge. For optical optimization tasks, coatings based on SiO_2 and TiO_2 remain leading choices due to their ability to reduce light reflection losses. ZnO, meanwhile, is a promising transparent conductive oxide because of its affordability, high electrical conductivity when doped, and suitability for use in thin-film silicon cells. At the same time, both TiO_2 and ZnO may require special technological measures to overcome potential drawbacks related to photocatalytic activity or chemical instability. CeO_2 shows promise as an innovative material for surface passivation and UV protection, though it still requires further investigation.

Table 7. Comparison of key oxide materials used in crystalline silicon (c-Si) solar cells.

Oxide Material	Main Functions in c-Si Cells	Advantages	Disadvantages and Limitations
Al_2O_3	Surface passivation, insulation	Excellent chemical passivation, negative charge (effective field-effect passivation), high thermal stability, chemical inertness	Does not conduct electrons (only a passivation layer), often requires an additional protective layer (e.g., SiN_x)
SiO_2	Surface passivation, antireflection coatings, tunneling layer	Exceptional chemical passivation, very stable interface with Si, excellent antireflection properties (low refractive index, ~1.45)	Lack of effective field-effect passivation (neutral/weakly positive charge), primarily used as a passive layer
TiO_2	Antireflection coatings, surface passivation of n-Si	High transparency, high refractive index (2.0–2.5), good chemical stability, low cost	Unintended shunting due to n-type conductivity, photocatalytic activity under UV, requires precise film quality control
ZnO	Transparent conductive oxide (TCO), buffer layer in heterojunctions	High transparency, high conductivity when doped (e.g., AZO), low cost, application flexibility	Lower chemical stability, sensitive to humidity and acidic environments, requires additional passivation
CeO_2	Experimental window layer, UV filter, potential passivation layer	Good chemical stability, UV absorption capability (Si protection), promising CeO_2/n-Si heterojunction	Low electron mobility, further research needed for deposition optimization

4.2. Perovskite Solar Cells (PSC)

Hybrid organic–inorganic perovskite solar cells (PSCs) have attracted significant scientific attention in recent years due to their high theoretical solar energy conversion efficiency and the potential cost-effectiveness of their production [280]. One of the crucial aspects of improving the efficiency and stability of such devices is the selection of optimal charge-selective layers, among which oxide materials play an essential role [281]. Typically, metal oxide thin films are employed in PSC architectures to facilitate selective charge transport, reduce carrier recombination, and ensure long-term device stability [282].

TiO_2 is one of the most widely used and extensively studied materials for electron transport layers (ETLs) in PSCs [283], particularly in the conventional n–i–p configuration [284]. A key reason for the widespread use of TiO_2 is its favorable band alignment: its conduction band matches well with that of the perovskite [285,286]. This enables efficient electron extraction from the active layer while blocking hole transport in the reverse direction, thereby reducing recombination. With its wide bandgap, TiO_2 remains transparent to most of the solar spectrum, minimizing photon absorption losses [287].

PSC devices using TiO_2-based mesoporous ETLs currently demonstrate power conversion efficiencies exceeding 20%, highlighting the exceptional suitability of this material [288]. TiO_2 is also favored for its high chemical stability under prolonged illumination and its relatively low manufacturing cost. Despite these advantages, TiO_2 also has several drawbacks. Notably, it is well known for its photocatalytic activity under UV light, which can degrade both the perovskite and adjacent organic layers in the device [289]. This creates a need for additional UV-blocking or protective layers, such as ultrathin Al_2O_3 or CeO_2 coatings. Another significant technological limitation is the high-temperature treatment required to

crystallize TiO_2 films and achieve high device performance [290]. This requirement complicates its use on flexible polymer substrates, prompting efforts to develop low-temperature deposition methods, such as solution processing, chemical bath deposition, or atomic layer deposition (ALD). Despite these challenges, TiO_2 remains the benchmark ETL material in PSC design due to its well-established processing protocols, stable and high performance, and ongoing improvements through fine-tuned layer engineering.

Among alternative ETL materials for PSCs, ZnO has drawn considerable attention [291]. Unlike traditional TiO_2, ZnO can be processed at low temperatures, including via solution-based methods [292]. This makes ZnO particularly attractive for use on flexible and polymer substrates, where high-temperature processing (as required for TiO_2) is not feasible [293]. For instance, sol–gel ZnO films can be formed at temperatures below 150 °C, greatly simplifying fabrication and reducing production costs [294].

Additionally, ZnO exhibits superior charge transport speed due to its higher electron mobility compared to TiO_2. This enhances the extraction of electrons from the perovskite active layer, potentially increasing short-circuit current density (J_SC) and fill factor (FF) [295]. The energy level alignment between ZnO and perovskite materials is also favorable—ZnO has a bandgap of approximately 3.3 eV, offering high transparency in the visible spectrum [296]. Combined with its strong electron affinity, ZnO is considered a promising candidate for ETL applications [297].

Despite its many advantages, the application of ZnO in PSCs faces significant challenges, particularly due to its chemical reactivity toward perovskite materials. It has been reported that perovskite layers deposited directly onto ZnO surfaces undergo rapid degradation [293]. This is caused by chemical interactions between the ZnO surface and the organic cations in the perovskite, resulting in the deprotonation of methylammonium cations and accelerated degradation of the perovskite layer. These processes substantially reduce the stability and longevity of devices with ZnO ETLs, despite their initially high performance.

To overcome this issue, researchers are actively developing various surface modification strategies for ZnO, including the introduction of interfacial protective layers. For example, the use of bilayer structures in which ZnO is coated with a compact TiO_2 layer has proven effective [298], as have coatings based on self-assembled monolayers of organic molecules or fullerene derivatives [299]. These solutions significantly enhance device stability while maintaining high initial efficiency in PSCs employing ZnO-based ETLs. Nanostructured forms of ZnO (such as nanorods or nanoparticles) further improve electron collection by increasing the effective interfacial area and providing direct pathways for charge transport [300].

Among other oxide materials that are gaining increasing prominence in perovskite photovoltaics, tin oxide (SnO_2) has emerged as especially important. Although SnO_2 was not part of the original list of analyzed materials, its role as an efficient ETL in PSCs warrants special attention due to its excellent performance and widespread use in modern device architectures [301]. Thanks to its combination of high stability, wide bandgap (~3.6 eV), and suitability for low-temperature processing, SnO_2 has emerged as a leading ETL candidate alongside TiO_2 and ZnO. Studies have shown that SnO_2 provides more stable performance than TiO_2 and demonstrates lower hysteresis behavior, which is crucial for the long-term operation of PSCs [302–304].

Aluminum oxide (Al_2O_3), in turn, occupies a unique niche among materials used in PSCs due to its insulating and passivating properties. In the early stages of solid-state PSC development, it was discovered that replacing the conductive mesoporous TiO_2 scaffold with insulating Al_2O_3 did not lead to a complete drop in performance; in fact, devices with efficiencies of about 10–11% were still achieved [305]. This was possible because

perovskite was able to infiltrate the mesoporous Al_2O_3 structure and directly transport electrons to the contact, eliminating the need for a conductive scaffold. Later research showed that mesoporous frameworks made of Al_2O_3 or other inert oxides could even increase the open-circuit voltage (V_OC) compared to TiO_2-based devices, due to reduced surface electron recombination [306].

Al_2O_3 is characterized by high chemical inertness toward perovskites, preventing degradation of the active layer and significantly improving device stability. This property is effectively utilized in PSC structures with carbon electrodes, where a triple mesoporous structure is employed: a bottom TiO_2 layer for efficient electron contact, a middle Al_2O_3 layer as an inert insulating spacer, and a top carbon layer serving as the electrode [307]. This configuration allows Al_2O_3 to efficiently isolate the perovskite layer from the carbon contact, reducing recombination and improving device longevity.

Another promising ETL material in PSCs under recent investigation is cerium oxide (CeO_2). Its high conduction band level aligns well with the energy levels of typical perovskite materials, enabling efficient electron extraction from the active layer. In addition, CeO_2 offers several unique advantages, particularly its ability to absorb ultraviolet (UV) radiation [308]. This property allows cerium oxide to serve as a protective UV-blocking layer, preventing degradation of organic–inorganic perovskites under UV exposure. As a result, the incorporation of CeO_2 layers significantly enhances the long-term stability of PSCs under continuous illumination [309].

An additional advantage of CeO_2 is the presence of oxygen vacancies, which not only facilitate electron transport but also enhance its chemical stability against oxygen and moisture. However, this material is still under active laboratory investigation. One of the main barriers to its widespread adoption is the difficulty of producing high-quality CeO_2 thin films without high-temperature annealing. Recent studies report that optimizing deposition processes, particularly solution-based CeO_2 film formation without post-deposition thermal treatment, can lead to improved device efficiency, demonstrating this material's significant potential [310]. Nevertheless, CeO_2 remains less technologically mature than conventional oxides such as TiO_2 and SnO_2 and requires further research before broad commercial deployment.

Another unconventional material gaining attention in perovskite photovoltaics is iron(III) oxide, commonly known as hematite (α-Fe_2O_3). Its appeal lies in its abundance, non-toxicity, and exceptional stability under ultraviolet and visible light exposure [311]. Hematite's availability and low cost make it a promising alternative for use as a compact ETL in PSCs [312]. Researchers have achieved power conversion efficiencies of around 13% in devices with compact Fe_2O_3 layers through precise control over the fabrication process, notably by forming dense, defect-free films using solution crystallization techniques [313].

At the same time, hematite suffers from several significant drawbacks that limit its widespread use. Its main limitation is low electron mobility and a high density of trap states, which lead to severe carrier recombination [314]. Additionally, due to its relatively narrow bandgap, hematite absorbs part of the visible spectrum, reducing the overall efficiency of devices where the ETL should be transparent [315]. Currently, the use of hematite remains confined mainly to laboratory settings, where ongoing efforts are focused on improving its electronic properties through doping and nanostructuring to make it more competitive with traditional oxides such as TiO_2 or SnO_2.

WO_3 is most commonly used as a hole transport layer (HTL), although some studies also demonstrate its applicability as an ETL in specific configurations [316]. This oxide has a wide bandgap, making it transparent across most of the solar spectrum [317]. However, the most valuable property of WO_3 is its tunable work function, which varies depending on stoichiometry. In its sub-stoichiometric form (WO_x), it has a high work function,

making it ideal for use as an inorganic HTL, especially in inverted (p–i–n) perovskite architectures [318]. Besides serving as an HTL, WO_3 is also actively investigated as an ETL material; for example, mesoporous WO_3 is used in PSCs as an additional layer to enhance electron transport [319].

Al_2O_3 and SiO_2 have limited applications in PSCs, mainly serving auxiliary functions, insulating and passivating (Al_2O_3) or anti-reflective (SiO_2), and rarely acting as primary charge-selective layers. Their inclusion in device architecture is often aimed at improving stability and optical performance. An inert mesoporous scaffold or ultrathin Al_2O_3 spacer helps passivate interfacial defect states at the perovskite/ETL junction, reducing recombination rates and thereby increasing V_OC. However, as Al_2O_3 is non-conductive, its thickness must be strictly controlled to avoid adding series resistance. SiO_2, on the other hand, is primarily used as an optical or insulating interlayer: it reduces light reflection, stabilizes the active layer morphology, and acts as a barrier to interfacial ion diffusion. Both oxides function indirectly by improving the durability and electrical performance of the cell but are not involved in selective charge transport, and therefore are excluded from the comparative table of transport oxides.

In summary, hole transport in PSCs is generally facilitated by p-type oxides with high work functions. WO_3, NiO, and MoO_3 (the latter two not included in this analysis) are typical representatives of such materials. The advantage of using oxide materials over organic HTLs lies in their significantly higher resistance to ultraviolet light, heat, and moisture, thereby greatly extending device lifetime. Notably, CeO_2 and WO_3 can also absorb UV light, protecting the perovskite layer from degradation.

However, some oxides such as TiO_2 and ZnO exhibit photocatalytic activity, which, under UV exposure, can lead to degradation of the perovskite and adjacent organic layers. To address this, specific approaches are employed—either by adding protective interlayers (such as CeO_2) or incorporating luminescent additives that convert UV radiation into visible light.

Therefore, the correct selection and combination of oxide materials, considering their specific properties, enables synergistic effects that enhance both efficiency and stability of perovskite solar cells. The key characteristics and application roles of these oxides in the context of PSCs are summarized in the comparative table below (Table 8).

Table 8. Comparison of key characteristics of oxide materials used in perovskite solar cells.

Oxide Material	Layer Type	Main Advantages and Functions	Drawbacks and Technological Features
TiO_2	ETL	High transparency; favorable band alignment with perovskite; thermal stability; efficiency > 20%	Photocatalytic activity (UV-induced perovskite degradation); requires high-temperature processing (>450 °C)
ZnO	ETL	High electron mobility; low-temperature deposition; compatible with solution-based methods	Chemical instability in contact with MA^+-based perovskites; requires interfacial protection or surface modification
CeO_2	ETL	UV absorption; chemical inertness; interface passivation; potential for enhanced stability	Lower electron mobility; difficulty in forming high-quality films without thermal treatment

Table 8. *Cont.*

Oxide Material	Layer Type	Main Advantages and Functions	Drawbacks and Technological Features
Fe_2O_3	ETL, also studied as experimental absorber	Low cost; environmental friendliness; high resistance to UV and moisture	Low electron mobility; high charge recombination; partial visible light absorption; lower efficiency (~13%)
WO_3	HTL/ETL	High work function (HTL); resistance to moisture and temperature; solution-processable; UV protection	Suboptimal band alignment when used as ETL; property variation depending on stoichiometry level

4.3. Dye-Sensitized Solar Cells (DSSC)

In dye-sensitized solar cells, the mesoporous oxide layer acts as a photoanode: it supports light-sensitive dyes and transports electrons to the transparent electrode [320,321]. The most common material in this role is TiO_2 [322]. Its popularity is due to its wide bandgap, chemical inertness, non-toxicity, low cost, and ability to form highly porous nanostructures that enable efficient light harvesting [323]. The main drawback of TiO_2 is the slow electron transport and the risk of recombination with oxidized electrolyte species; however, this can be mitigated through surface modification, core–shell structures, and other engineering strategies [324–326].

An alternative is ZnO, which has a similar bandgap and favorable energy alignment, but features higher electron mobility [327]. Due to the ease of forming nanostructures such as nanorods, ZnO provides direct pathways for electrons and can reduce recombination [328,329]. Moreover, ZnO can be deposited at low temperatures, making it suitable for flexible photovoltaic devices [330,331]. However, common dyes, especially those based on ruthenium, may interact with its surface, leading to dissolution or defect formation, thus limiting efficiency [332,333]. This issue can be addressed via interface engineering and the use of alternative dyes [334,335].

Other semiconductor oxides, such as WO_3, SnO_2, and Fe_2O_3, are also under investigation as photoanodes [336–338]. WO_3, when combined with TiO_2, can enhance UV sensitivity [339]. SnO_2 is notable for its high electron mobility and its ability to increase open-circuit voltage due to a deeper conduction band. However, it requires blocking layers to counteract recombination with the electrolyte caused by its high mobility and deep conduction band [340]. Hematite absorbs visible light, but suffers from an extremely short hole diffusion length and high recombination, which limits its industrial applicability in DSSCs [341].

Inert oxides such as Al_2O_3 and SiO_2, although not conductive, play important auxiliary roles. Ultrathin Al_2O_3 layers deposited on TiO_2 surfaces can passivate defect states and reduce recombination, thereby increasing the open-circuit voltage [342]. SiO_2, meanwhile, is used as a scattering additive in the anode or as a barrier layer that prolongs the photon path and improves light absorption [343].

Table 9 summarizes oxide materials that play key roles in the functional layers of DSSCs. CeO_2 currently has limited or auxiliary applications and requires further experimental verification for widespread use.

Table 9. Characteristics of Oxide Materials for DSSC.

Oxide Material	Role in DSSC	Advantages	Limitations
TiO_2	Photoanode	Ideal energy alignment with dyes; high chemical stability; large surface area for dye adsorption	Slow electron transport; recombination with oxidized electrolyte species
ZnO	Photoanode	High electron mobility; easy nanostructuring (nanorods, nanoparticles); low-temperature deposition	Chemical instability in the presence of some dyes (especially acidic); risk of defect formation
WO_3	Photoanode/Additive	UV absorption; chemical stability; electron conductivity	Less favorable energy alignment; high recombination; low efficiency
Fe_2O_3 (Hematite)	Experimental Photoanode	Visible light absorption; non-toxicity; UV stability	Very short hole diffusion length (~2–4 nm); intense recombination; low photovoltage
Al_2O_3	Passivating Barrier	Defect passivation; reduced recombination; increased V_OC	Insulator—does not conduct electrons; requires precise thickness control
SiO_2	Optical Additive/Barrier	Enhanced light scattering; structural stabilization; chemical inertness	Non-conductive; indirect effect via morphology and optics

4.4. Thin-Film Chalcogenide and Inorganic Solar Cells

In thin-film solar cells based on CIGS, CdTe, CZTS, and amorphous silicon (a-Si:H), oxide ceramics play a key role as transparent conductive oxides (TCOs), buffer layers, or passivating dielectrics [344–346]. The most common configuration is a bilayer TCO composed of an inner ZnO layer and an outer conductive layer providing lateral conductivity [347]. Thanks to its wide band gap, good transparency, and doping ability, AZO is widely used not only in CIGS and CZTS, but also in CdTe and silicon-based cells [348–350].

TiO_2 is being investigated as an alternative to CdS in CIGS and CdTe for cadmium-free structures [351,352]. TiO_2 is also used to passivate grain boundaries in CIGS [353]. SnO_2 serves as a standard transparent electrode in CdTe and some CIGS cells. Insulating oxides such as Al_2O_3 and SiO_2 are applied for surface passivation, grain boundary recombination suppression, and the creation of dielectric interlayers [354]. High-work-function oxides like WO_3 are placed between the absorber (e.g., CdTe or CIGS) and the metal contact to improve hole extraction [355]. These materials provide better energy level alignment, reduce contact losses, and can act as recombination barriers.

Table 10 summarizes the roles and technological characteristics of oxide materials in thin-film chalcogenide and inorganic solar cells. It includes only those oxides that have demonstrated practical effectiveness as transparent contacts, buffer, or passivating layers for CIGS, CdTe, CZTS, and a-Si:H. Experimentally promising but still less commonly used oxides, such as CeO_2 (due to insufficient conductivity and less mature passivation control) and Fe_2O_3 (high optical absorption and low electron mobility limiting its use as TCO or buffer), remain primarily at the lab stage and require further validation for widespread implementation in thin-film PV technologies.

Table 10. Role of Oxides in Thin-Film Chalcogenide and Inorganic Solar Cells.

Oxide Material	Role in the Device	Advantages	Limitations or Application Conditions
ZnO	Transparent contact, buffer, textured layer	High transparency, good conductivity when doped, texturing capability	May require protection during deposition, vulnerable to acids
TiO_2	Buffer layer, grain boundary passivation	Cd-free replacement for CdS, visible-range transparency, thermal stability	Requires interface control due to risk of recombination
Al_2O_3	Passivating layer, dielectric barrier	Reduces recombination, improves V_OC, used in nanopatterned structures	Insulator—does not conduct charge, precise thickness critical
SiO_2	Dielectric layer, diffusion barrier	Optical transparency, thermal stability, interlayer diffusion barrier	Does not contribute to charge transport, auxiliary function
WO_3	Back contact buffer (CdTe, CIGS)	High work function, transparency, improved hole extraction	Requires thin deposition (a few nm), critical energy level alignment
CeO_2	Experimental buffer/window layer between absorber; surface passivation; UV barrier	Wide band gap, high transparency; chemical inertness; Cd-free; UV absorption and surface recombination reduction	Low electron mobility increases series resistance; electrical properties sensitive to oxygen vacancies; requires optimized deposition methods (ALD, solution processes) and post-treatment; efficiency demonstrated only on lab-scale samples

4.5. Organic and Emerging Types of Solar Cells

In emerging photovoltaic technologies, including organic solar cells (OSCs) and quantum dot (QD) solar cells, metal oxides are used as charge-selective transport layers due to their stability, suitable energy alignment, and transparency [356,357].

ZnO and TiO_2 are widely used as electron transport layers (ETLs) in inverted OSC architectures [358,359]. High-work-function oxides, such as WO_3, are also commonly used in OSCs [360,361]. These materials efficiently extract holes and provide favorable alignment with the valence band of donor polymers. When oxides like Fe_2O_3 or WO_3 are used as absorbers, tandem or multilayer structures can be developed to broaden the spectral response. The main advantages of such systems include stability, low cost, and the absence of volatile or toxic components, making them promising for use in harsh environments such as space or in solar fuel production.

Table 11 summarizes the properties of oxide layers that have already found practical application in organic, quantum dot, and "all-oxide" solar cells. Notably, Al_2O_3, SiO_2, and CeO_2 mostly serve auxiliary functions, dielectric encapsulation, passivation, or UV-barrier, and have only a limited effect on charge-selective transport in these architectures.

Table 11. Oxide Materials in Organic, Quantum Dot, and "All-Oxide" Solar Cells: Functions, Advantages, and Technological Limitations.

Oxide Material	Role in the Device	Advantages	Limitations or Application Conditions
ZnO	ETL (OSC, QD)	High transparency; solution-processable; high electron mobility; chemical stability	Generates reactive radicals under UV; requires surface modification or encapsulation
TiO_2	ETL (OSC, QD); contact in Cu_2O cells	Wide band gap; stability; solution-processable	Low electron mobility; interface quality is critical
WO_3	HTL (OSC); rear contact (QD)	High work function; transparency; thermal stability; UV protection	Lower work function than MoO_3; sensitive to stoichiometry and thickness
Fe_2O_3	Absorber (experimental)	Low cost; non-toxic; stable	Requires cascade/tandem architecture; limited spectral absorption; low carrier mobility; low efficiency
CeO_2	ETL or protective interlayer/UV filter in all-oxide cells	UV absorption prevents degradation of the active layer; chemically inert; compatible with low-temperature deposition	Low electron mobility; properties sensitive to oxygen vacancies; large-scale solution processing not yet optimized
Al_2O_3	Inert encapsulation, passivating/optical spacer	Reduces surface recombination; stabilizes morphology; chemically/thermally inert; may enhance V_OC	Does not conduct charge; thickness must be <3 nm to avoid adding series resistance
SiO_2	Anti-reflective front (AR) coating or dielectric stabilizing barrier	Low refractive index (~1.45) reduces reflection; barrier to oxygen/moisture diffusion; low-T compatible	Not charge-selective; effect is purely optical/encapsulation-related, requiring careful integration with ETL/HTL

4.6. Application Matrix of Oxide Ceramics in Solar Cells: Analytical Summary

The universality or specialization of oxide materials in solar cells is determined not only by their electronic structure and stability, but also by how they function in the devices—as active charge transport layers or as auxiliary passivating or optical components. Table 12 and Figure 12 summarize the key roles of each oxide in various photovoltaic architectures. This application matrix allows for simultaneous evaluation of the maturity, functional flexibility, and technological relevance of the materials, visually reflecting which ones are already implemented, have limited use, or are currently under active investigation.

TiO_2 and ZnO have proven to be versatile solutions for most architectures (PSC, DSSC, OSC, QD), as evidenced by their leading citation counts in the literature and frequent appearance among keywords such as electron transport layer, mesoporous, dye-sensitized, and UV stability. Their flexibility is enabled by a combination of wide bandgap, high transparency, various nanostructuring options, and stable energetic alignment with active layers.

Table 12. Applications of Key Binary Oxides in Different Types of Solar Cells.

Oxide Material	c-Si	PSC	DSSC	Thin-Film (CIGS, CdTe, CZTS, a-Si:H)	OSC, QD, All-Oxide
TiO_2	Passivation, anti-reflection	ETL, barrier, mesoporous scaffold	Photoanode (ETL)	Buffer, grain boundary passivation	ETL, contact with Cu_2O
ZnO	TCO, buffer	ETL	Photoanode (ETL)	TCO, buffer, textured layer	ETL, all-oxide component
Al_2O_3	Passivation, dielectric	Passivation, inert insulator	Barrier, passivation of TiO_2	Passivation, dielectric barrier	Optical spacer, inert interlayer
SiO_2	Anti-reflective, tunnel layer	Anti-reflective, optical layer	Optical additive, light scatterer	Diffusion barrier, optical stabilization	Dielectric, optical substrate
CeO_2	UV protection, passivation	ETL, UV filter, stabilization	–	Potential passivation, buffer (experimental)	ETL, absorber, protective layer
Fe_2O_3	–	Absorber (experimental)	Photoanode (low efficiency)	–	Absorber in all-oxide architectures
WO_3	–	HTL, ETL (investigated)	Photoanode/additive	Rear buffer contact (HTL)	HTL, absorber, rear contact

ETL—electron transport layer; HTL—hole transport layer; TCO—transparent conductive oxide; Barrier/buffer—for energetic or chemical alignment; Passivation—reduction in recombination; Absorber—light-absorbing layer.

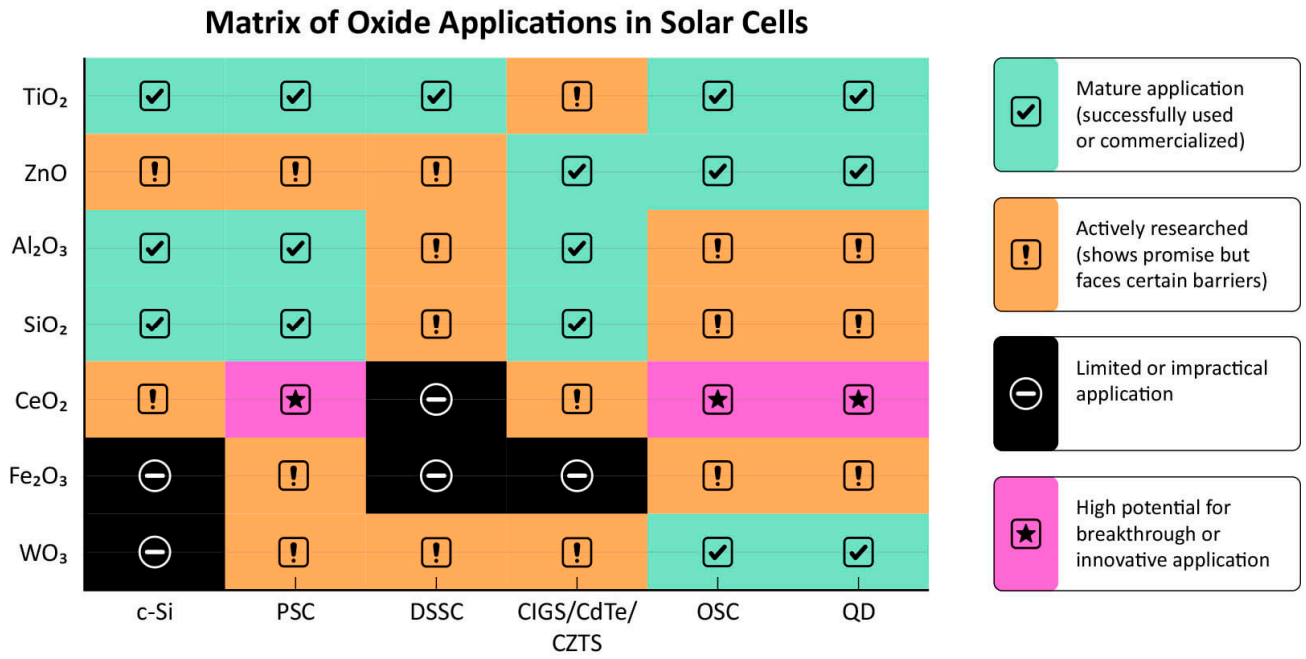

Figure 12. Matrix of Oxide Ceramic Applications in Solar Cells.

In contrast, SiO_2 and Al_2O_3 serve clearly defined specialized roles—passivation, dielectric separation, and optical stabilization. This is reflected in a narrower range of keywords (e.g., surface passivation, antireflective coating) and in their lower, though stable, citation

levels. While they are not charge carriers, they are essential for the stability and longevity of devices.

Oxides with potential (CeO_2, Fe_2O_3, WO_3) appear in the literature as emerging materials but have not yet achieved widespread implementation. Our bibliometric analysis shows that publications on CeO_2 are often accompanied by tags such as UV filter, stability enhancement, and interface engineering, whereas Fe_2O_3 is typically associated with PEC, low mobility, and visible light absorber. Nevertheless, major barriers remain: unfavorable band alignment, low charge mobility, and complex interfacial chemistry.

Therefore, in the next generation of architectures (such as all-oxide, tandem, and inverted designs), combined structures look promising—where the drawbacks of one material are compensated by the advantages of another (e.g., TiO_2@CeO_2 or ZnO/WO_3). This aligns with our bibliometric findings on keyword co-occurrence, where pairings such as ZnO + buffer layer, TiO_2 + passivation, and WO_3 + HTL are appearing with increasing frequency.

The publication peak we identified in the 2010s aligns with the strengthening of global and regional policies in the field of decarbonization and the deployment of renewable energy. At the global level, the Paris Agreement (2015) set the framework by institutionalizing long-term climate goals and the regular review of ambition [362]. At the EU level, momentum was reinforced by Directive (EU) 2018/2001 (RED II), which established binding targets and harmonized support rules for renewable energy [363]. National mechanisms also played a key role: in China, the introduction of a nationwide feed-in tariff for solar energy in 2011 sharply improved the investment attractiveness of PV projects [364], while in the United States, the ARRA program (2009) provided substantial investments in "clean" energy, grid infrastructure, and R&D [365,366]. The combined effect of these policies was reflected in empirical series: according to IEA and IEA-PVPS data, in the 2010s the installed capacity and generation of solar energy grew at explosive rates, correlating with our bibliometric peak in studies on ETL materials, passivation, and optical stacks (TiO_2, ZnO, Al_2O_3, SiO_2), as well as with a parallel rise of interest in "emerging" oxides (WO_3, Fe_2O_3, CeO_2) [367,368].

In conclusion, a comparative analysis of physical properties, device functions, and the publication landscape indicates that oxide ceramics are no longer auxiliary components but are emerging as a full-fledged platform for next-generation photovoltaic technologies. Their flexibility, chemical stability, and multifunctionality allow for material adaptation to specific architectures, opening pathways for interface engineering, integration into hybrid structures, and the development of stable, environmentally friendly solar cells.

4.7. Future Directions

The further development of oxide ceramics for solar energy primarily hinges on refined engineering of well-established materials, particularly TiO_2 and ZnO. Despite their high efficiency in perovskite, organic, and quantum dot solar cells, the stability of these oxides remains limited by surface chemical reactivity: ZnO rapidly degrades in humid or acidic environments, while mesoporous TiO_2 requires careful control of porosity and crystal phase. One of the most promising strategies is the deposition of ultrathin buffer layers of Al_2O_3, SiO_2, or CeO_2, as has been implemented for other architectures [369–371].

Beyond binary systems, the insights gained from our systematic review can also inspire the rational design of ternary and multicomponent oxide ceramics with more complex crystal structures. In particular, ZnO–Al_2O_3 spinels exhibit composition-dependent tunability of electronic and mechanical properties, making them attractive as transport or buffer layers [372]. Similarly, Al_2O_3–SiO_2 mullite phases show favorable combinations of stability and electronic structure, which could be harnessed for dielectric or passivation

functions in solar devices [373]. Although these systems are more challenging to model and synthesize, their structural flexibility offers greater opportunities for fine-tuning interfacial and optoelectronic properties, thereby broadening the design space for next-generation solar cell architectures.

For the next-generation group of oxides (CeO_2, Fe_2O_3, and WO_3), the main challenge is transitioning from laboratory prototypes to stable devices. CeO_2 requires optimization of its crystal phase and integration with conventional ETLs; hematite can serve as an absorber or photoelectrode only if charge transport is enhanced through doping or heterostructure design; WO_3 demonstrates excellent reliability, but its properties are highly sensitive to stoichiometry, requiring precise control during deposition.

A promising direction is the concept of fully oxide-based architectures, where the same class of materials serves as both the absorbing layer and selective contacts. Combinations such as ZnO/Cu_2O, TiO_2/NiO, or WO_3/Fe_2O_3 have demonstrated the feasibility of environmentally friendly and thermally stable 'all-oxide' solar cells, which hold promise for competing with conventional technologies in certain applications [374,375]. An additional boost is expected from the rapid advancement of SnO_2, which, alongside TiO_2 and ZnO, is becoming a versatile electron transport layer in perovskite solar cells.

This trajectory can be accelerated by integrating bibliometric mapping with materials science analytics: systematic analysis of keywords and co-authorship networks can help identify overlooked oxides and optimally allocate research efforts across hybrid architectures, interfacial chemistry, and long-term stability. Taken together, these approaches constitute a roadmap for the development of efficient, durable, and environmentally sustainable next-generation photovoltaic technologies.

Beyond device performance, the sustainability profile of oxide ceramics will increasingly shape their research prioritization and industrial uptake. Al_2O_3 offers excellent passivation but is associated with energy-intensive alumina production and the generation of bauxite residue ("red mud"), calling for low-temperature deposition routes and waste-minimization strategies at the precursor stage [376]. ZnO is widely used as an ETL/TCO; however, it is classified by ECHA as Aquatic Acute/Chronic 1 (H400/H410), which underscores the need for responsible use, effluent treatment, and end-of-life (EOL) handling of nanostructured ZnO [377]. WO_3 depends on tungsten, listed among the EU critical/strategic raw materials, highlighting supply risk exposure and the importance of precursor efficiency, recycling of sputtering targets, and supplier diversification. CeO_2 relies on light rare-earth element (cerium); rare earths feature on EU criticality lists due to geographical concentration of deposits, making substitution, loading minimization, and circular-economy approaches pertinent [378,379]. In contrast, Fe_2O_3 and SiO_2 generally exhibit benign toxicological profiles and broad availability; nonetheless, high-temperature synthesis for dense or textured films raises embodied energy concerns that LCA should capture [380].

Looking ahead, these sustainability considerations should not be seen merely as constraints, but rather as opportunities to reshape material strategies in photovoltaics. The move toward low-energy and low-temperature synthesis routes—from aerosol deposition to advanced atomic-layer techniques—offers not only lower environmental footprints but also novel microstructural control. Pursuing material thrift, such as ultrathin functional layers and judicious use of dopants, can reduce costs while opening avenues for flexible or tandem designs. The vision of design-for-disassembly—enabling oxide layers to be cleanly separated and recovered at end of life—points to a future where solar modules can become part of a circular economy rather than a waste burden. Addressing the supply risks of tungsten and rare earths by diversifying sources or substituting scarce elements may also stimulate innovation in alloying and doping strategies. Finally, the integration

of prospective life-cycle assessments (LCA) and criticality analyses alongside traditional performance metrics promises to transform how new oxides are evaluated, ensuring that breakthroughs in efficiency go hand in hand with environmental responsibility.

Taken together, these directions outline a pathway where oxide ceramics evolve from being reliable functional layers to becoming the backbone of sustainable, recyclable, and globally resilient photovoltaic technologies.

5. Conclusions

This study presents a comprehensive bibliometric and comparative analysis of binary oxide materials used in modern solar cells. By combining quantitative analytics (based on Web of Science data), in-depth exploration of physicochemical properties, and role-based analysis of oxides across various device architectures, we not only synthesized current knowledge but also identified emerging directions for future research.

The bibliometric findings indicate the dominance of TiO_2 and ZnO in the scientific discourse, which correlates with their versatility as charge transport layers in multiple solar cell types. At the same time, oxides with more specialized functions (such as Al_2O_3 and SiO_2) show consistent citation patterns in niche areas, reaffirming their key role in enhancing device stability and surface passivation. Trends in keyword usage and co-authorship networks reveal the formation of knowledge clusters around specific oxide functions, including charge transport, stabilization, nanostructuring, and interface engineering.

Functional analysis revealed that the effectiveness of an oxide is determined not only by its bandgap or electron affinity but also by its adaptability to the specific operating requirements of the device. In particular, CeO_2, Fe_2O_3, and WO_3 hold considerable potential but still face challenges related to interfacial compatibility, charge transport, and phase stability.

The proposed classification of materials across different solar cell architectures provides a holistic understanding of the role of oxide ceramics in modern photovoltaics. The identified future directions point toward the development of stable, efficient, and environmentally safe next-generation photovoltaic technologies, especially within the scope of all-oxide concepts and hybrid device architectures.

Altogether, this comparative review demonstrates that binary oxides are not merely auxiliary materials but are evolving into a platform for next-generation photovoltaics. The analysis highlights that their future potential lies in interface engineering, stability enhancement, and environmentally safe device design. In particular, TiO_2 and ZnO will continue to dominate through nanostructuring and heterojunction engineering, while Al_2O_3 and SiO_2 remain indispensable for passivation and optical control. CeO_2, Fe_2O_3, and WO_3, though still emerging, offer promising opportunities in UV protection, photoelectrochemical hydrogen generation, and multifunctional device integration. Beyond binary systems, the bibliometric evidence and functional mapping presented here also point to ternary and multicomponent oxides (e.g., spinels, mullites) as logical extensions where compositional tunability could unlock new device concepts. By linking bibliometric trends to functional performance gaps, this study provides a roadmap that may inspire targeted innovations and guide future experimental and theoretical research in oxide-based solar energy technologies.

Author Contributions: Conceptualization, Y.S., S.N. and A.I.P.; methodology, Y.S. and S.N.; software, S.N.; validation, Y.S. and S.N.; formal analysis, Y.S. and S.N.; investigation, Y.S., S.N. and A.I.P.; resources, S.N.; data curation, Y.S., S.N., M.K. and A.I.P.; writing—original draft preparation, Y.S. and S.N.; writing—review and editing, M.K. and A.I.P.; visualization, Y.S. and S.N.; supervision, Y.S. and A.I.P.; project administration, A.I.P.; funding acquisition, Y.S. All authors have read and agreed to the published version of the manuscript.

Funding: This research was funded by the National Research Fund of Ukraine with the support of the University of Cambridge, Great Britain, grant number 0124U000223 "Design and Research of Oxide Heterostructures for Portable Solar Cells.".

Data Availability Statement: No new data were created or analyzed in this study.

Acknowledgments: Yana Suchikova and Serhii Nazarovets would like to thank all Ukrainian defenders for the possibility to finalize and publish this work.

Conflicts of Interest: The authors declare that they have no competing financial or non-financial interests.

References

1. Bergmann, R. Crystalline Si thin-film solar cells: A review. *Appl. Phys. A* **1999**, *69*, 187–194. [CrossRef]
2. Andreani, L.C.; Bozzola, A.; Kowalczewski, P.; Liscidini, M.; Redorici, L. Silicon solar cells: Toward the efficiency limits. *Adv. Phys. X* **2018**, *4*, 1548305. [CrossRef]
3. Green, M.A. Silicon solar cells: State of the art. *Philos. Trans. R. Soc. A Math. Phys. Eng. Sci.* **2013**, *371*, 20110413. [CrossRef]
4. Ferekides, C.; Balasubramanian, U.; Mamazza, R.; Viswanathan, V.; Zhao, H.; Morel, D. CdTe thin film solar cells: Device and technology issues. *Sol. Energy* **2004**, *77*, 823–830. [CrossRef]
5. Ali, M.; Khan, Q.; Din, M.F.U.; Kasi, J.K.; Kasi, A.K.; Ali, A.; Ullah, S. Simulation-based optimization of CdS/CdTe solar cells incorporating MXene-enhanced SnO_2 buffer layer: Insights from experimentally validated material properties. *Sol. Energy* **2025**, *294*, 113510. [CrossRef]
6. Barbato, M.; Artegiani, E.; Bertoncello, M.; Meneghini, M.; Trivellin, N.; Mantoan, E.; Romeo, A.; Mura, G.; Ortolani, L.; Zanoni, E.; et al. CdTe solar cells: Technology, operation and reliability. *J. Phys. D Appl. Phys.* **2021**, *54*, 333002. [CrossRef]
7. Mufti, N.; Amrillah, T.; Taufiq, A.; Diantoro, M.; Nur, H. Review of CIGS-based solar cells manufacturing by structural engineering. *Sol. Energy* **2020**, *207*, 1146–1157. [CrossRef]
8. Suchikova, Y.; Bohdanov, I.; Kovachov, S.; Popov, A.I. Thin CIGS Films Obtained by Spray Pyrolysis. In *Nanomaterials and Nanocomposites, Nanostructures, and Their Applications. NANO 2023*; Fesenko, O., Yatsenko, L., Eds.; Springer Proceedings in Physics; Springer: Cham, Switzerland, 2024; Volume 253. [CrossRef]
9. Lin, L.; Ravindra, N.M. Temperature dependence of CIGS and perovskite solar cell performance: An overview. *SN Appl. Sci.* **2020**, *2*, 1361. [CrossRef]
10. Lu, S.; Chen, C.; Tang, J. Possible top cells for next-generation Si-based tandem solar cells. *Front. Optoelectron.* **2020**, *13*, 246–255. [CrossRef]
11. Panigrahi, J.; Komarala, V.K. Progress on the intrinsic a-Si:H films for interface passivation of silicon heterojunction solar cells: A review. *J. Non-Cryst. Solids* **2021**, *574*, 121166. [CrossRef]
12. Zhou, J.; Su, X.; Huang, Q.; Zhang, B.; Yang, J.; Zhao, Y.; Hou, G. Recent advancements in poly-Si/SiO_xpassivating contacts for high-efficiency silicon solar cells: Technology review and perspectives. *J. Mater. Chem. A* **2022**, *10*, 20147–20173. [CrossRef]
13. Raza, E.; Ahmad, Z. Review on two-terminal and four-terminal crystalline-silicon/perovskite tandem solar cells; progress, challenges, and future perspectives. *Energy Rep.* **2022**, *8*, 5820–5851. [CrossRef]
14. Jiang, L.; Cui, S.; Sun, P.; Wang, Y.; Yang, C. Comparison of Monocrystalline and Polycrystalline Solar Modules. In Proceedings of the 2020 IEEE 5th Information Technology and Mechatronics Engineering Conference (ITOEC), Chongqing, China, 12–14 June 2020; pp. 341–344. [CrossRef]
15. Enaganti, P.K.; Dwivedi, P.K.; Srivastava, A.K.; Goel, S. Study of solar irradiance and performance analysis of submerged monocrystalline and polycrystalline solar cells. *Prog. Photovolt. Res. Appl.* **2020**, *28*, 725–735. [CrossRef]
16. Suchikova, Y. Provision of environmental safety through the use of porous semiconductors for solar energy sector. *East.-Eur. J. Enterp. Technol.* **2016**, *6*, 26–33. [CrossRef]
17. Santos, I.M.D.L.; Courel, M.; Moreno-Oliva, V.I.; Dueñas-Reyes, E.; Díaz-Cruz, E.B.; Ojeda-Martínez, M.; Pérez, L.M.; Laroze, D. The study of inorganic absorber layers in perovskite solar cells: The influence of CdTe and CIGS incorporation. *Sci. Rep.* **2025**, *15*, 10353. [CrossRef] [PubMed]
18. Iqbal, N.; Colvin, D.J.; Schneller, E.J.; Sakthivel, T.S.; Ristau, R.; Huey, B.D.; Yu, B.X.; Jaubert, J.-N.; Curran, A.J.; Wang, M.; et al. Characterization of front contact degradation in monocrystalline and multicrystalline silicon photovoltaic modules following damp heat exposure. *Sol. Energy Mater. Sol. Cells* **2022**, *235*, 111468. [CrossRef]
19. Wijewardane, S.; Kazmerski, L.L. Inventions, innovations, and new technologies: Flexible and lightweight thin-film solar PV based on CIGS, CdTe, and a-Si:H. *Sol. Compass* **2023**, *7*, 100053. [CrossRef]
20. Gao, B.; Shao, Y.; Liu, W.; Xiang, H.; Yu, Y.; Liu, Z. Out-door reliability and degradation of HIT, CIGS, n-type multi-busbar, PERC, and CdTe modules in Shanghai, China. *Sol. Energy Mater. Sol. Cells* **2022**, *236*, 111490. [CrossRef]

21. Bosio, A.; Pasini, S.; Romeo, N. The History of Photovoltaics with Emphasis on CdTe Solar Cells and Modules. *Coatings* **2020**, *10*, 344. [CrossRef]
22. Fang, Z.; Wang, X.C.; Wu, H.C.; Zhao, C.Z. Achievements and Challenges of CdS/CdTe Solar Cells. *Int. J. Photoenergy* **2011**, *2011*, 297350. [CrossRef]
23. Khrypunov, G.; Vambol, S.; Deyneko, N.; Sychikova, Y. Increasing the efficiency of film solar cells based on cadmium telluride. *East.-Eur. J. Enterp. Technol.* **2016**, *6*, 12–18. [CrossRef]
24. Romeo, A.; Artegiani, E.; Menossi, D. Low substrate temperature CdTe solar cells: A review. *Sol. Energy* **2018**, *175*, 9–15. [CrossRef]
25. Balakhayeva, R.; Akilbekov, A.; Baimukhanov, Z.; Usseinov, A.; Giniyatova, S.; Zdorovets, M.; Vlasukova, L.; Popov, A.I.; Dauletbekova, A. CdTe Nanocrystal Synthesis in SiO_2/Si Ion-Track Template: The Study of Electronic and Structural Properties. *Phys. Status Solidi (A)* **2020**, *218*, 2000231. [CrossRef]
26. Zghaibeh, M.; Okonkwo, P.C.; Emori, W.; Ahmed, T.; Mohamed, A.; Aliyu, M.; Ogunleye, G.J. CdTe solar cells fabrication and examination techniques: A focused review. *Int. J. Green Energy* **2022**, *20*, 555–570. [CrossRef]
27. Fthenakis, V.; Athias, C.; Blumenthal, A.; Kulur, A.; Magliozzo, J.; Ng, D. Sustainability evaluation of CdTe PV: An update. *Renew. Sustain. Energy Rev.* **2020**, *123*, 109776. [CrossRef]
28. Curtin, A.; Vail, C.; Buckley, H. CdTe in thin film photovoltaic cells: Interventions to protect drinking water in production and end-of-life. *Water-Energy Nexus* **2020**, *3*, 15–28. [CrossRef]
29. Lin, L.; Ravindra, N.M. CIGS and perovskite solar cells—An overview. *Emerg. Mater. Res.* **2020**, *9*, 812–824. [CrossRef]
30. Ramanujam, J.; Singh, U.P. Copper indium gallium selenide based solar cells—A review. *Energy Environ. Sci.* **2017**, *10*, 1306–1319. [CrossRef]
31. Ong, K.H.; Agileswari, R.; Maniscalco, B.; Arnou, P.; Kumar, C.C.; Bowers, J.W.; Marsadek, M.B. Review on Substrate and Molybdenum Back Contact in CIGS Thin Film Solar Cell. *Int. J. Photoenergy* **2018**, *2018*, 9106269. [CrossRef]
32. Romanyuk, Y.E.; Hagendorfer, H.; Stücheli, P.; Fuchs, P.; Uhl, A.R.; Sutter-Fella, C.M.; Werner, M.; Haass, S.; Stückelberger, J.; Broussillou, C.; et al. All Solution-Processed Chalcogenide Solar Cells—From Single Functional Layers Towards a 13.8% Efficient CIGS Device. *Adv. Funct. Mater.* **2014**, *25*, 12–27. [CrossRef]
33. Feurer, T.; Reinhard, P.; Avancini, E.; Bissig, B.; Löckinger, J.; Fuchs, P.; Carron, R.; Weiss, T.P.; Perrenoud, J.; Stutterheim, S.; et al. Progress in thin film CIGS photovoltaics—Research and development, manufacturing, and applications. *Prog. Photovolt. Res. Appl.* **2016**, *25*, 645–667. [CrossRef]
34. Zhao, C.; Yu, S.; Tang, W.; Yuan, X.; Zhou, H.; Qi, T.; Zheng, X.; Ning, D.; Ma, M.; Zhu, J.; et al. Advances in CIGS thin film solar cells with emphasis on the alkali element post-deposition treatment. *Mater. Rep. Energy* **2023**, *3*, 100214. [CrossRef]
35. Kim, S.; Van Quy, H.; Bark, C.W. Photovoltaic technologies for flexible solar cells: Beyond silicon. *Mater. Today Energy* **2021**, *19*, 100583. [CrossRef]
36. Dhere, N.G. Toward GW/year of CIGS production within the next decade. *Sol. Energy Mater. Sol. Cells* **2007**, *91*, 1376–1382. [CrossRef]
37. Singh, B.P.; Goyal, S.K.; Kumar, P. Solar PV cell materials and technologies: Analyzing the recent developments. *Mater. Today Proc.* **2021**, *43*, 2843–2849. [CrossRef]
38. Wang, M.; Obene, P.; Questianx, M.; Harris, M.; Singh, R.; Choy, K.L. Electrostatic InkJet printed silver grids for non-vacuum processed CIGS solar cells. *Sci. Rep.* **2025**, *15*, 11048. [CrossRef]
39. Tong, Y.; Xiao, Z.; Du, X.; Zuo, C.; Li, Y.; Lv, M.; Yuan, Y.; Yi, C.; Hao, F.; Hua, Y.; et al. Progress of the key materials for organic solar cells. *Sci. China Chem.* **2020**, *63*, 758–765. [CrossRef]
40. Li, X.; Li, P.; Wu, Z.; Luo, D.; Yu, H.-Y.; Lu, Z.-H. Review and perspective of materials for flexible solar cells. *Mater. Rep. Energy* **2021**, *1*, 100001. [CrossRef]
41. Suchikova, Y.; Bogdanov, I.; Kovachov, S.; Kamensky, D.; Myroshnychenko, V.; Panova, N. Optimal ranges determination of morphological parameters of nanopatterned semiconductors quality for solar cells. *Arch. Mater. Sci. Eng.* **2020**, *1*, 15–24. [CrossRef]
42. Li, J.; Aierken, A.; Liu, Y.; Zhuang, Y.; Yang, X.; Mo, J.H.; Fan, R.K.; Chen, Q.Y.; Zhang, S.Y.; Huang, Y.M.; et al. A Brief Review of High Efficiency III-V Solar Cells for Space Application. *Front. Phys.* **2021**, *8*, 631925. [CrossRef]
43. Yao, H.; Wang, J.; Xu, Y.; Zhang, S.; Hou, J. Recent Progress in Chlorinated Organic Photovoltaic Materials. *Acc. Chem. Res.* **2020**, *53*, 822–832. [CrossRef]
44. Fan, B.; Lin, F.; Wu, X.; Zhu, Z.; Jen, A.K.-Y. Selenium-Containing Organic Photovoltaic Materials. *Acc. Chem. Res.* **2021**, *54*, 3906–3916. [CrossRef] [PubMed]
45. Kim, J.Y.; Lee, J.-W.; Jung, H.S.; Shin, H.; Park, N.-G. High-Efficiency Perovskite Solar Cells. *Chem. Rev.* **2020**, *120*, 7867–7918. [CrossRef] [PubMed]
46. Kumar, N.S.; Naidu, K.C.B. A review on perovskite solar cells (PSCs), materials and applications. *J. Mater.* **2021**, *7*, 940–956. [CrossRef]
47. Liu, L.; Najar, A.; Wang, K.; Du, M.; Liu, S. Perovskite Quantum Dots in Solar Cells. *Adv. Sci.* **2022**, *9*, 2104577. [CrossRef]

48. Albaladejo-Siguan, M.; Baird, E.C.; Becker-Koch, D.; Li, Y.; Rogach, A.L.; Vaynzof, Y. Stability of Quantum Dot Solar Cells: A Matter of (Life)Time. *Adv. Energy Mater.* **2021**, *11*, 2003457. [CrossRef]
49. Duan, L.; Hu, L.; Guan, X.; Lin, C.; Chu, D.; Huang, S.; Liu, X.; Yuan, J.; Wu, T. Quantum Dots for Photovoltaics: A Tale of Two Materials. *Adv. Energy Mater.* **2021**, *11*, 2100354. [CrossRef]
50. Schileo, G.; Grancini, G. Lead or no lead? Availability, toxicity, sustainability and environmental impact of lead-free perovskite solar cells. *J. Mater. Chem. C* **2021**, *9*, 67–76. [CrossRef]
51. Huang, Z.; Beard, M.C. Dye-Sensitized Multiple Exciton Generation in Lead Sulfide Quantum Dots. *J. Am. Chem. Soc.* **2022**, *144*, 15855–15861. [CrossRef]
52. Sahu, A.; Garg, A.; Dixit, A. A review on quantum dot sensitized solar cells: Past, present and future towards carrier multiplication with a possibility for higher efficiency. *Sol. Energy* **2020**, *203*, 210–239. [CrossRef]
53. Rakshit, S.; Piatkowski, P.; Mora-Seró, I.; Douhal, A. Combining Perovskites and Quantum Dots: Synthesis, Characterization, and Applications in Solar Cells, LEDs, and Photodetectors. *Adv. Opt. Mater.* **2022**, *10*, 2102566. [CrossRef]
54. Kim, T.; Lim, S.; Yun, S.; Jeong, S.; Park, T.; Choi, J. Design Strategy of Quantum Dot Thin-Film Solar Cells. *Small* **2020**, *16*, e2002460. [CrossRef]
55. Zhang, G.; Lin, F.R.; Qi, F.; Heumüller, T.; Distler, A.; Egelhaaf, H.-J.; Li, N.; Chow, P.C.Y.; Brabec, C.J.; Jen, A.K.-Y.; et al. Renewed Prospects for Organic Photovoltaics. *Chem. Rev.* **2022**, *122*, 14180–14274. [CrossRef]
56. Li, Y.; Huang, X.; Sheriff, H.K.M.; Forrest, S.R. Semitransparent organic photovoltaics for building-integrated photovoltaic applications. *Nat. Rev. Mater.* **2022**, *8*, 186–201. [CrossRef]
57. Akinoglu, B.G.; Tuncel, B.; Badescu, V. Beyond 3rd generation solar cells and the full spectrum project. Recent advances and new emerging solar cells. *Sustain. Energy Technol. Assess.* **2021**, *46*, 101287. [CrossRef]
58. Cramer, C.L.; Ionescu, E.; Graczyk-Zajac, M.; Nelson, A.T.; Katoh, Y.; Haslam, J.J.; Wondraczek, L.; Aguirre, T.G.; LeBlanc, S.; Wang, H.; et al. Additive manufacturing of ceramic materials for energy applications: Road map and opportunities. *J. Eur. Ceram. Soc.* **2022**, *42*, 3049–3088. [CrossRef]
59. Suchikova, Y.; Lazarenko, A.; Kovachov, S.; Usseinov, A.; Karipbaev, Z.; Popov, A.I. Formation of porous Ga_2O_3/GaAs layers for electronic devices. In Proceedings of the 2022 IEEE 16th International Conference on Advanced Trends in Radioelectronics, Telecommunications and Computer Engineering (TCSET), Lviv-Slavske, Ukraine, 22–26 February 2022. [CrossRef]
60. Kadyrzhanov, K.K.; Kozlovskiy, A.A.; Konuhova, M.; Popov, A.I.; Shlimas, D.D.; Borgekov, D.B. Determination of gamma radiation shielding efficiency by radiation-resistant composite ZrO_2–Al_2O_3—TiO_2–WO_3—Nb_2O_5 ceramics. *Opt. Mater.* **2024**, *154*, 115752. [CrossRef]
61. Usseinov, A.; Koishybayeva, Z.; Platonenko, A.; Akilbekov, A.; Purans, J.; Pankratov, V.; Suchikova, Y.; Popov, A.I. Ab-Initio Calculations of Oxygen Vacancy in Ga_2O_3 Crystals. *Latv. J. Phys. Tech. Sci.* **2021**, *58*, 3–10. [CrossRef]
62. Suchikova, Y.; Nazarovets, S.; Popov, A.I. Ga_2O_3 solar-blind photodetectors: From civilian applications to missile detection and research agenda. *Opt. Mater.* **2024**, *157*, 116397. [CrossRef]
63. Zhou, S.; Pu, Y.; Zhang, X.; Shi, Y.; Gao, Z.; Feng, Y.; Shen, G.; Wang, X.; Wang, D. High energy density, temperature stable lead-free ceramics by introducing high entropy perovskite oxide. *Chem. Eng. J.* **2022**, *427*, 131684. [CrossRef]
64. Usseinov, A.; Koishybayeva, Z.; Platonenko, A.; Pankratov, V.; Suchikova, Y.; Akilbekov, A.; Zdorovets, M.; Purans, J.; Popov, A.I. Vacancy Defects in Ga_2O_3: First-Principles Calculations of Electronic Structure. *Materials* **2021**, *14*, 7384. [CrossRef]
65. Jiao, Y.; Dai, J.; Fan, Z.; Cheng, J.; Zheng, G.; Grema, L.; Zhong, J.; Li, H.-F.; Wang, D. Overview of high-entropy oxide ceramics. *Mater. Today* **2024**, *77*, 92–117. [CrossRef]
66. Wang, Z.; Lin, R.; Huo, Y.; Li, H.; Wang, L. Formation, Detection, and Function of Oxygen Vacancy in Metal Oxides for Solar Energy Conversion. *Adv. Funct. Mater.* **2021**, *32*, 2109503. [CrossRef]
67. Ming, W.; Jiang, Z.; Luo, G.; Xu, Y.; He, W.; Xie, Z.; Shen, D.; Li, L. Progress in Transparent Nano-Ceramics and Their Potential Applications. *Nanomaterials* **2022**, *12*, 1491. [CrossRef] [PubMed]
68. Bondarchuk, A.N.; Corrales-Mendoza, I.; Aguilar-Martínez, J.A.; Tomás, S.A.; Gómez-Caiceros, D.A.; Hernández-Méndez, A.; Marken, F. A BiVO4 photoanode grown on porous and conductive SnO_2 ceramics for water splitting driven by solar energy. *Ceram. Int.* **2020**, *46*, 9040–9049. [CrossRef]
69. Freitas, A.L.M.; Muche, D.N.F.; Leite, E.R.; Souza, F.L. Interface engineering of nanoceramic hematite photoelectrode for solar energy conversion. *J. Am. Ceram. Soc.* **2020**, *103*, 6833–6846. [CrossRef]
70. Ahmad, W.; Tahir, S.; Ali, A.; Mahmood, K. A novel approach to reduce both front and rear side power losses in PERC solar cells using different combinations of transparent metal oxides. *Ceram. Int.* **2022**, *49*, 2821–2828. [CrossRef]
71. Möllmann, A.; Bialuschewski, D.; Fischer, T.; Tachibana, Y.; Mathur, S. Functional metal oxide ceramics as electron transport medium in photovoltaics and photo-electrocatalysis. In *Advanced Ceramics for Energy Conversion and Storage*; Elsevier: Amsterdam, The Netherlands, 2020; pp. 207–273. [CrossRef]
72. Almakayeel, N.; Kaliyannan, G.V.; Gunasekaran, R. Enhancing power conversion efficiency of polycrystalline silicon photovoltaic cells using yttrium oxide anti-reflective coating via electro-spraying method. *Ceram. Int.* **2024**, *50*, 42392–42403. [CrossRef]

73. Maqsood, S.; Ali, Z.; Ali, K.; Ishaq, M.; Sajid, M.; Farhan, A.; Rahdar, A.; Pandey, S. Assessment of different optimized anti-reflection coatings for ZnO/Si heterojunction solar cells. *Ceram. Int.* **2023**, *49*, 37118–37126. [CrossRef]
74. Sadiq, I.; Ali, S.A.; Ahmad, T. Advanced Hybrid Ceramics for Nuclear and Hydrogen Energy Applications. *ChemistrySelect* **2023**, *8*, e202300837. [CrossRef]
75. Alizadeh, A.; Roudgar-Amoli, M.; Bonyad-Shekalgourabi, S.-M.; Shariatinia, Z.; Mahmoudi, M.; Saadat, F. Dye sensitized solar cells go beyond using perovskite and spinel inorganic materials: A review. *Renew. Sustain. Energy Rev.* **2022**, *157*, 112047. [CrossRef]
76. Kusuma, J.; Balakrishna, R.G. Ceramic grains: Highly promising hole transport material for solid state QDSSC. *Sol. Energy Mater. Sol. Cells* **2020**, *209*, 110445. [CrossRef]
77. Mozafari, H.; Hamidinezhad, H. Effect of electrospun bilayer titanium oxide–tin oxide nanofibers on the performance of dye-sensitized solar cells. *Opt. Mater.* **2023**, *144*, 114297. [CrossRef]
78. Szindler, M.; Szindler, M.; Drygała, A.; Lukaszkowicz, K.; Kaim, P.; Pietruszka, R. Dye-Sensitized Solar Cell for Building-Integrated Photovoltaic (BIPV) Applications. *Materials* **2021**, *14*, 3743. [CrossRef]
79. Exeler, J.; Jüstel, T. Advances in Functional Ceramics for Water Splitting: A Comprehensive Review. *Photochem* **2024**, *4*, 271–284. [CrossRef]
80. Hassan, N.S.; Jalil, A.A.; Khusnun, N.F.; Ahmad, A.; Abdullah, T.A.T.; Kasmani, R.M.; Norazahar, N.; Kamaroddin, M.F.A.; Vo, D.V.N. Photoelectrochemical water splitting using post-transition metal oxides for hydrogen production: A review. *Environ. Chem. Lett.* **2021**, *20*, 311–333. [CrossRef]
81. Halfadji, A.; Bennabi, L.; Giannakis, S.; Marrani, A.G.; Bellucci, S. Sono-synthesis and characterization of next-generation antimicrobial ZnO/TiO_2 and Fe3O4/TiO_2 bi-nanocomposites, for antibacterial and antifungal applications. *Ceram. Int.* **2024**, *50*, 39097–39108. [CrossRef]
82. Kaler, V.; Pandel, U.; Duchaniya, R. Development of TiO_2/PVA nanocomposites for application in solar cells. *Mater. Today Proc.* **2018**, *5*, 6279–6287. [CrossRef]
83. Serga, V.; Burve, R.; Krumina, A.; Pankratova, V.; Popov, A.I.; Pankratov, V. Study of phase composition, photocatalytic activity, and photoluminescence of TiO_2 with Eu additive produced by the extraction-pyrolytic method. *J. Mater. Res. Technol.* **2021**, *13*, 2350–2360. [CrossRef]
84. Rakhman, K.A.; Budhyantoro, A.; Aprilita, N.H.; Kartini, I. One-pot synthesis of hollow sphere TiO_2/Ag nanoparticles co-sensitized with peonidin: Pelargonidin for dye-sensitized solar cells applications. *J. Mater. Sci. Mater. Electron.* **2024**, *35*, 1926. [CrossRef]
85. Khan, M.; Ali, S.; Alwadai, N.; Haq, I.U.; Irfan, M.; Albalawi, H.; Almuqrin, A.H.; Almoneef, M.M.; Iqbal, M. Structural, electrical and optical properties of hetrostructured MoS2/ZnO thin films for potential perovskite solar cells application. *J. Mater. Res. Technol.* **2022**, *20*, 1616–1623. [CrossRef]
86. Wibowo, A.; Marsudi, M.A.; Amal, M.I.; Ananda, M.B.; Stephanie, R.; Ardy, H.; Diguna, L.J. ZnO nanostructured materials for emerging solar cell applications. *RSC Adv.* **2020**, *10*, 42838–42859. [CrossRef]
87. Hajji, M.; Ajili, M.; Jebbari, N.; Loreiro, A.G.; Kamoun, N.T. Photocatalytic performance and solar cell applications of coupled semiconductor CuO– ZnO sprayed thin films: Coupling effect between oxides. *Opt. Mater.* **2023**, *140*, 113798. [CrossRef]
88. Alsmadi, A.K.M.; Salameh, B.; Alshammari, O.; Bumajdad, A.; Madkour, M. Synthesis, photocatalytic, and photoelectric performance of mesoporous Au/TiO_2 and Au/TiO_2/MWCNT nanocomposites. *J. Phys. Chem. Solids* **2025**, *207*, 112874. [CrossRef]
89. Tyagi, J.; Gupta, H.; Purohit, L. Mesoporous ZnO/TiO_2 photoanodes for quantum dot sensitized solar cell. *Opt. Mater.* **2021**, *115*, 111014. [CrossRef]
90. Kaur, N.; Singh, D.P.; Mahajan, A. Plasmonic Engineering of TiO_2 Photoanodes for Dye-Sensitized Solar Cells: A Review. *J. Electron. Mater.* **2022**, *51*, 4188–4206. [CrossRef]
91. Lana, G.M.; Bello, I.T.; Adedokun, O.M.; Adenigba, V.O.; Jubu, P.R.; Adedokun, O.; Sanusi, Y.K.; Dhlamini, M.S.; Awodugba, A.O. One-Dimensional TiO_2 Nanocomposite-based Photoanode for Dye-Sensitized solar Cells: A review. *Sol. Energy* **2024**, *279*, 112850. [CrossRef]
92. Sha, S.; Lu, H.; Yang, S.; Li, T.; Wu, J.; Ma, J.; Wang, K.; Hou, C.; Sheng, Z.; Li, Y. One-step electrodeposition of ZnO/graphene composite film as photoanode for dye-sensitised solar cells. *Colloids Surf. A Physicochem. Eng. Asp.* **2021**, *630*, 127491. [CrossRef]
93. Almakayeel, N.; Kaliyannan, G.V.; Gunasekaran, R.; Rathanasamy, R. Enhanced photovoltaic efficiency through 3D-Printed COC/Al_2O_3 anti-reflective coversheets. *J. Mater. Res. Technol.* **2024**, *33*, 3093–3105. [CrossRef]
94. Shablonin, E.; Popov, A.; Prieditis, G.; Vasil'CHenko, E.; Lushchik, A. Thermal annealing and transformation of dimer F centers in neutron-irradiated Al_2O_3 single crystals. *J. Nucl. Mater.* **2021**, *543*, 152600. [CrossRef]
95. Yuliantini, L.; Nursam, N.M.; Pranoto, L.M.; Hidayat, J.; Sova, R.R.; Rahayu, E.S.; Djamal, M.; Yasaka, P.; Boonin, K.; Kaewkhao, J. Photon up-conversion in Er^{3+} ion-doped ZnO-Al_2O_3-BaO-B_2O_3 glass for enhancing the performance of dye-sensitized solar cells. *J. Alloys Compd.* **2023**, *954*, 170163. [CrossRef]

96. Verma, M.; Mishra, G.P. High Electric Field Sensing in Ultrathin SiO_2 and Tunnel Region to Enhance GaInP/Si Dual Junction Solar Cell Performance. *IEEE Sens. J.* **2021**, *22*, 1273–1279. [CrossRef]
97. Wang, Z.; Zhang, X.; Liu, Q.; Luo, G.; Lu, J.; Xie, Y.; Zhao, X.; Tian, S. Superhydrophilic antireflection films with excellent optical and mechanical performance for perovskite solar cells. *Inorg. Chem. Commun.* **2024**, *168*, 112876. [CrossRef]
98. Molina-Lozano, A.E.; Lanza, M.R.V.; Ortiz, P.; Cortés, M.T. Photoelectrochemical and Structural Insights of Electrodeposited CeO_2 Photoanodes. *Surfaces* **2024**, *7*, 898–919. [CrossRef]
99. Ravi, G.; Thyagarajan, K. $CoFe_2O_4/NiFe_2O_4/CeO_2$ nanocomposites: Structural, FTIR, XPS, BET, and magnetic properties. *Appl. Phys. A* **2024**, *130*, 726. [CrossRef]
100. Kumar, P.; Ratan, J.K.; Divya, N.; Mummaneni, K.; Rawat, G. Investigation of CeO_2/rGO Nanocomposites as Diesel Additives to Enhance Engine Performance and Reduce Exhaust Emissions. In Proceedings of the 2023 9th International Conference on Signal Processing and Communication (ICSC), Noida, India, 21–23 December 2023; pp. 714–719. [CrossRef]
101. Nien, Y.-H.; Zhuang, S.-W.; Chou, J.-C.; Yang, P.-H.; Lai, C.-H.; Kuo, P.-Y.; Ho, C.-S.; Wu, Y.-T.; Syu, R.-H.; Chen, P.-F. Photovoltaic Measurement Under Different Illumination of the Dye-Sensitized Solar Cell With the Photoanode Modified by Fe_2O_3/g-C_3N_4/TiO_2 Heterogeneous Nanofibers Prepared by Electrospinning With Dual Jets. *IEEE Trans. Semicond. Manuf.* **2023**, *36*, 291–297. [CrossRef]
102. Wu, S.; Cheng, C.-H.; Hsiao, Y.-J.; Juang, R.-C.; Wen, W.-F. Fe_2O_3 films on stainless steel for solar absorbers. *Renew. Sustain. Energy Rev.* **2016**, *58*, 574–580. [CrossRef]
103. Kamil, A.F.; Abdullah, H.I.; Rheima, A.M.; Mohammed, S.H. UV-Irradiation synthesized α-Fe_2O_3 nanoparticles based dye-sensitized solar cells. *Mater. Today Proc.* **2022**, *61*, 820–825. [CrossRef]
104. Shinde, S.S.; Bansode, R.A.; Bhosale, C.H.; Rajpure, K.Y. Physical properties of hematite α-Fe_2O_3thin films: Application to photoelectrochemical solar cells. *J. Semicond.* **2011**, *32*, 013001. [CrossRef]
105. Chen, L.; Wu, S.; Ma, D.; Shang, A.; Li, X. Optoelectronic modeling of the Si/α-Fe_2O_3 heterojunction photoanode. *Nano Energy* **2018**, *43*, 177–183. [CrossRef]
106. Dadkhah, M.; Nine, J.; Purasinhala, K.; Sandhu, G.S.; Losic, D. Nanostructure-dependent colouration efficiency of electrochromic coatings using 0D, 1D, and 2D WO_3 for smart windows. *Nano Mater. Sci.* **2024**. [CrossRef]
107. Wang, L.; Zhai, Z.; Li, L. Rapid Fabrication of Tungsten Oxide-Based Electrochromic Devices through Femtosecond Laser Processing. *Micromachines* **2024**, *15*, 785. [CrossRef] [PubMed]
108. Aldirham, S.H.; Helal, A.; Shkir, M.; Sayed, M.A.; Ali, A.M. Enhancement Study of the Photoactivity of TiO_2 Photocatalysts during the Increase of the WO_3 Ratio in the Presence of Ag Metal. *Catalysts* **2024**, *14*, 633. [CrossRef]
109. Matalkeh, M.; Nasrallah, G.K.; Shurrab, F.M.; Al-Absi, E.S.; Mohammed, W.; Elzatahry, A.; Saoud, K.M. Visible Light Photocatalytic Activity of Ag/WO_3 Nanoparticles and its Antibacterial Activity Under Ambient Light and in The Dark. *Results Eng.* **2022**, *13*, 100313. [CrossRef]
110. Ghattavi, S.; Nezamzadeh-Ejhieh, A. Nanoscale AgI-WO_3 binary photocatalyst: Synthesis, brief characterization, and investigation of its photocatalytic activity. *Mater. Res. Bull.* **2022**, *158*, 112085. [CrossRef]
111. Hedayati, M.; Fouladvand, M.; Rouhollahi, A. Fabrication of WO_3/Co_3O_4 nanorods as a p-n heterojunction photoanode for efficient photoelectrochemical oxygen evolution. *Int. J. Hydrogen Energy* **2024**, *84*, 288–295. [CrossRef]
112. Lee, D.; Chae, M.; Ahmad, I.; Kim, J.-R.; Kim, H.-D. Influence of WO_3-Based Antireflection Coatings on Current Density in Silicon Heterojunction Solar Cells. *Nanomaterials* **2023**, *13*, 1550. [CrossRef] [PubMed]
113. Diebold, U. The surface science of titanium dioxide. *Surf. Sci. Rep.* **2003**, *48*, 53–229. [CrossRef]
114. Imanishi, A.; Tsuji, E.; Nakato, Y. Dependence of the Work Function of TiO_2 (Rutile) on Crystal Faces, Studied by a Scanning Auger Microprobe. *J. Phys. Chem. C* **2007**, *111*, 2128–2132. [CrossRef]
115. Kadoshima, M.; Hiratani, M.; Shimamoto, Y.; Torii, K.; Miki, H.; Kimura, S.; Nabatame, T. Rutile-type TiO_2 thin film for high-k gate insulator. *Thin Solid Film.* **2003**, *424*, 224–228. [CrossRef]
116. Dewasi, A.; Mitra, A. Effect of variation of thickness of TiO_2 on the photovoltaic performance of n-TiO_2/p-Si heterostructure. *J. Mater. Sci. Mater. Electron.* **2017**, *28*, 18075–18084. [CrossRef]
117. Falson, J.; Kozuka, Y.; Uchida, M.; Smet, J.H.; Arima, T.-H.; Tsukazaki, A.; Kawasaki, M. MgZnO/ZnO heterostructures with electron mobility exceeding 1×10^6 cm^2/Vs. *Sci. Rep.* **2016**, *6*, 26598. [CrossRef]
118. Ozgür, Ü.; Alivov, Y.I.; Liu, C.; Teke, A.; Reshchikov, M.A.; Doğan, S.; Avrutin, V.; Cho, S.-J.; Morkoç, H. A comprehensive review of ZnO materials and devices. *J. Appl. Phys.* **2005**, *98*, 041301. [CrossRef]
119. Look, D. Recent advances in ZnO materials and devices. *Mater. Sci. Eng. B* **2001**, *80*, 383–387. [CrossRef]
120. Kim, S.K.; Lee, S.W.; Hwang, C.S.; Min, Y.-S.; Won, J.Y.; Jeong, J. Low Temperature (<100 °C) Deposition of Aluminum Oxide Thin Films by ALD with O_3 as Oxidant. *J. Electrochem. Soc.* **2006**, *153*, F69–F76. [CrossRef]
121. Liu, D.; Robertson, J. Oxygen vacancy levels and interfaces of Al_2O_3. *Microelectron. Eng.* **2009**, *86*, 1668–1671. [CrossRef]
122. Costina, I.; Franchy, R. Band gap of amorphous and well-ordered Al_2O_3 on Ni3Al(100). *Appl. Phys. Lett.* **2001**, *78*, 4139–4141. [CrossRef]

123. Guerreiro, A.N.; Costa, I.B.; Vale, A.B.; Braga, M.H. Distinctive Electric Properties of Group 14 Oxides: SiO_2, SiO, and SnO_2. *Int. J. Mol. Sci.* **2023**, *24*, 15985. [CrossRef] [PubMed]
124. Li, Z.; Zhang, Z.; Tian, J.; Wu, G.; He, Y.; Yu, B.; Zhan, F.; Wang, Y.; Sun, M.; Yang, W.; et al. Efficient and Dense Electron Emission from a SiO_2 Tunneling Diode with Low Poisoning Sensitivity. *Nano Lett.* **2022**, *22*, 1270–1277. [CrossRef] [PubMed]
125. Kim, T.; Oh, C.; Park, S.H.; Lee, J.W.; Lee, S.I.; Kim, B.S. Electrical properties of low-temperature SiO_2 thin films prepared by plasma-enhanced atomic layer deposition with different plasma times. *AIP Adv.* **2021**, *11*, 115126. [CrossRef]
126. Kusmierek, E. A CeO_2 Semiconductor as a Photocatalytic and Photoelectrocatalytic Material for the Remediation of Pollutants in Industrial Wastewater: A Review. *Catalysts* **2020**, *10*, 1435. [CrossRef]
127. Wang, B.; Zhu, B.; Yun, S.; Zhang, W.; Xia, C.; Afzal, M.; Cai, Y.; Liu, Y.; Wang, Y.; Wang, H. Fast ionic conduction in semiconductor CeO_2-δ electrolyte fuel cells. *NPG Asia Mater.* **2019**, *11*, 51. [CrossRef]
128. Zhang, N.; Zhang, G.; Chong, S.; Zhao, H.; Huang, T.; Zhu, J. Ultrasonic impregnation of MnO_2/CeO_2 and its application in catalytic sono-degradation of methyl orange. *J. Environ. Manag.* **2018**, *205*, 134–141. [CrossRef] [PubMed]
129. Avellaneda, C.O.; Berton, M.A.; Bulhões, L.O. Optical and electrochemical properties of CeO_2 thin film prepared by an alkoxide route. *Sol. Energy Mater. Sol. Cells* **2008**, *92*, 240–244. [CrossRef]
130. Erlebach, A.; Kurland, H.-D.; Grabow, J.; Müller, F.A.; Sierka, M. Structure evolution of nanoparticulate Fe_2O_3. *Nanoscale* **2014**, *7*, 2960–2969. [CrossRef]
131. Cong-Zhou, L.; Wei-Pin, C. High dielectric constants of hematite (α-Fe_2O_3) and its anomalous characteristics. *Ferroelectrics* **1981**, *38*, 926. [CrossRef]
132. Shaheen, W.; Hong, K. Thermal characterization and physicochemical properties of Fe_2O_3–Mn_2O_3/Al_2O_3 system. *Thermochim. Acta* **2002**, *381*, 153–164. [CrossRef]
133. Mahmoud, H.R.; El-Molla, S.A.; Saif, M. Improvement of physicochemical properties of Fe_2O_3/MgO nanomaterials by hydrothermal treatment for dye removal from industrial wastewater. *Powder Technol.* **2013**, *249*, 225–233. [CrossRef]
134. Walter, C.W.; Hertzler, C.F.; Devynck, P.; Smith, G.P.; Peterson, J.R. Photodetachment of WO^-_3: The electron affinity of WO_3. *J. Chem. Phys.* **1991**, *95*, 824–827. [CrossRef]
135. Vuong, N.M.; Hieu, H.N.; Kim, D. An edge-contacted pn-heterojunction of a p-SWCNT/n-WO_3 thin film. *J. Mater. Chem. C* **2013**, *1*, 5153–5160. [CrossRef]
136. Sanchez, F.; Marot, L.; Dmitriev, A.; Antunes, R.; Steiner, R.; Meyer, E. WO_3 work function enhancement induced by filamentous films deposited by resistive heating evaporation technique. *J. Alloys Compd.* **2023**, *968*, 171888. [CrossRef]
137. Passas, I. Bibliometric Analysis: The Main Steps. *Encyclopedia* **2024**, *4*, 1014–1025. [CrossRef]
138. Donthu, N.; Kumar, S.; Mukherjee, D.; Pandey, N.; Lim, W.M. How to conduct a bibliometric analysis: An overview and guidelines. *J. Bus. Res.* **2021**, *133*, 285–296. [CrossRef]
139. Ellegaard, O.; Wallin, J.A. The bibliometric analysis of scholarly production: How great is the impact? *Scientometrics* **2015**, *105*, 1809–1831. [CrossRef]
140. Suchikova, Y.; Nazarovets, S.; Popov, A.I. Electrochemical Etching vs. Electrochemical Deposition: A Comparative Bibliometric Analysis. *Electrochem* **2025**, *6*, 18. [CrossRef]
141. Menéndez-Manjón, A.; Moldenhauer, K.; Wagener, P.; Barcikowski, S. Nano-energy research trends: Bibliometrical analysis of nanotechnology research in the energy sector. *J. Nanoparticle Res.* **2011**, *13*, 3911–3922. [CrossRef]
142. Sales, M.B.; Neto, J.G.L.; Braz, A.K.D.S.; Junior, P.G.D.S.; Melo, R.L.F.; Valério, R.B.R.; Serpa, J.d.F.; Lima, A.M.D.S.; De Lima, R.K.C.; Guimarães, A.P.; et al. Trends and Opportunities in Enzyme Biosensors Coupled to Metal-Organic Frameworks (MOFs): An Advanced Bibliometric Analysis. *Electrochem* **2023**, *4*, 181–211. [CrossRef]
143. Zhang, F.; Xu, W.; Deng, Z.; Huang, J. A bibliometric and visualization analysis of electrochemical biosensors for early diagnosis of eye diseases. *Front. Med.* **2025**, *11*, 1487981. [CrossRef]
144. Dong, B.; Xu, G.; Luo, X.; Cai, Y.; Gao, W. A bibliometric analysis of solar power research from 1991 to 2010. *Scientometrics* **2012**, *93*, 1101–1117. [CrossRef]
145. Obaideen, K.; Olabi, A.G.; Al Swailmeen, Y.; Shehata, N.; Abdelkareem, M.A.; Alami, A.H.; Rodriguez, C.; Sayed, E.T. Solar Energy: Applications, Trends Analysis, Bibliometric Analysis and Research Contribution to Sustainable Development Goals (SDGs). *Sustainability* **2023**, *15*, 1418. [CrossRef]
146. Fauzi, M.A.; Abidin, N.H.Z.; Suki, N.M.; Budiea, A.M.A. Residential rooftop solar panel adoption behavior: Bibliometric analysis of the past and future trends. *Renew. Energy Focus* **2023**, *45*, 1–9. [CrossRef]
147. Yousef, B.A.; Obaideen, K.; AlMallahi, M.N.; Alajmi, N.; Radwan, A.; Al-Shihabi, S.; Elgendi, M. On the contribution of concentrated solar power (CSP) to the sustainable development goals (SDGs): A bibliometric analysis. *Energy Strat. Rev.* **2024**, *52*, 101356. [CrossRef]
148. David, T.M.; Rizol, P.M.S.R.; Machado, M.A.G.; Buccieri, G.P. Future research tendencies for solar energy management using a bibliometric analysis, 2000–2019. *Heliyon* **2020**, *6*, e04452. [CrossRef] [PubMed]

149. Du, H.; Li, N.; Brown, M.A.; Peng, Y.; Shuai, Y. A bibliographic analysis of recent solar energy literatures: The expansion and evolution of a research field. *Renew. Energy* **2014**, *66*, 696–706. [CrossRef]
150. Zwane, N.; Tazvinga, H.; Botai, C.; Murambadoro, M.; Botai, J.; de Wit, J.; Mabasa, B.; Daniel, S.; Mabhaudhi, T. A Bibliometric Analysis of Solar Energy Forecasting Studies in Africa. *Energies* **2022**, *15*, 5520. [CrossRef]
151. Saikia, K.; Vallès, M.; Fabregat, A.; Saez, R.; Boer, D. A bibliometric analysis of trends in solar cooling technology. *Sol. Energy* **2020**, *199*, 100–114. [CrossRef]
152. Mongeon, P.; Paul-Hus, A. The journal coverage of Web of Science and Scopus: A comparative analysis. *Scientometrics* **2016**, *106*, 213–228. [CrossRef]
153. Archambault, É.; Campbell, D.; Gingras, Y.; Larivière, V. Comparing bibliometric statistics obtained from the Web of Science and Scopus. *J. Am. Soc. Inf. Sci. Technol.* **2009**, *60*, 1320–1326. [CrossRef]
154. Franceschet, M. A comparison of bibliometric indicators for computer science scholars and journals on Web of Science and Google Scholar. *Scientometrics* **2009**, *83*, 243–258. [CrossRef]
155. Arruda, H.; Silva, E.R.; Lessa, M.; Domício Proença, J.; Bartholo, R. VOSviewer and Bibliometrix. *J. Med. Libr. Assoc.* **2022**, *110*, 392–395. [CrossRef]
156. Wong, D. VOSviewer. *Tech. Serv. Q.* **2018**, *35*, 219–220. [CrossRef]
157. Bukar, U.A.; Sayeed, S.; Razak, S.F.A.; Yogarayan, S.; Amodu, O.A.; Mahmood, R.A.R. A method for analyzing text using VOSviewer. *MethodsX* **2023**, *11*, 102339. [CrossRef] [PubMed]
158. Schmidt, M. The Sankey Diagram in Energy and Material Flow Management. *J. Ind. Ecol.* **2008**, *12*, 82–94. [CrossRef]
159. Lupton, R.; Allwood, J. Hybrid Sankey diagrams: Visual analysis of multidimensional data for understanding resource use. *Resour. Conserv. Recycl.* **2017**, *124*, 141–151. [CrossRef]
160. Daniel, D.; West-Mitchell, K. The Sankey diagram: An exploratory application of a data visualization tool. *Transfusion* **2024**, *64*, 967–968. [CrossRef]
161. Muruganandham, M.; Zhang, Y.; Suri, R.; Lee, G.-J.; Chen, P.-K.; Hsieh, S.-H.; Sillanpyää, M.; Wu, J.J. Environmental Applications of ZnO Materials. *J. Nanosci. Nanotechnol.* **2015**, *15*, 6900–6913. [CrossRef]
162. Gonçalves, R.A.; Toledo, R.P.; Joshi, N.; Berengue, O.M. Green Synthesis and Applications of ZnO and TiO_2 Nanostructures. *Molecules* **2021**, *26*, 2236. [CrossRef] [PubMed]
163. Šebesta, M.; Kolenčík, M.; Sunil, B.R.; Illa, R.; Mosnáček, J.; Ingle, A.P.; Urík, M. Field Application of ZnO and TiO_2 Nanoparticles on Agricultural Plants. *Agronomy* **2021**, *11*, 2281. [CrossRef]
164. Navidpour, A.H.; Hosseinzadeh, A.; Zhou, J.L.; Huang, Z. Progress in the application of surface engineering methods in immobilizing TiO_2 and ZnO coatings for environmental photocatalysis. *Catal. Rev.* **2021**, *65*, 822–873. [CrossRef]
165. Najaf, Z.; Nguyen, D.L.T.; Chae, S.Y.; Joo, O.-S.; Shah, A.U.H.A.; Vo, D.-V.N.; Nguyen, V.-H.; Van Le, Q.; Rahman, G. Recent trends in development of hematite (α-Fe_2O_3) as an efficient photoanode for enhancement of photoelectrochemical hydrogen production by solar water splitting. *Int. J. Hydrogen Energy* **2021**, *46*, 23334–23357. [CrossRef]
166. Tahir, A.A.; Wijayantha, K.G.U.; Saremi-Yarahmadi, S.; Mazhar, M.; McKee, V. Nanostructured α-Fe_2O_3Thin Films for Photoelectrochemical Hydrogen Generation. *Chem. Mater.* **2009**, *21*, 3763–3772. [CrossRef]
167. Emin, S.; de Respinis, M.; Mavrič, T.; Dam, B.; Valant, M.; Smith, W. Photoelectrochemical water splitting with porous α-Fe_2O_3 thin films prepared from Fe/Fe-oxide nanoparticles. *Appl. Catal. A Gen.* **2016**, *523*, 130–138. [CrossRef]
168. Kalantarian, K.; Sheibani, S. Ag and carbon quantum dot-modified Fe_2O_3/g-C_3N_4 nanocomposites for efficient photocatalytic degradation of organic pollutants and hydrogen production. *Int. J. Hydrogen Energy* **2025**, *140*, 343–361. [CrossRef]
169. Mohamed, H.O.; Obaid, M.; Poo, K.-M.; Abdelkareem, M.A.; Talas, S.A.; Fadali, O.A.; Kim, H.Y.; Chae, K.-J. Fe/Fe_2O_3 nanoparticles as anode catalyst for exclusive power generation and degradation of organic compounds using microbial fuel cell. *Chem. Eng. J.* **2018**, *349*, 800–807. [CrossRef]
170. Ashraf, M.; Khan, I.; Usman, M.; Khan, A.; Shah, S.S.; Khan, A.Z.; Saeed, K.; Yaseen, M.; Ehsan, M.F.; Tahir, M.N.; et al. Hematite and Magnetite Nanostructures for Green and Sustainable Energy Harnessing and Environmental Pollution Control: A Review. *Chem. Res. Toxicol.* **2019**, *33*, 1292–1311. [CrossRef]
171. Suchea, M.P.; Tudose, I.V.; Romanitan, C.; Pachiu, C.; Popescu, M.; Mouratis, K.; Manica, M.; Antohe, S.; Couris, S.; Zisopol, D.G.; et al. Study of evolution for 3D structured surface with nano-balls and walls-like features with thickness variation for WO_3 thin films made by spray deposition. *Sci. Rep.* **2025**, *15*, 4275. [CrossRef]
172. Phogat, P.; Rawat, S.; Thakur, J.; Jha, R.; Singh, S. Influence of metal ion doping on the photo-electrochemical detection performance of WO_3. *Sens. Actuators A Phys.* **2024**, *382*, 116150. [CrossRef]
173. Yao, Y.; Sang, D.; Zou, L.; Wang, Q.; Liu, C. A Review on the Properties and Applications of WO_3 Nanostructure−Based Optical and Electronic Devices. *Nanomaterials* **2021**, *11*, 2136. [CrossRef]
174. Buch, V.R.; Chawla, A.K.; Rawal, S.K. Review on electrochromic property for WO_3 thin films using different deposition techniques. *Mater. Today Proc.* **2016**, *3*, 1429–1437. [CrossRef]

175. Vezzoli, G.; Chen, M.; Caslavsky, J. New high dielectric constant materials: Micro/nanocomposites of suspended Au clusters in SiO_2/SiO_2, Al_2O_3, Li_2O gels and relevant theory for high capacitance applications. *Nanostruct. Mater.* **1994**, *4*, 985–1009. [CrossRef]
176. Na Kim, R.; Yun, H.W.; Lee, J.; Kim, W.-B. Dipole Formation and Electrical Properties According to SiO_2 Layer Thickness at an Al_2O_3/SiO_2 Interface. *J. Phys. Chem. C* **2021**, *125*, 14486–14492. [CrossRef]
177. Kim, D.; Choi, J.; Ryu, S.W.; Kim, W. Improved Interface and Electrical Properties by Inserting an Ultrathin SiO_2 Buffer Layer in the Al_2O_3/Si Heterojunction. *Adv. Funct. Mater.* **2019**, *29*, 1807271. [CrossRef]
178. Kim, A.S.; Serko, N.A.; Khakuashev, P.E.; Kolky, A.N.; Yurchuck, S.Y. Application of Al_2O_3 Film for Stabilization of the Charge Properties of the SiO_2/p-Si Interface. *Russ. Microelectron.* **2023**, *52*, 835–841. [CrossRef]
179. Sen, M.T.S.K.A.; Bronsveld, P.; Weeber, A. Thermally stable MoOx hole selective contact with Al_2O_3 interlayer for industrial size silicon solar cells. *Sol. Energy Mater. Sol. Cells* **2021**, *230*, 111139. [CrossRef]
180. Bullock, J.; Yan, D.; Cuevas, A. Passivation of aluminium–n^+ silicon contacts for solar cells by ultrathin Al_2O_3 and SiO_2 dielectric layers. *Phys. Status Solidi (RRL)—Rapid Res. Lett.* **2013**, *7*, 946–949. [CrossRef]
181. Yang, Y.; He, J.; Wu, G.; Hu, J. "Thermal Stabilization Effect" of Al_2O_3 nano-dopants improves the high-temperature dielectric performance of polyimide. *Sci. Rep.* **2015**, *5*, 16986. [CrossRef] [PubMed]
182. Bartzsch, H.; Glöß, D.; Böcher, B.; Frach, P.; Goedicke, K. Properties of SiO_2 and Al_2O_3 films for electrical insulation applications deposited by reactive pulse magnetron sputtering. *Surf. Coat. Technol.* **2003**, *174–175*, 774–778. [CrossRef]
183. Ren, Y.; Zhang, B.; Zhong, Z.; Ye, J.; Zhang, J.; Fang, Z.; Ye, F. Reusable, high specific surface areas, and excellent thermal stability Al_2O_3–SiO_2 aerogel composites as high-temperature thermal insulators for radome applications. *J. Alloys Compd.* **2024**, *984*, 173990. [CrossRef]
184. Gayathri, P.; Akila, T.; Sibu, G.A.; Selvaraj, M.; Assiri, M.A.; Matheswaran, P.; Balasubramani, V. Enhancing photovoltaic applications through precipitating agents in ITO/CIS/CeO_2/Al heterojunction solar cell. *Inorg. Chem. Commun.* **2024**, *168*, 112866. [CrossRef]
185. Aklalouch, M.; Calleja, A.; Granados, X.; Ricart, S.; Boffa, V.; Ricci, F.; Puig, T.; Obradors, X. Hybrid sol–gel layers containing CeO_2 nanoparticles as UV-protection of plastic lenses for concentrated photovoltaics. *Sol. Energy Mater. Sol. Cells* **2014**, *120*, 175–182. [CrossRef]
186. Li, Z.; Tong, L.; Ma, Y.; Zhao, L. Fabrication of CeO_2/CaO nanocomposite as ultraviolet screening agent and its application in sunscreen. *Ceram. Int.* **2024**, *50*, 20431–20440. [CrossRef]
187. Zhao, Y.; Gao, Z.; Lv, C.; Zhao, H.; Li, J.; Lv, Y. Synthesis and applications of polymorphic CeO_2 and AgI/CeO_2 nanocomposites. *J. Mater. Sci. Mater. Eng.* **2025**, *20*, 56. [CrossRef]
188. Saha, S.; Keerthi, C.J.; Roy, S.; Sahatiya, P.; Dan, S.S.; Pal, S. Engineering Oxygen Vacancies in CeO_2 for High-Performance UV-Vis Photodetector. *IEEE Photon-Technol. Lett.* **2023**, *35*, 1207–1210. [CrossRef]
189. Semwal, N.; Mahar, D.; Arya, M.C. Response surface methodology-driven optimization of dye-sensitized Fe-doped CeO_2 photocatalysts for efficient phenol degradation. *J. Mol. Struct.* **2025**, *1341*, 142639. [CrossRef]
190. Qiu, G.; Yang, X.; Zhang, Y.; Zhao, J.; Liu, Q. Highly dispersed MoC quantum dots assist CeO_2 for photocatalytic hydrogen production under visible light. *Int. J. Hydrogen Energy* **2025**, *106*, 423–431. [CrossRef]
191. O'Regan, B.; Grätzel, M. A low-cost, high-efficiency solar cell based on dye-sensitized colloidal TiO_2 films. *Nature* **1991**, *353*, 737–740. [CrossRef]
192. Kojima, A.; Teshima, K.; Shirai, Y.; Miyasaka, T. Organometal Halide Perovskites as Visible-Light Sensitizers for Photovoltaic Cells. *J. Am. Chem. Soc.* **2009**, *131*, 6050–6051. [CrossRef]
193. Grätzel, M. Photoelectrochemical cells. *Nature* **2001**, *414*, 338–344. [CrossRef]
194. Kim, H.-S.; Lee, C.-R.; Im, J.-H.; Lee, K.-B.; Moehl, T.; Marchioro, A.; Moon, S.-J.; Humphry-Baker, R.; Yum, J.-H.; Moser, J.E.; et al. Lead Iodide Perovskite Sensitized All-Solid-State Submicron Thin Film Mesoscopic Solar Cell with Efficiency Exceeding 9%. *Sci. Rep.* **2012**, *2*, 591. [CrossRef]
195. Nazeeruddin, M.K.; Kay, A.; Rodicio, I.; Humphry-Baker, R.; Mueller, E.; Liska, P.; Vlachopoulos, N.; Graetzel, M. Conversion of light to electricity by cis-X2bis(2,2′-bipyridyl-4,4′-dicarboxylate)ruthenium(II) charge-transfer sensitizers (X = Cl-, Br-, I-, CN-, and SCN-) on nanocrystalline titanium dioxide electrodes. *J. Am. Chem. Soc.* **1993**, *115*, 6382–6390. [CrossRef]
196. Law, M.; Greene, L.E.; Johnson, J.C.; Saykally, R.; Yang, P. Nanowire dye-sensitized solar cells. *Nat. Mater.* **2005**, *4*, 455–459. [CrossRef]
197. Grätzel, M. Dye-sensitized solar cells. *J. Photochem. Photobiol. C Photochem. Rev.* **2003**, *4*, 145–153. [CrossRef]
198. Liu, D.; Kelly, T.L. Perovskite solar cells with a planar heterojunction structure prepared using room-temperature solution processing techniques. *Nat. Photonics* **2013**, *8*, 133–138. [CrossRef]
199. Liu, B.; Aydil, E.S. Growth of Oriented Single-Crystalline Rutile TiO_2 Nanorods on Transparent Conducting Substrates for Dye-Sensitized Solar Cells. *J. Am. Chem. Soc.* **2009**, *131*, 3985–3990. [CrossRef] [PubMed]

200. Kay, A.; Cesar, I.; Grätzel, M. New Benchmark for Water Photooxidation by Nanostructured α-Fe_2O_3 Films. *J. Am. Chem. Soc.* **2006**, *128*, 15714–15721. [CrossRef]
201. Cushing, S.K.; Li, J.; Meng, F.; Senty, T.R.; Suri, S.; Zhi, M.; Li, M.; Bristow, A.D.; Wu, N. Photocatalytic Activity Enhanced by Plasmonic Resonant Energy Transfer from Metal to Semiconductor. *J. Am. Chem. Soc.* **2012**, *134*, 15033–15041. [CrossRef] [PubMed]
202. Palomares, E.; Clifford, J.N.; Haque, S.A.; Lutz, T.; Durrant, J.R. Control of Charge Recombination Dynamics in Dye Sensitized Solar Cells by the Use of Conformally Deposited Metal Oxide Blocking Layers. *J. Am. Chem. Soc.* **2002**, *125*, 475–482. [CrossRef]
203. Zou, S.; Liu, Y.; Li, J.; Liu, C.; Feng, R.; Jiang, F.; Li, Y.; Song, J.; Zeng, H.; Hong, M.; et al. Stabilizing Cesium Lead Halide Perovskite Lattice through Mn(II) Substitution for Air-Stable Light-Emitting Diodes. *J. Am. Chem. Soc.* **2017**, *139*, 11443–11450. [CrossRef]
204. Aberle, A.G. Surface passivation of crystalline silicon solar cells: A review. *Prog. Photovolt. Res. Appl.* **2000**, *8*, 473–487. [CrossRef]
205. Mor, G.K.; Varghese, O.K.; Paulose, M.; Shankar, K.; Grimes, C.A. A review on highly ordered, vertically oriented TiO_2 nanotube arrays: Fabrication, material properties, and solar energy applications. *Sol. Energy Mater. Sol. Cells* **2006**, *90*, 2011–2075. [CrossRef]
206. Huang, Z.; Geyer, N.; Werner, P.; de Boor, J.; Gösele, U. Metal-Assisted Chemical Etching of Silicon: A Review. *Adv. Mater.* **2010**, *23*, 285–308. [CrossRef]
207. Malinkiewicz, O.; Yella, A.; Lee, Y.H.; Espallargas, G.M.; Graetzel, M.; Nazeeruddin, M.K.; Bolink, H.J. Perovskite solar cells employing organic charge-transport layers. *Nat. Photonics* **2013**, *8*, 128–132. [CrossRef]
208. Niu, G.; Li, W.; Meng, F.; Wang, L.; Dong, H.; Qiu, Y. Study on the stability of $CH_3NH_3PbI_3$films and the effect of post-modification by aluminum oxide in all-solid-state hybrid solar cells. *J. Mater. Chem. A* **2013**, *2*, 705–710. [CrossRef]
209. Sivula, K.; Le Formal, F.; Grätzel, M. Solar Water Splitting: Progress Using Hematite (α-Fe_2O_3) Photoelectrodes. *ChemSusChem* **2011**, *4*, 432–449. [CrossRef] [PubMed]
210. Osterloh, F.E. Inorganic nanostructures for photoelectrochemical and photocatalytic water splitting. *Chem. Soc. Rev.* **2012**, *42*, 2294–2320. [CrossRef] [PubMed]
211. Kango, S.; Kalia, S.; Celli, A.; Njuguna, J.; Habibi, Y.; Kumar, R. Surface modification of inorganic nanoparticles for development of organic–inorganic nanocomposites—A review. *Prog. Polym. Sci.* **2013**, *38*, 1232–1261. [CrossRef]
212. Park, J.H.; Kim, S.; Bard, A.J. Novel Carbon-Doped TiO_2 Nanotube Arrays with High Aspect Ratios for Efficient Solar Water Splitting. *Nano Lett.* **2005**, *6*, 24–28. [CrossRef]
213. Wang, C.-C.; Li, J.-R.; Lv, X.-L.; Zhang, Y.-Q.; Guo, G. Photocatalytic organic pollutants degradation in metal–organic frameworks. *Energy Environ. Sci.* **2014**, *7*, 2831–2867. [CrossRef]
214. Bak, T.; Nowotny, J.; Rekas, M.; Sorrell, C.C. Photo-electrochemical hydrogen generation from water using solar energy. Materials-related aspects. *Int. J. Hydrogen Energy* **2002**, *27*, 991–1022. [CrossRef]
215. Granqvist, C. Electrochromic tungsten oxide films: Review of progress 1993–1998. *Sol. Energy Mater. Sol. Cells* **2000**, *60*, 201–262. [CrossRef]
216. Meyer, J.; Hamwi, S.; Kröger, M.; Kowalsky, W.; Riedl, T.; Kahn, A. Transition Metal Oxides for Organic Electronics: Energetics, Device Physics and Applications. *Adv. Mater.* **2012**, *24*, 5408–5427. [CrossRef]
217. Baetens, R.; Jelle, B.P.; Gustavsen, A. Properties, requirements and possibilities of smart windows for dynamic daylight and solar energy control in buildings: A state-of-the-art review. *Sol. Energy Mater. Sol. Cells* **2010**, *94*, 87–105. [CrossRef]
218. Liu, X.; Iocozzia, J.; Wang, Y.; Cui, X.; Chen, Y.; Zhao, S.; Li, Z.; Lin, Z. Noble metal–metal oxide nanohybrids with tailored nanostructures for efficient solar energy conversion, photocatalysis and environmental remediation. *Energy Environ. Sci.* **2016**, *10*, 402–434. [CrossRef]
219. Corma, A.; Atienzar, P.; García, H.; Chane-Ching, J.-Y. Hierarchically mesostructured doped CeO_2 with potential for solar-cell use. *Nat. Mater.* **2004**, *3*, 394–397. [CrossRef]
220. Ou, G.; Xu, Y.; Wen, B.; Lin, R.; Ge, B.; Tang, Y.; Liang, Y.; Yang, C.; Huang, K.; Zu, D.; et al. Tuning defects in oxides at room temperature by lithium reduction. *Nat. Commun.* **2018**, *9*, 1302. [CrossRef]
221. Abanades, S.; Flamant, G. Thermochemical hydrogen production from a two-step solar-driven water-splitting cycle based on cerium oxides. *Sol. Energy* **2006**, *80*, 1611–1623. [CrossRef]
222. Boyjoo, Y.; Sun, H.; Liu, J.; Pareek, V.K.; Wang, S. A review on photocatalysis for air treatment: From catalyst development to reactor design. *Chem. Eng. J.* **2017**, *310*, 537–559. [CrossRef]
223. Talebi, H.; Rad, R.R.; Emami, F. Synergistic effects of SiO_2 and Au nanostructures for enhanced broadband light absorption in perovskite solar cells. *Sci. Rep.* **2025**, *15*, 11548. [CrossRef]
224. Dkhili, M.; Khalifa, M.; Aouida, S.; Ezzaouia, H.; Brown, T.M. Unveiling interface dynamics in perovskite solar cells with CeO_2/SnO_2 bilayer: Insights from electrochemical impedance spectroscopy. *Mater. Today Commun.* **2025**, *46*, 112786. [CrossRef]
225. Haque, M.M.; Mahjabin, S.; Islam, M.A.; Selvanathan, V.; Putthisigamany, Y.; Abdullah, H.B.; Arith, F.; Akhtaruzzaman, M.; Ibrahim, M.A.; Chelvanathan, P. Modulation of optoelectronic properties of WO_3 thin film via Cr doping through RF co-sputtering. *Inorg. Chem. Commun.* **2025**, *177*, 114300. [CrossRef]

226. Liu, H.; Du, Y.; Yin, X.; Bai, M.; Liu, W. Micro/Nanostructures for Light Trapping in Monocrystalline Silicon Solar Cells. *J. Nanomater.* **2022**, *2022*, 8139174. [CrossRef]
227. Saga, T. Advances in crystalline silicon solar cell technology for industrial mass production. *NPG Asia Mater.* **2010**, *2*, 96–102. [CrossRef]
228. Green, M.A. Crystalline and thin-film silicon solar cells: State of the art and future potential. *Sol. Energy* **2003**, *74*, 181–192. [CrossRef]
229. Rath, J. Low temperature polycrystalline silicon: A review on deposition, physical properties and solar cell applications. *Sol. Energy Mater. Sol. Cells* **2003**, *76*, 431–487. [CrossRef]
230. Schropp, R.E.; Carius, R.; Beaucarne, G. Amorphous Silicon, Microcrystalline Silicon, and Thin-Film Polycrystalline Silicon Solar Cells. *MRS Bull.* **2007**, *32*, 219–224. [CrossRef]
231. Zhang, H.; Wang, X.; Chen, X.; Zhang, Y. Research progress of compound-based dopant-free asymmetric heterogeneous contact silicon solar cell. *Nano Energy* **2025**, *136*, 110715. [CrossRef]
232. Liang, B.; Chen, X.; Wang, X.; Yuan, H.; Sun, A.; Wang, Z.; Hu, L.; Hou, G.; Zhao, Y.; Zhang, X. Progress in crystalline silicon heterojunction solar cells. *J. Mater. Chem. A* **2024**, *13*, 2441–2477. [CrossRef]
233. Kirchartz, T.; Yan, G.; Yuan, Y.; Patel, B.K.; Cahen, D.; Nayak, P.K. The state of the art in photovoltaic materials and device research. *Nat. Rev. Mater.* **2025**, *10*, 335–354. [CrossRef]
234. Melskens, J.; Theeuwes, R.J.; Black, L.E.; Berghuis, W.-J.H.; Macco, B.; Bronsveld, P.C.P.; Kessels, W.M.M. Excellent Passivation of *n*-Type Silicon Surfaces Enabled by Pulsed-Flow Plasma-Enhanced Chemical Vapor Deposition of Phosphorus Oxide Capped by Aluminum Oxide. *Phys. Status Solidi (RRL)—Rapid Res. Lett.* **2020**, *15*, 2000399. [CrossRef]
235. Banerjee, S.; Das, M.K. A review of Al_2O_3 as surface passivation material with relevant process technologies on c-Si solar cell. *Opt. Quantum Electron.* **2021**, *53*, 60. [CrossRef]
236. Madani, K.; Rohatgi, A.; Min, K.H.; Song, H.-E.; Huang, Y.-Y.; Upadhyaya, A.D.; Upadhyaya, V.; Rounsaville, B.; Ok, Y.-W. Comparison of passivation properties of plasma-assisted ALD and APCVD deposited Al_2O_3 with SiNx capping. *Sol. Energy Mater. Sol. Cells* **2020**, *218*, 110718. [CrossRef]
237. Grant, N.; Pain, S.; Khorani, E.; Jefferies, R.; Wratten, A.; McNab, S.; Walker, D.; Han, Y.; Beanland, R.; Bonilla, R.; et al. Activation of Al_2O_3 surface passivation of silicon: Separating bulk and surface effects. *Appl. Surf. Sci.* **2023**, *645*, 158786. [CrossRef]
238. Berghuis, W.J.H.-J.; Melskens, J.; Macco, B.; Theeuwes, R.J.; Black, L.E.; Verheijen, M.A.; Kessels, W.M.M. Excellent surface passivation of germanium by a-Si:H/Al_2O_3 stacks. *J. Appl. Phys.* **2021**, *130*, 135303. [CrossRef]
239. Ramos-Carrazco, A.; Berman-Mendoza, D.; Ramirez-Espinoza, R.; Gutierrez, R.G.; Vazquez-Arce, J.L.; Rangel, R.; Melendrez-Amavizca, R.; Bartolo-Pérez, P. Al_2O_3/Si NPs multilayered antireflective coating to enhance the photovoltaic performance of solar cells. *J. Mater. Sci. Mater. Electron.* **2023**, *34*, 2328. [CrossRef]
240. Huang, Y.-C.; Chuang, R.W. Study on Annealing Process of Aluminum Oxide Passivation Layer for PERC Solar Cells. *Coatings* **2021**, *11*, 1052. [CrossRef]
241. Uzum, A.; Kanmaz, I. Passivation properties of HfO_2-SiO_2 mixed metal oxide thin films with low reflectivity on silicon substrates for semiconductor devices. *Thin Solid Film.* **2021**, *738*, 138965. [CrossRef]
242. Prishya, A.A.; Chopra, L. Comprehensive review on uses of silicon dioxide in solar cell. *Mater. Today Proc.* **2022**, *72*, 1471–1478. [CrossRef]
243. Yang, Y.; Chen, D.; Li, D.; Zhao, T.; Zhang, W.; Qiao, W.; Liang, Y.; Yang, Y. Research on the Evolution of Defects Initiation and the Diffusion of Dopant on the Si/SiO_2 Interface. *Adv. Mater. Interfaces* **2024**, *12*, 2400751. [CrossRef]
244. van de Loo, B.; Knoops, H.; Dingemans, G.; Janssen, G.; Lamers, M.; Romijn, I.; Weeber, A.; Kessels, W. "Zero-charge" SiO_2/Al_2O_3 stacks for the simultaneous passivation of n+ and p+ doped silicon surfaces by atomic layer deposition. *Sol. Energy Mater. Sol. Cells* **2015**, *143*, 450–456. [CrossRef]
245. Hoex, B.; Schmidt, J.; Bock, R.; Altermatt, P.P.; van de Sanden, M.C.M.; Kessels, W.M.M. Excellent passivation of highly doped p-type Si surfaces by the negative-charge-dielectric Al_2O_3. *Appl. Phys. Lett.* **2007**, *91*, 112107. [CrossRef]
246. Smirnov, M.; Roginskii, E.; Savin, A.; Mazhenov, N.; Pankin, D. Density-Functional Study of the Si/SiO_2 Interfaces in Short-Period Superlattices: Structures and Energies. *Coatings* **2023**, *13*, 1231. [CrossRef]
247. Glunz, S.W.; Steinhauser, B.; Polzin, J.; Luderer, C.; Grübel, B.; Niewelt, T.; Okasha, A.M.O.M.; Bories, M.; Nagel, H.; Krieg, K.; et al. Silicon-based passivating contacts: The TOPCon route. *Prog. Photovolt. Res. Appl.* **2021**, *31*, 341–359. [CrossRef]
248. Yousuf, H.; Khokhar, M.Q.; Zahid, M.A.; Rabelo, M.; Kim, S.; Pham, D.P.; Kim, Y.; Yi, J. Tunnel Oxide Deposition Techniques and Their Parametric Influence on Nano-Scaled SiO_x Layer of TOPCon Solar Cell: A Review. *Energies* **2022**, *15*, 5753. [CrossRef]
249. Rahman, R.U.; Khokhar, M.Q.; Hussain, S.Q.; Mehmood, H.; Yousuf, H.; Jony, J.A.; Park, S.; Yi, J. Progress in TOPCon solar cell technology: Investigating hafnium oxide through simulation. *Curr. Appl. Phys.* **2024**, *63*, 96–104. [CrossRef]
250. Li, S.; Liu, C.; Zhu, T.; Wang, Y.; He, J.; Yang, G.; Sun, P.; Li, H.; Liu, H.; Jiang, N. Effects of the thermal treatments on the optical properties of SiO_2 anti-reflective coatings on sapphire windows. *Infrared Phys. Technol.* **2024**, *137*, 105151. [CrossRef]

251. Jimenéz-Vivanco, M.R.; García, G.; Carrillo, J.; Agarwal, V.; Díaz-Becerril, T.; Doti, R.; Faubert, J.; Lugo, J.E. Porous Si-SiO_2 based UV Microcavities. *Sci. Rep.* **2020**, *10*, 2220. [CrossRef]
252. Pliskin, W.A.; Esch, R.P. Refractive Index of SiO_2 Films Grown on Silicon. *J. Appl. Phys.* **1965**, *36*, 2011–2013. [CrossRef]
253. Ali, K.; Khan, S.A.; Jafri, M.M. Effect of Double Layer (SiO_2/TiO_2) Anti-reflective Coating on Silicon Solar Cells. *Int. J. Electrochem. Sci.* **2014**, *9*, 7865–7874. [CrossRef]
254. Rad, A.S.; Afshar, A.; Azadeh, M. Anti-reflection and self-cleaning meso-porous TiO_2 coatings as solar systems protective layer: Investigation of effect of porosity and roughness. *Opt. Mater.* **2020**, *107*, 110027. [CrossRef]
255. Richards, B.S. Comparison of $TiO_2$and other dielectric coatings for buried-contact solar cells: A review. *Prog. Photovolt. Res. Appl.* **2004**, *12*, 253–281. [CrossRef]
256. Elrashidi, A.; Elleithy, K. High-Efficiency Crystalline Silicon-Based Solar Cells Using Textured TiO_2 Layer and Plasmonic Nanoparticles. *Nanomaterials* **2022**, *12*, 1589. [CrossRef]
257. Richards, B.S.; Cotter, J.E.; Honsberg, C.B. Enhancing the surface passivation of TiO_2 coated silicon wafers. *Appl. Phys. Lett.* **2002**, *80*, 1123–1125. [CrossRef]
258. Yadav, C.; Kumar, S. Numerical Simulation for Optimization of Ultra-thin n-type AZO and TiO_2 Based Textured p-type c-Si Heterojunction Solar Cells. *Silicon* **2021**, *14*, 4291–4299. [CrossRef]
259. Lettieri, S.; Pavone, M.; Fioravanti, A.; Amato, L.S.; Maddalena, P. Charge Carrier Processes and Optical Properties in TiO_2 and TiO_2-Based Heterojunction Photocatalysts: A Review. *Materials* **2021**, *14*, 1645. [CrossRef] [PubMed]
260. Singh, M.; Singh, D.; Mishra, V.; Singh, V.; Singh, S.; Dev, R.; Singh, D. Efficiency and environmental stability of TiO_2 based solar cells for green electricity production. *Int. J. Chem. React. Eng.* **2023**, *22*, 69–77. [CrossRef]
261. Park, G.S.; Lee, S.; Kim, D.; Park, S.Y.; Koh, J.H.; Won, D.H.; Lee, P.; Do, Y.R.; Min, B.K. Amorphous TiO_2 Passivating Contacts for Cu(In,Ga)$(S,Se)_2$ Ultrathin Solar Cells: Defect-State-Mediated Hole Conduction. *Adv. Energy Mater.* **2023**, *13*, 2203183. [CrossRef]
262. Khir, H.; Pandey, A.; Saidur, R.; Ahmad, M.S.; Rahim, N.A.; Dewika, M.; Samykano, M. Recent advancements and challenges in flexible low temperature dye sensitised solar cells. *Sustain. Energy Technol. Assess.* **2022**, *53*, 102745. [CrossRef]
263. Shukla, G.; Angappane, S. Dimensional constraints favour high temperature anatase phase stability in TiO_2 nanorods. *Appl. Surf. Sci.* **2022**, *577*, 151874. [CrossRef]
264. Cui, W.; Chen, F.; Li, Y.; Su, X.; Sun, B. Status and perspectives of transparent conductive oxide films for silicon heterojunction solar cells. *Mater. Today Nano* **2023**, *22*, 100329. [CrossRef]
265. Dong, G.; Li, J.; Zhao, Y.; Ran, X.; Peng, C.; He, D.; Jin, C.; Wang, Q.; Jiang, H.; Zhang, Y.; et al. Highly efficient silicon heterojunction solar cells with ZnO:Al transparent electrode and transition metal doped indium oxide interfacial layer. *Prog. Photovolt. Res. Appl.* **2023**, *31*, 931–938. [CrossRef]
266. Wang, J.; Meng, C.; Liu, H.; Hu, Y.; Zhao, L.; Wang, W.; Xu, X.; Zhang, Y.; Yan, H. Application of Indium Tin Oxide/Aluminum-Doped Zinc Oxide Transparent Conductive Oxide Stack Films in Silicon Heterojunction Solar Cells. *ACS Appl. Energy Mater.* **2021**, *4*, 13586–13592. [CrossRef]
267. Kumari, P.; Srivastava, A.; Sharma, R.K.; Sharma, D.; Srivastava, S.K. Zinc Oxide: A Fascinating Material for Photovoltaic Applications. In *Materials Horizons from Nature to Nanomaterials*; Springer Nature: Singapore, 2022; pp. 173–241. [CrossRef]
268. Üzar, N.; Abdulaziz, U. Investigation of the effects of coating numbers of thin films and metal contact type on physical properties of undoped ZnO, Fe-doped ZnO, and Fe–B co-doped ZnO thin films. *J. Mater. Sci. Mater. Electron.* **2024**, *35*, 1136. [CrossRef]
269. Aberle, A.G. Overview on SiN surface passivation of crystalline silicon solar cells. *Sol. Energy Mater. Sol. Cells* **2001**, *65*, 239–248. [CrossRef]
270. Tepner, S.; Lorenz, A. Printing technologies for silicon solar cell metallization: A comprehensive review. *Prog. Photovolt. Res. Appl.* **2023**, *31*, 557–590. [CrossRef]
271. Suchikova, Y.; Kovachov, S.; Bohdanov, I.; Karipbayev, Z.T.; Zhydachevskyy, Y.; Lysak, A.; Pankratov, V.; Popov, A.I. Advanced Synthesis and Characterization of CdO/CdS/ZnO Heterostructures for Solar Energy Applications. *Materials* **2024**, *17*, 1566. [CrossRef]
272. Suchikova, Y.; Kovachov, S.; Bohdanov, I.; Karipbaev, Z.T.; Pankratov, V.; Popov, A.I. Study of the structural and morphological characteristics of the CdxTeyOz nanocomposite obtained on the surface of the CdS/ZnO heterostructure by the SILAR method. *Appl. Phys. A* **2023**, *129*, 116625. [CrossRef]
273. Balasubramani, V.; Akila, T.; Suresh, R.; Alodhay, A.N.; Muthuramamoorthy, M.; Sasikumar, K. Optimizing Oxygen Vacancy Concentrations in CeO_2 Thin Films for Enhanced Photodetector Sensitivity. *Opt. Mater.* **2025**, *159*, 116625. [CrossRef]
274. Ali, Z.; Ali, K. Modeling of improved efficiency and spectral response of a Si-based heterojunction solar cell by using CeO_2 as a buffer layer. *J. Comput. Electron.* **2022**, *21*, 1320–1328. [CrossRef]
275. Kanneboina, V. The simulated performance of c-Si/a-Si:H heterojunction solar cells with nc-Si:H, μc-Si:H, a-SiC:H, and a-SiGe:H emitter layers. *J. Comput. Electron.* **2020**, *20*, 344–352. [CrossRef]
276. Vikhrov, S.P.; Vishnyakov, N.V.; Gudzev, V.V.; Ermachikhin, A.V.; Shilina, D.V.; Litvinov, V.G.; Maslov, A.D.; Mishustin, V.G.; Terukov, E.I.; Titov, A.S. Study of Deep Levels in a HIT Solar Cell. *Semiconductors* **2018**, *52*, 926–930. [CrossRef]

277. Crovetto, A.; Yan, C.; Iandolo, B.; Zhou, F.; Stride, J.; Schou, J.; Hao, X.; Hansen, O. Lattice-matched Cu_2ZnSnS_4/CeO_2 solar cell with open circuit voltage boost. *Appl. Phys. Lett.* **2016**, *109*, 233904. [CrossRef]
278. Maniglia, R.; Reed, K.J.; Texter, J. Reactive CeO_2 nanofluids for UV protective films. *J. Colloid Interface Sci.* **2017**, *506*, 346–354. [CrossRef]
279. Caputo, F.; De Nicola, M.; Sienkiewicz, A.; Giovanetti, A.; Bejarano, I.; Licoccia, S.; Traversa, E.; Ghibelli, L. Cerium oxide nanoparticles, combining antioxidant and UV shielding properties, prevent UV-induced cell damage and mutagenesis. *Nanoscale* **2015**, *7*, 15643–15656. [CrossRef]
280. Han, J.; Park, K.; Tan, S.; Vaynzof, Y.; Xue, J.; Diau, E.W.-G.; Bawendi, M.G.; Lee, J.-W.; Jeon, I. Perovskite solar cells. *Nat. Rev. Methods Prim.* **2025**, *5*, 3. [CrossRef]
281. Prince, K.J.; Mirletz, H.M.; Gaulding, E.A.; Wheeler, L.M.; Kerner, R.A.; Zheng, X.; Schelhas, L.T.; Tracy, P.; Wolden, C.A.; Berry, J.J.; et al. Sustainability pathways for perovskite photovoltaics. *Nat. Mater.* **2024**, *24*, 22–33. [CrossRef]
282. Elangovan, N.K.; Kannadasan, R.; Beenarani, B.; Alsharif, M.H.; Kim, M.-K.; Inamul, Z.H. Recent developments in perovskite materials, fabrication techniques, band gap engineering, and the stability of perovskite solar cells. *Energy Rep.* **2024**, *11*, 1171–1190. [CrossRef]
283. Sewela, T.; Ocaya, R.O.; Malevu, T.D. Recent insights into the transformative role of Graphene-based/TiO_2 electron transport layers for perovskite solar cells. *Energy Sci. Eng.* **2024**, *13*, 4–26. [CrossRef]
284. Liao, Y.-H.; Chang, Y.-H.; Lin, T.-H.; Lee, K.-M.; Wu, M.-C. Recent Advances in Metal Oxide Electron Transport Layers for Enhancing the Performance of Perovskite Solar Cells. *Materials* **2024**, *17*, 2722. [CrossRef]
285. Chen, X.; Yue, Z.; Yang, H.; Xu, B.; Cheng, Y. N-Type Self-Assembled Monolayers (SAMs): The Next Star Materials in the Perovskite Photovoltaic Field. *Small* **2025**, *21*, e2411312. [CrossRef] [PubMed]
286. Samantaray, M.R.; Wang, Z.; Hu, D.; Yuan, M.; Song, H.; Li, F.; Jia, G.; Ji, L.; Zou, X.; Shen, H.; et al. Scalable Fabrication Methods of Large-Area (n-*i*-p) Perovskite Solar Panels. *Sol. RRL* **2024**, *8*, 2400235. [CrossRef]
287. Kothandaraman, R.K.; Jiang, Y.; Feurer, T.; Tiwari, A.N.; Fu, F. Near-Infrared-Transparent Perovskite Solar Cells and Perovskite-Based Tandem Photovoltaics. *Small Methods* **2020**, *4*, 2000395. [CrossRef]
288. Lin, L.; Jones, T.W.; Yang, T.C.; Duffy, N.W.; Li, J.; Zhao, L.; Chi, B.; Wang, X.; Wilson, G.J. Inorganic Electron Transport Materials in Perovskite Solar Cells. *Adv. Funct. Mater.* **2020**, *31*, 2008300. [CrossRef]
289. Arora, I.; Chawla, H.; Chandra, A.; Sagadevan, S.; Garg, S. Advances in the strategies for enhancing the photocatalytic activity of TiO_2: Conversion from UV-light active to visible-light active photocatalyst. *Inorg. Chem. Commun.* **2022**, *143*, 109700. [CrossRef]
290. Gopinath, V.M.; Arulvel, S. A review on the steels, alloys/high entropy alloys, composites and coatings used in high temperature wear applications. *Mater. Today Proc.* **2021**, *43*, 817–823. [CrossRef]
291. Manabeng, M.; Mwankemwa, B.S.; Ocaya, R.O.; Motaung, T.E.; Malevu, T.D. A Review of the Impact of Zinc Oxide Nanostructure Morphology on Perovskite Solar Cell Performance. *Processes* **2022**, *10*, 1803. [CrossRef]
292. Abidin, N.A.Z.; Arith, F.; Noorasid, N.S.; Sarkawi, H.; Mustafa, A.N.; Safie, N.E.; Shah, A.S.M.; Azam, M.A.; Chelvanathan, P.; Amin, N. Dopant engineering for ZnO electron transport layer towards efficient perovskite solar cells. *RSC Adv.* **2023**, *13*, 33797–33819. [CrossRef]
293. Apergi, S.; Brocks, G.; Tao, S.; Olthof, S. Probing the Reactivity of ZnO with Perovskite Precursors. *ACS Appl. Mater. Interfaces* **2024**, *16*, 14984–14994. [CrossRef] [PubMed]
294. Znaidi, L. Sol–gel-deposited ZnO thin films: A review. *Mater. Sci. Eng. B* **2010**, *174*, 18–30. [CrossRef]
295. Han, Y.; Guo, J.; Luo, Q.; Ma, C.-Q. Solution-Processable Zinc Oxide for Printed Photovoltaics: Progress, Challenges, and Prospect. *Adv. Energy Sustain. Res.* **2023**, *4*, 2200179. [CrossRef]
296. Luo, J.; Wang, Y.; Zhang, Q. Progress in perovskite solar cells based on ZnO nanostructures. *Sol. Energy* **2018**, *163*, 289–306. [CrossRef]
297. Qiu, C.; Wu, Y.; Song, J.; Wang, W.; Li, Z. Efficient Planar Perovskite Solar Cells with ZnO Electron Transport Layer. *Coatings* **2022**, *12*, 1981. [CrossRef]
298. Otalora, C.; Botero, M.A.; Ordoñez, G. ZnO compact layers used in third-generation photovoltaic devices: A review. *J. Mater. Sci.* **2021**, *56*, 15538–15571. [CrossRef]
299. Kim, S.Y.; Cho, S.J.; Byeon, S.E.; He, X.; Yoon, H.J. Self-Assembled Monolayers as Interface Engineering Nanomaterials in Perovskite Solar Cells. *Adv. Energy Mater.* **2020**, *10*, 2002606. [CrossRef]
300. Sekar, K.; Doineau, R.; Mayarambakam, S.; Schmaltz, B.; Poulin-Vittrant, G. Control of ZnO nanowires growth in flexible perovskite solar cells: A mini-review. *Heliyon* **2024**, *10*, e24706. [CrossRef] [PubMed]
301. Jiang, Q.; Zhang, X.; You, J. SnO_2: A Wonderful Electron Transport Layer for Perovskite Solar Cells. *Small* **2018**, *14*, e1801154. [CrossRef]
302. Deng, K.; Chen, Q.; Li, L. Modification Engineering in SnO_2 Electron Transport Layer toward Perovskite Solar Cells: Efficiency and Stability. *Adv. Funct. Mater.* **2020**, *30*, 2004209. [CrossRef]

303. Chen, Y.; Meng, Q.; Zhang, L.; Han, C.; Gao, H.; Zhang, Y.; Yan, H. SnO_2-based electron transporting layer materials for perovskite solar cells: A review of recent progress. *J. Energy Chem.* **2019**, *35*, 144–167. [CrossRef]
304. Ahmmed, S.; He, Y.; Kayesh, E.; Karim, A.; Matsuishi, K.; Islam, A. Ce-Doped SnO_2 Electron Transport Layer for Minimizing Open Circuit Voltage Loss in Lead Perovskite Solar Cells. *ACS Appl. Mater. Interfaces* **2024**, *16*, 32282–32290. [CrossRef]
305. Lee, M.M.; Teuscher, J.; Miyasaka, T.; Murakami, T.N.; Snaith, H.J. Efficient Hybrid Solar Cells Based on Meso-Superstructured Organometal Halide Perovskites. *Science* **2012**, *338*, 643–647. [CrossRef]
306. Noh, M.F.M.; Teh, C.H.; Daik, R.; Lim, E.L.; Yap, C.C.; Ibrahim, M.A.; Ludin, N.A.; Yusoff, A.R.b.M.; Jang, J.; Teridi, M.A.M. The architecture of the electron transport layer for a perovskite solar cell. *J. Mater. Chem. C* **2017**, *6*, 682–712. [CrossRef]
307. Al-Shujaa, S.; Zhao, P.; He, D.; Al-Anesi, B.; Feng, Y.; Xia, J.; Zhang, B.; Zhang, Y. Improving the Efficiency and Stability of Perovskite Solar Cells by Refining the Perovskite-Electron Transport Layer Interface and Shielding the Absorber from UV Effects. *ACS Appl. Mater. Interfaces* **2024**, *16*, 28493–28504. [CrossRef]
308. Bhattarai, S.; Borah, D.; Rout, J.; Pandey, R.; Madan, J.; Hossain, I.; Handique, P.; Ansari, M.Z.; Hossain, M.K.; Rahman, F. Designing an efficient lead-free perovskite solar cell with green-synthesized $CuCrO_2$ and CeO_2 as carrier transport materials. *RSC Adv.* **2023**, *13*, 34693–34702. [CrossRef]
309. Hu, T.; Xiao, S.; Yang, H.; Chen, L.; Chen, Y. Cerium oxide as an efficient electron extraction layer for p–i–n structured perovskite solar cells. *Chem. Commun.* **2017**, *54*, 471–474. [CrossRef]
310. Chen, W.; Luo, Q.; Zhang, C.; Shi, J.; Deng, X.; Yue, L.; Wang, Z.; Chen, X.; Huang, S. Effects of down-conversion CeO_2:Eu^{3+} nanophosphors in perovskite solar cells. *J. Mater. Sci. Mater. Electron.* **2017**, *28*, 11346–11357. [CrossRef]
311. Abdulrahman, A.; Basem, A.; Algarni, Z.; Soliman, N.F.; Amari, A.; Saydullaev, B.; Abduvokhidov, A.; Khudoynazarov, E.; Mahariq, I. Sustainable Synthesis of a Novel α-Fe_2O_3/ZIF-8/PANI Composite Electrodes for High-Energy Hybrid Supercapacitors. *J. Alloys Compd.* **2025**, *1040*, 183422. [CrossRef]
312. Dissanayake, D.M.S.N.; Mantilaka, M.M.M.G.P.G.; Palihawadana, T.C.; Chandrakumara, G.T.D.; De Silva, R.T.; Pitawala, H.M.T.G.A.; de Silva, K.M.N.; Amaratunga, G.A.J. Facile and low-cost synthesis of pure hematite (α-Fe_2O_3) nanoparticles from naturally occurring laterites and their superior adsorption capability towards acid-dyes. *RSC Adv.* **2019**, *9*, 21249–21257. [CrossRef] [PubMed]
313. Qureshi, A.A.; Javed, S.; Akram, M.A.; Schmidt-Mende, L.; Fakharuddin, A. Solvent-Assisted Crystallization of an α-Fe_2O_3 Electron Transport Layer for Efficient and Stable Perovskite Solar Cells Featuring Negligible Hysteresis. *ACS Omega* **2023**, *8*, 18106–18115. [CrossRef] [PubMed]
314. Piccinin, S. The band structure and optical absorption of hematite (α-Fe_2O_3): A first-principles GW-BSE study. *Phys. Chem. Chem. Phys.* **2019**, *21*, 2957–2967. [CrossRef]
315. Fan, X.; Zhu, F.; Wang, Z.; Wang, X.; Zou, Y.; Gao, B.; Song, L.; He, J.; Wang, T. Preparation of p-type Fe_2O_3 nanoarray and its performance as photocathode for photoelectrochemical water splitting. *Front. Chem.* **2025**, *13*, 1526745. [CrossRef]
316. Rahman, A.U.; El Astal-Quirós, A.; Susanna, G.; Javanbakht, H.; Calabrò, E.; Polino, G.; Paci, B.; Generosi, A.; Riva, F.R.; Brunetti, F.; et al. Scaling-Up of Solution-Processable Tungsten Trioxide (WO_3) Nanoparticles as a Hole Transport Layer in Inverted Organic Photovoltaics. *Energies* **2024**, *17*, 814. [CrossRef]
317. Ávila-López, A.; Cruz, J.C.; Díaz-Real, J.A.; García-Uitz, K.; Cante-Góngora, D.; Rodríguez-May, G. A Review of Perovskite-Based Solar Cells over the Last Decade: The Evolution of the Hole Transport Layer and the Use of WO_3 as an Electron Transport Layer. *Coatings* **2025**, *15*, 132. [CrossRef]
318. Haque, M.M.; Mahjabin, S.; Abdullah, H.B.; Akhtaruzzaman, M.; Almohamadi, H.; Islam, M.A.; Hossain, M.I.; Ibrahim, M.A.; Chelvanathan, P. Exploring the Theoretical Potential of Tungsten Oxide (WOx) as a Universal Electron Transport Layer (ETL) for Various Perovskite Solar Cells through Interfacial Energy Band Alignment Modulation. *J. Phys. Chem. Solids* **2024**, *196*, 112324. [CrossRef]
319. Roy, A.; Bhandari, S.; Ghosh, A.; Sundaram, S.; Mallick, T.K. Incorporating Solution-Processed Mesoporous WO_3 as an Interfacial Cathode Buffer Layer for Photovoltaic Applications. *J. Phys. Chem. A* **2020**, *124*, 5709–5719. [CrossRef]
320. Sengupta, D.; Das, P.; Mondal, B.; Mukherjee, K. Effects of doping, morphology and film-thickness of photo-anode materials for dye sensitized solar cell application—A review. *Renew. Sustain. Energy Rev.* **2016**, *60*, 356–376. [CrossRef]
321. Grätzel, M. Mesoporous oxide junctions and nanostructured solar cells. *Curr. Opin. Colloid Interface Sci.* **1999**, *4*, 314–321. [CrossRef]
322. Zhang, Y.; Zhang, B.; Peng, X.; Liu, L.; Dong, S.; Lin, L.; Chen, S.; Meng, S.; Feng, Y. Preparation of dye-sensitized solar cells with high photocurrent and photovoltage by using mesoporous titanium dioxide particles as photoanode material. *Nano Res.* **2015**, *8*, 3830–3841. [CrossRef]
323. Di Carlo, G.; Calogero, G.; Brucale, M.; Caschera, D.; de Caro, T.; Di Marco, G.; Ingo, G.M. Insights into meso-structured photoanodes based on titanium oxide thin film with high dye adsorption ability. *J. Alloys Compd.* **2014**, *609*, 116–124. [CrossRef]
324. Agarwala, S.; Kevin, M.; Wong, A.S.W.; Peh, C.K.N.; Thavasi, V.; Ho, G.W. Mesophase Ordering of TiO_2 Film with High Surface Area and Strong Light Harvesting for Dye-Sensitized Solar Cell. *ACS Appl. Mater. Interfaces* **2010**, *2*, 1844–1850. [CrossRef]

325. Li, W.; Elzatahry, A.; Aldhayan, D.; Zhao, D. Core–shell structured titanium dioxide nanomaterials for solar energy utilization. *Chem. Soc. Rev.* **2018**, *47*, 8203–8237. [CrossRef] [PubMed]
326. Korir, B.K.; Kibet, J.K.; Ngari, S.M. A review on the current status of dye-sensitized solar cells: Toward sustainable energy. *Energy Sci. Eng.* **2024**, *12*, 3188–3226. [CrossRef]
327. Kumar, D. A short review on the advancement in the development of TiO_2 and ZnO based photo-anodes for the application of Dye-Sensitized Solar Cells (DSSCs). *Eng. Res. Express* **2021**, *3*, 042004. [CrossRef]
328. Clarke, B.; Ghandi, K. The Interplay of Growth Mechanism and Properties of ZnO Nanostructures for Different Applications. *Small* **2023**, *19*, e2302864. [CrossRef] [PubMed]
329. Ali, J.; Bibi, S.; Jatoi, W.B.; Tuzen, M.; Jakhrani, M.A.; Feng, X.; Saleh, T.A. Green synthesized zinc oxide nanostructures and their applications in dye-sensitized solar cells and photocatalysis: A review. *Mater. Today Commun.* **2023**, *36*, 106840. [CrossRef]
330. Vittal, R.; Ho, K.-C. Zinc oxide based dye-sensitized solar cells: A review. *Renew. Sustain. Energy Rev.* **2017**, *70*, 920–935. [CrossRef]
331. Boro, B.; Gogoi, B.; Rajbongshi, B.; Ramchiary, A. Nano-structured TiO_2/ZnO nanocomposite for dye-sensitized solar cells application: A review. *Renew. Sustain. Energy Rev.* **2018**, *81*, 2264–2270. [CrossRef]
332. Kumar, R.; Umar, A.; Kumar, G.; Nalwa, H.S.; Kumar, A.; Akhtar, M.S. Zinc oxide nanostructure-based dye-sensitized solar cells. *J. Mater. Sci.* **2017**, *52*, 4743–4795. [CrossRef]
333. Abdellah, I.M. Molecular engineering and electrolyte optimization strategies for enhanced performance of Ru(ii) polypyridyl-sensitized DSSCs. *RSC Adv.* **2025**, *15*, 9763–9786. [CrossRef]
334. Bouclé, J.; Ackermann, J. Solid-state dye-sensitized and bulk heterojunction solar cells using TiO_2 and ZnO nanostructures: Recent progress and new concepts at the borderline. *Polym. Int.* **2011**, *61*, 355–373. [CrossRef]
335. Prabavathy, N.; Shalini, S.; Balasundaraprabhu, R.; Velauthapillai, D.; Prasanna, S.; Muthukumarasamy, N. Enhancement in the photostability of natural dyes for dye-sensitized solar cell (DSSC) applications: A review. *Int. J. Energy Res.* **2017**, *41*, 1372–1396. [CrossRef]
336. Zheng, H.; Tachibana, Y.; Kalantar-Zadeh, K. Dye-Sensitized Solar Cells Based on WO_3. *Langmuir* **2010**, *26*, 19148–19152. [CrossRef]
337. Chen, W.; Qiu, Y.; Zhong, Y.; Wong, K.S.; Yang, S. High-Efficiency Dye-Sensitized Solar Cells Based on the Composite Photoanodes of SnO_2 Nanoparticles/ZnO Nanotetrapods. *J. Phys. Chem. A* **2010**, *114*, 3127–3138. [CrossRef]
338. Memar, A.; Phan, C.M.; Tade, M.O. Photocatalytic activity of WO_3/Fe_2O_3 nanocomposite photoanode. *Int. J. Hydrogen Energy* **2015**, *40*, 8642–8649. [CrossRef]
339. Younas, M.; Gondal, M.; Dastageer, M.; Baig, U. Fabrication of cost effective and efficient dye sensitized solar cells with WO_3-TiO_2 nanocomposites as photoanode and MWCNT as Pt-free counter electrode. *Ceram. Int.* **2019**, *45*, 936–947. [CrossRef]
340. Kim, M.-H.; Kwon, Y.-U. Semiconducting Divalent Metal Oxides as Blocking Layer Material for SnO_2-Based Dye-Sensitized Solar Cells. *J. Phys. Chem. C* **2011**, *115*, 23120–23125. [CrossRef]
341. Shahpari, M.; Behjat, A.; Khajaminian, M.; Torabi, N. The influence of morphology of hematite (α-Fe_2O_3) counter electrodes on the efficiency of dye-sensitized solar cells. *Sol. Energy* **2015**, *119*, 45–53. [CrossRef]
342. Suh, D. Status of Al_2O_3/TiO_2-Based Antireflection and Surface Passivation for Silicon Solar Cells. *Phys. Status Solidi (RRL)—Rapid Res. Lett.* **2021**, *15*, 2100236. [CrossRef]
343. Lee, M.-J.; Park, J.-Y.; Kim, C.-S.; Okuyama, K.; Lee, S.-E.; Kim, T.-O. Improvement of light scattering capacity in dye-sensitized solar cells by doping with SiO_2 nanoparticles. *J. Power Sources* **2016**, *327*, 96–103. [CrossRef]
344. Ramanujam, J.; Bishop, D.M.; Todorov, T.K.; Gunawan, O.; Rath, J.; Nekovei, R.; Artegiani, E.; Romeo, A. Flexible CIGS, CdTe and a-Si:H based thin film solar cells: A review. *Prog. Mater. Sci.* **2020**, *110*, 100619. [CrossRef]
345. Luque, A.; Hegedus, S. (Eds.) *Handbook of Photovoltaic Science and Engineering*; John Wiley & Sons, Ltd.: Hoboken, NJ, USA, 2011. [CrossRef]
346. Vijayan, K.; Vijayachamundeeswari, S.; Sivaperuman, K.; Ahsan, N.; Logu, T.; Okada, Y. A review on advancements, challenges, and prospective of copper and non-copper based thin-film solar cells using facile spray pyrolysis technique. *Sol. Energy* **2022**, *234*, 81–102. [CrossRef]
347. Ishizuka, S.; Sakurai, K.; Yamada, A.; Matsubara, K.; Fons, P.; Iwata, K.; Nakamura, S.; Kimura, Y.; Baba, T.; Nakanishi, H.; et al. Fabrication of wide-gap Cu(In1−xGax)Se2 thin film solar cells: A study on the correlation of cell performance with highly resistive i-ZnO layer thickness. *Sol. Energy Mater. Sol. Cells* **2005**, *87*, 541–548. [CrossRef]
348. Efaz, E.T.; Rhaman, M.; Al Imam, S.; Bashar, K.L.; Kabir, F.; Mourtaza, E.; Sakib, S.N.; Mozahid, F.A. A review of major technologies of thin-film solar cells. *Eng. Res. Express* **2021**, *3*, 032001. [CrossRef]
349. Romeo, A.; Artegiani, E. CdTe-Based Thin Film Solar Cells: Past, Present and Future. *Energies* **2021**, *14*, 1684. [CrossRef]
350. Salhi, B. The Photovoltaic Cell Based on CIGS: Principles and Technologies. *Materials* **2022**, *15*, 1908. [CrossRef]
351. Rahman, M.A. Enhancing the photovoltaic performance of Cd-free Cu2ZnSnS4 heterojunction solar cells using SnS HTL and TiO_2 ETL. *Sol. Energy* **2021**, *215*, 64–76. [CrossRef]

352. Qin, D.; Yang, P.; Pan, Y.; Wang, Y.; Pan, Y.; Weng, G.; Hu, X.; Tao, J.; Chu, J.; Akiyama, H.; et al. Non-Cadmium $TiO_2/Sb_2(Se, S)_3$ Heterojunction Solar Cells with Improved Efficiency by NaCl-Treated Interface Engineering. *ACS Appl. Mater. Interfaces* **2025**, *17*, 22050–22059. [CrossRef] [PubMed]
353. Werner, F.; Veith-Wolf, B.; Spindler, C.; Barget, M.R.; Babbe, F.; Guillot, J.; Schmidt, J.; Siebentritt, S. Oxidation as Key Mechanism for Efficient Interface Passivation in Cu(In,Ga)Se2 Thin-Film Solar Cells. *Phys. Rev. Appl.* **2020**, *13*, 054004. [CrossRef]
354. Cunha, J.M.V.; Fernandes, P.A.; Hultqvist, A.; Teixeira, J.P.; Bose, S.; Vermang, B.; Garud, S.; Buldu, D.; Gaspar, J.; Edoff, M.; et al. Insulator Materials for Interface Passivation of Cu(In,Ga)Se_2Thin Films. *IEEE J. Photovolt.* **2018**, *8*, 1313–1319. [CrossRef]
355. Abbas, K.J.; Bahrami, A. Investigating the potential of WO_3 and WS_2 as Cd-free buffer layers in Sb2Se3-Based thin-film solar cells: A numerical study with SCAPS-1D software. *Sol. Energy Mater. Sol. Cells* **2024**, *272*, 112891. [CrossRef]
356. Ouyang, D.; Huang, Z.; Choy, W.C.H. Solution-Processed Metal Oxide Nanocrystals as Carrier Transport Layers in Organic and Perovskite Solar Cells. *Adv. Funct. Mater.* **2018**, *29*, 1804660. [CrossRef]
357. Concina, I.; Vomiero, A. Metal Oxide Semiconductors for Dye- and Quantum-Dot-Sensitized Solar Cells. *Small* **2014**, *11*, 1744–1774. [CrossRef]
358. Pandi, K.; Kumar, T.R.N.; Lakhera, S.K.; Neppolian, B. Simultaneous Passivation of Surface Vacancies and Enhancement in Charge Transfer Property of ZnO Electron Transport Layer for Inverted Organic Solar Cells. *Energy Technol.* **2020**, *8*, 2000481. [CrossRef]
359. Chaudhary, D.K.; Dhawan, P.K.; Patel, S.P.; Bhasker, H. Large area semitransparent inverted organic solar cells with enhanced operational stability using TiO_2 electron transport layer for building integrated photovoltaic devices. *Mater. Lett.* **2021**, *283*, 128725. [CrossRef]
360. Bivour, M.; Temmler, J.; Steinkemper, H.; Hermle, M. Molybdenum and tungsten oxide: High work function wide band gap contact materials for hole selective contacts of silicon solar cells. *Sol. Energy Mater. Sol. Cells* **2015**, *142*, 34–41. [CrossRef]
361. Tan, Z.; Li, L.; Cui, C.; Ding, Y.; Xu, Q.; Li, S.; Qian, D.; Li, Y. Solution-Processed Tungsten Oxide as an Effective Anode Buffer Layer for High-Performance Polymer Solar Cells. *J. Phys. Chem. C* **2012**, *116*, 18626–18632. [CrossRef]
362. United Nations Framework Convention on Climate Change (UNFCCC). *Paris Agreement*; UNFCCC: Bonn, Germany, 2015. Available online: https://unfccc.int/sites/default/files/english_paris_agreement.pdf (accessed on 5 September 2025).
363. European Union. Directive (EU) 2018/2001 of the European Parliament and of the Council of 11 December 2018 on the Pro-motion of the Use of Energy from Renewable Sources (Recast). Official Journal of the European Union L 328 (21 December 2018), 82–209. Available online: https://eur-lex.europa.eu/legal-content/en/ALL/?uri=CELEX:32018L2001 (accessed on 5 September 2025).
364. International Energy Agency (IEA). Solar PV Feed-in Tariff (China)—IEA Policies Database, 2011 (Notice No. 1594). Available online: https://www.iea.org/policies/5100-solar-pv-feed-in-tariff (accessed on 5 September 2025).
365. U.S. Department of Energy (DOE). Recovery Act (American Recovery and Reinvestment Act of 2009). Available online: https://www.energy.gov/recovery-act (accessed on 5 September 2025).
366. Alternative Fuels Data Center (AFDC). American Recovery and Reinvestment Act of 2009 (Public Law 111-5)—Energy-Related Provisions. Available online: https://afdc.energy.gov/laws/arra.html (accessed on 5 September 2025).
367. International Energy Agency (IEA). Solar PV—Analysis (Overview of Global Trends and Market Dynamics). IEA: Paris, France, 2024–2025 (Living Page). Available online: https://www.iea.org/energy-system/renewables/solar-pv (accessed on 5 September 2025).
368. IEA Photovoltaic Power Systems Programme (IEA-PVPS). *A Snapshot of Global PV—1992–2016*, 5th ed.; IEA-PVPS: Paris, France, 2017. Available online: https://iea-pvps.org/wp-content/uploads/2020/01/IEA-PVPS_-_A_Snapshot_of_Global_PV_-_1992-2016__1_.pdf (accessed on 5 September 2025).
369. Suchikova, Y.; Kovachov, S.; Bohdanov, I.; Konuhova, M.; Zhydachevskyy, Y.; Kumarbekov, K.; Pankratov, V.; Popov, A.I. Wet Chemical Synthesis of $Al_xGa_{1-x}As$ Nanostructures: Investigation of Properties and Growth Mechanisms. *Crystals* **2024**, *14*, 633. [CrossRef]
370. Suchikova, Y.; Kovachov, S.; Bohdanov, I.; Popova, E.; Moskina, A.; Popov, A. Characterization of $Cd_xTe_yO_z$/CdS/ZnO Heterostructures Synthesized by the SILAR Method. *Coatings* **2023**, *13*, 639. [CrossRef]
371. Kovachov, S.; Bohdanov, I.; Karipbayev, Z.; Suchikova, Y.; Tsebriienko, T.; Popov, A.I. Layer-by-Layer Synthesis and Analysis of the the Phase Composition of Cd_x Te_yO_z/CdS/por-ZnO/ZnO Heterostructure. In Proceedings of the 2022 IEEE 3rd KhPI Week on Advanced Technology (KhPIWeek), Kharkiv, Ukraine, 3–7 October 2022; pp. 1–6. [CrossRef]
372. Xu, P.; Wang, H.; Ren, L.; Tu, B.; Wang, W.; Fu, Z. Theoretical study on composition-dependent properties of ZnO·$n$$Al_2O_3$ spinels. Part I: Optical and dielectric. *J. Am. Ceram. Soc.* **2021**, *104*, 5099–5109. [CrossRef]
373. Aryal, S.; Rulis, P.; Ching, W.; Green, D.J. Mechanical Properties and Electronic Structure of Mullite Phases Using First-Principles Modeling. *J. Am. Ceram. Soc.* **2012**, *95*, 2075–2088. [CrossRef]
374. Edan, T.S.; Haider, A.J.; Sultan, F.I. Core–Shell Nanostructures in Self-Cleaning Surface Technology: A Mini Review. *Plasmonics* **2025**, 1–20. [CrossRef]

375. Arulkumar, E.; Manivannan, R.K.; Dhamodaran, G.; Krishnan, R. CuO@α-Fe_2O_3 nanocomposite via one-pot synthesis for multifunctional photocatalytic, optoelectronic and antimicrobial applications. *J. Sol-Gel Sci. Technol.* **2025**, 1–33. [CrossRef]
376. de Freitas Mendes, M.V.; Pedroti, L.G.; de Carvalho, J.M.F.; Ferreira, F.A.; Mendes, B.C.; Xavier, L.M.; Fernandes, W.E.H.; Oliveira, N.M.A. Characterization of Yellow and Red Clays and Bauxite Residue: Analysis of Properties and Potential for Ceramic Products. In *Characterization of Minerals, Metals, and Materials 2025*; Peng, Z., Xie, K.Y., Zhang, M., Li, J., Li, B., Monteiro, S.N., Soman, R., Hwang, J.-Y., Kalay, Y.E., Escobedo-Diaz, J.P., et al., Eds.; TMS 2025. The Minerals, Metals & Materials Series; Springer: Cham, Switzerland, 2025. [CrossRef]
377. European Chemicals Agency (ECHA). Hazardous to the Aquatic Environment (Long-Term). ECHA Registration Dossier; ECHA: Helsinki, Finland, [Online]. Available online: https://echa.europa.eu/registration-dossier/-/registered-dossier/16139/2/1 (accessed on 7 September 2025).
378. RMIS (Raw Materials Information System—Tungsten): European Commission, Joint Research Centre (JRC). RMIS—Raw Materials Information System: Tungsten. European Commission: Brussels, Belgium, [Online]. Available online: https://rmis.jrc.ec.europa.eu/rmp/Tungsten (accessed on 7 September 2025).
379. European Commission, Directorate-General for Internal Market, Industry, Entrepreneurship and SMEs (DG GROW). Critical Raw Materials. European Commission: Brussels, Belgium, [Online]. Available online: https://single-market-economy.ec.europa.eu/sectors/raw-materials/areas-specific-interest/critical-raw-materials_en (accessed on 7 September 2025).
380. Jungbluth, N. Life cycle assessment of crystalline photovoltaics in the Swiss ecoinvent database. *Prog. Photovolt. Res. Appl.* **2005**, *13*, 429–446. [CrossRef]